Removal of Emerging Contaminants from Aqueous Solutions by Using Polymeric Resins

---

A Thesis
Submitted to
the Temple University Graduate Board

In Partial Fulfillment
Of the Requirements for the Degree of
MASTER of SCIENCE
in
ENVIRONMENTAL ENGINEERING

By
Dan Liu
May, 2011

Thesis Approval(s):

____
Thesis advisor:
Dr. Rominder Suri, Ph.D., P.E. Civil & Environmental Engineering

Dr. Tony Singh, Ph.D. Civil & Environmental Engineering
Dr. Judy (Huichun) Zhang, Ph.D. Civil & Environmental Engineering

ABSTRACT

The emerging contaminants (ECs) such as estrogen hormones, perfluorinated compounds (PFCs), bisphenol A (BPA) and 1, 4-dioxane have been detected in natural water bodies at a noticeable level worldwide. The presence of ECs in the aquatic environment can pose potential threats to aquatic organisms as well as human world. Ion-exchange is a highly efficient technology for the removal of heavy metal ions and natural organic materials (NOMs) due to the nature of exchanging similar charged ions. However, this technology has not been explored for removing ECs.

In this study, four categories of ECs: estrogen hormones (12), perfluorinated compounds (10), bisphenol A and 1, 4-dioxane were used as model contaminants. The adsorption of each category of ECs onto various types of polymeric resins (MN100, MN200, A530E, A532E and C115) was investigated. The removal of ECs was tested under batch and column mode. The effects of pH, resin dosage, and contact time on the removal of ECs were studied in batch mode; isotherm and kinetics models were applied to fit the experimental data. Column experiments were conducted to verify the practicability of the polymeric resins. Adsorption results have shown that both MN100 and MN200 resins could efficiently remove estrogen hormones mixture (more than 95%), and bisphenol A (more than 80%) with the initial concentration of 100 μg/L; A532E and A530E could remove perfuorinated compounds mixture (more than 99%) with the initial concentration of 100 μg/L. As pH increased from 9 to 11, the adsorption capacity onto polymeric resins decreased dramatically for estrogen hormones such as 17α-ethinylestradiol, estriol, 17β-estradiol, 17α-estradiol, estrone, 17α-dihydroequilin and equilin as well as bisphenol A. The adsorption of estrogen hormones and bisphenol A onto MN100 and MN200 resins reached the equilibrium within 24 hours, whereas the adsorption of perfluorinated compounds onto A532E and A530E reached the equilibrium within 8 hours. It was also observed that the adsorption of PFCs largely depends on the C-C chain length. PFCs with longer chain yielded lower adsorption efficiency onto the ion-exchange resins A532E and A530E. Adding salinity decreased the first-order rate constants for the adsorption of bisphenol A onto MN100 and MN200 resins. Fixed-bed column experiment results with estrogen hormones mixtures confirmed that the polymeric resins were good candidates in the removal of estrogen hormones. Trimegestone was the first compound detected in the effluent in the column test while 17β-estradiol, 17α-estradiol were the last. 80% of the exhausted resins (MN100 and MN200) by bisphenol A were regenerated by using pure methanol as regeneration solution. Polymeric resins were not effectively removing 1, 4-dioxane from the aqueous solution.

ACKNOWLEDGEMENTS

First of all I would like to express my sincere gratitude to my supervisor Dr. Rominder Suri. He provided me constant care on both mental and financial perspectives since the first day I joined his research group. He gave me many helpful suggestions, sage advice and constant encouragements during the pursuit of my Master's degree.

I would like to thank the members of my thesis committee: Dr. Rominder Suri, Dr. Tony Singh and Dr. Judy Zhang for their great source of wisdom and providing me with valuable insights.

I would like to thank Temple University for financial support during my time here. Special thanks to NSF Water and Environmental Technology center for the funding provided to complete my research work. I would like to appreciate the help from Purolite Inc. USA for the supply of materials to finish this project.

I would like to thank Dr. Tony Singh for his guidance during the entire term of my research work in the laboratory. I would also like to thank Dr. Muruganardham for the generous help on the revision of my thesis and the guidance to write scientific articles. Special thanks to Dr. Weiyue Qu for teaching me analytical techniques and for the help on the analytical support for my experiments. I would like to thank Dr. Katie Fenlon for the help on GC/MS/MS analysis as well.

Also, I would like to thank my colleagues: Dr. Gangadhar Andaluri, Bikash Bhattarai, Sagar Vattikonda, Marianne C Curran, Candice M Johnson, Rupam Rani, Tugba Akgun, Thida Chan for their considerate support in the lab.

Finally I would like to thank my family, my wife and my friends for their love and support during the past few years.

DEDICATION

This Thesis is dedicated to

My Parents Mr. Xiaoming Liu and Mrs. Cuiyun Ren

For teaching me to prepare and face the

Joy and challenges in my life

They are my constant source of inspiration and courage

My loving Wife, Mrs. Huihui Xu

For her unconditional love and mental support

She made my tough life sweet

TABLE OF CONTENTS

LIST OF FIGURES

LIST OF TABLES

CHAPTER 1

INTRODUCTION

The world population has grown faster than ever before in the past decades. Population growth is straining limited natural resources and raising more environmental issues such as water pollution and water shortage. For example, more than half of the 667 major cities in China were facing water shortage [He et al., 2001]. 27% of China's surface water quality was much lower than the lowest class of national water standard, which was usable only for agricultural irrigation [FAO, 1999]. Across America, the picture is even critically clear — the nation's freshwater supplies can no longer quench its thirst. For example, an epic drought in Georgia threatens the water supply for millions; Florida doesn't have nearly enough water for its expected population boom; The Great Lakes are shrinking; Upstate New York's reservoirs have dropped to record lows; And in the West, the Sierra Nevada snowpack is melting faster each year, etc. [MSNBC, 2007]. Asian countries and U.S.A. are not the only nations suffering this crisis. The clean water shortage problem is spreading worldwide.

In addition, the development of resources and technologies such as development of new pharmaceuticals and materials has generated huge amount of new chemicals and compounds. Some of the compounds are known as emerging contaminants which might consequently increase the potential threat to the environment and the humans. The existing water and wastewater treatment plants have been designed for the best in treatment and removal of traditional contaminants such as BOD, COD, germs and pathogens, especially those which are specified in the existing regulations. However, these treatment technologies cannot efficiently remove emerging contaminants from wastewater.

1.1 Emerging Contaminants

Emerging contaminants (ECs) (also known as microconstituents, micropollutants, contaminants of emerging concern or trace contaminants) generally refers to chemicals, biological agents and materials recently detected in the environment that may pose a potential or real threat to human health or the environment, but which are not generally regulated at present or are expected to undergo changes in regulations.

In earlier 90s, there have been growing concerns about potential adverse effects of emerging contaminants present in the environment [National Research Council, 1999]. Endocrine disrupting compounds (EDC) are one category of the emerging contaminants that can mimic the function of hormones in mammal's endocrine system and disrupt the physiologic function of endogenous hormones. One of the most potent of all the EDCs are hormones classified as natural and synthetic estrogens. Some of the natural and synthetic estrogens are considered as endocrine disruptors even at ng/L level in wastewater [Routledge et al., 1998]. For example, certain estrogenic compounds such as 17β-estradiol and 17α-ethinylestradiol (with the concentration of ng/L) can cause endocrine disrupting effects in fish species such as trouts, minnows and estuarine flounders [Staples et al., 1998, Kim et al., 2007, Zhang et al., 2006]. These chemicals are either produced naturally in mammal's body, or are synthetically created for use in birth control pills and hormone replacement therapy [Yoon et al., 2010, Kim et al., 2007].

Typical ECs include: endocrine disrupting compounds (EDCs), pharmaceuticals and personal care products (PPCPs), persistent organic pollutants (POPs), nanomaterials, etc. The representative structures of estrogen hormones are shown in Figure 1.1:

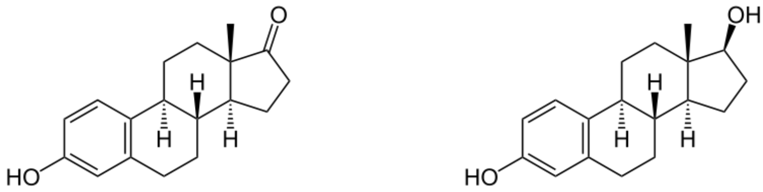

Figure 1.1 Structure of estrone (left) and 17β-estradiol (right)

Natural estrogens such as 17β-estradiol and estrone along with synthetic estrogen such as 17α-ethynylestradiol are excreted into environment by human and mammals mainly through their urine [Hashimoto et al., 2009]. These estrogen hormones are eventually detected in municipal wastewater treatment plant (WWTP) or receiving water [Auriol et al., 2006 and 2007]. Some of the most important pathways in which estrogen hormones enter the environment are:

- Effluent from municipal, sewage and wastewater treatment plants;
- Industrial effluents;
- Runoff from animal waste storage and from confined animal feeding operations;
- Agricultural applications of animal wastes.

Estrogens could get adsorbed onto the surrounding soil from the water bodies and eventually leach back into the water bodies, making it even difficult to remove [Hashimoto et al., 2009].

Perfluorinated compounds (PFCs) are used as surface protectors of textile, carpet, paper repelling water and oil and they are released to the environment primarily during the manufacturing and coating process [Mclachlan et al., 2007]. Concerns are raised since these synthetic fluorinated organic compounds are now found almost everywhere in the environment. Perfluorooctane sulfonate (PFOS) and perfluorooctanonic acid (PFOA) are two common representatives of the perfluorinated compounds (PFCs) which have received a great deal of attention, the structure of PFOS and PFOA are displayed in Figure 1.2:

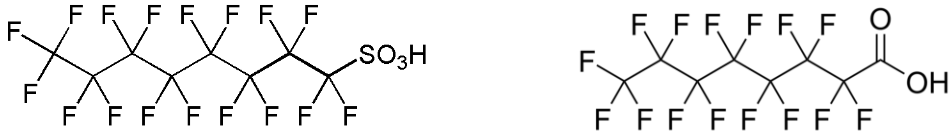

Figure 1.2 Structure of perfluorooctane sulfonate acid (PFOS) (left) and perfluorooctanoate acid (PFOA) (right)

PFCs can be found everywhere in the ecosystem all around the world. Michael et al. (2007) reported that PFOS concentration was found to be 200 ng/L in surface water. Researchers studied the sediments in water and wastewater treatment plants (WWTPs). Results showed that the concentration was ranging from 0.1-0.9 ng/g and 2.6-30.7 ng/g for PFOA and PFOS, respectively [Ma et al., 2010]. Giesy et al., (2001) studied on the concentration of PFCs in body parts of different wildlife. PFOS was also detected in the tissues of wildlife, including, fish, birds, and marine mammals. And relative high concentrations were also found in all the plasma samples of the wildlife. Jin et al., (2007) studied on historical trends in human serum levels of PFCs in China, it was reported for the total male and female subjects, the median level of serum PFOA increased significantly from 0.08 μg/L in 1987 to 4.3 μg/L in 2002; while for PFOS, increased from 0.03 μg/L in 1987 to 22.4 μg/L in 2002.

Large amount of bisphenol A (BPA) is produced worldwide. Most of it is being used as a monomer for the production of polycarbonate and epoxy resins [Staples et al., 1998]. The release of BPA into the environment is believed to be during manufacturing processes and by leaching from final products. Earlier study shows that the release of BPA into streams and rivers was mainly due to the discharges of sewage treatment plants (STPs), which have led to elevated levels both in surface waters and in sediments [Bolz et al., 2001]. The chemical structure of BPA is shown in Figure 1.3:

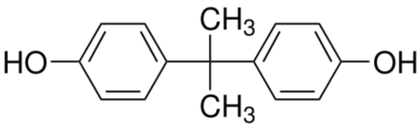

Figure 1.3 Structure of BPA

The exposure of BPA to humans is not limited to the aquatic and soil environments [Fromme et al., 2002]. Fu et al., (2010) also detected BPA in ambient aerosol samples from urban, rural, marine and even polar regions which indicated that BPA is a ubiquitous component in the atmosphere. Food, drinking water, dental sealants, cell phones, and inhalation of indoor dusts could also increase the exposure of BPA to humans. Studies have reported that BPA could also be found in human serum, urine, amniotic fluid, placental fluid and umbilical cord blood [Vandenberg et al., 2007].

There are a lot of debates for BPA on the harmful effect towards aquatic creatures and human health. Takahashi et al., (2001) reported that within the range of 23–2300 μg/L, BPA could pose mutagenic and estrogenic effects on humans. In addition, Vandenberg et al., (2007) declared there was a risk to the entire population at current exposure levels. However, US Food and Drug administration gave a report one year after saying there was no risk at all [US Food and Drug Administration, 2008]. The overall analysis of controversies on BPA is contributed to how assessment factors have been determined and applied.

The cyclic ether 1, 4-dioxane is a synthetic industrial chemical which is used as a solvent for paints, lacquers and in processes such as organic chemical manufacturing. The symmetrical structure of 1, 4-dioxane is shown in Figure 1.4:

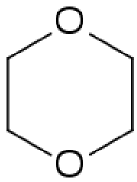

Figure 1.4 Structure of 1, 4-dioxane

1, 4-dioxane is completely miscible with water, hence, could migrate rapidly in groundwater. Once dissolved, the chemical's transport in groundwater is only weakly retarded by sorption to soil particles or suspended sediments because of its extremely low K_{ow} [Zenker et al., 2003]. The special properties of 1, 4-dioxane makes the in-situ treatment very difficult. several ex-situ treatments were developed to remediate the contaminated water and soil [Adams et al., 1994].

The occurrence of the ECs is everywhere especially in aquatic environment. The potential harmful effect of ECs towards aquatic creatures and human body is not negligible as discussed above. The rise of this issue requires an efficient removal technology to remove these compounds from the environment. The next section will focus on the typical wastewater treatment technologies, the advantages and shortcomings will be discussed.

1.2 Wastewater treatment technologies

Typical wastewater treatment technologies include: activated sludge system, chlorination, advanced oxidation processes, bioremediation and adsorption processes.

Activated sludge treatment is a predominant technology used in water and water and wastewater treatment plants (WWTPs). This process introduces air or oxygen into a mixture of activated sludge and wastewater. Living organisms in the activated sludge consume the oxygen and develop a biological floc which reduces the organic content of the sewage. However, the overall efficiency of WWTPs in removing the estrogen hormones was reported to be as low as 20% in the primary treatment [Kolpin et al., 2002]. The effluent residue concentrations of the estrogen hormones were still high enough to affect the aquatic creatures [Halling-Sorensen et al., 1998, Adams et al., 2002]. Other traditional treatment processes such as trickling filtration, anaerobic digestion have also been studied [Gabet-Giraud et al., 2010, Zhao et al., 2010]. The results showed that these processes were inefficient for the removal of PFCs. It was also found that microbial communities in the activated sludge could not digest PFCs [Sundstrom et al., 1979]. On the other hand, the PFCs concentration in the effluent of (WWTPs) sometimes found higher than the influent which indicated that microbial transformation process took place [Sinclair et al., 2006]. Numerous reports have indicated that activated sludge system as well as other traditional sewage treatment processes were found inefficient in removing BPA and 1,4-dioxane [Chang et al., 2009, Abe, 1999]

Chlorination is the process of adding chlorine to water as a water disinfection method to make it fit for human consumption as drinking water. Chlorine is effective in preventing the spread of waterborne diseases. Chlorine is a strong oxidant, once introduced into water sample, kills most of the bacteria and viruses. The disadvantage of such technique is the formations of other disinfection by-products while react with organic compounds [Chen et al., 2008]. Lee and Gunten (2009) studied the pathways of 17α-ethinylestradiol (EE2) transformation during chlorination of water with and without bromide (Br^-) to evaluate the effect of chlorination on the fate of EE2. They discovered that the transformation of EE2 during chlorination became considerably faster with the presence of Br^-. Yamamoto and Yasuhara (2002) investigated the chlorination of BPA in aqueous solutions. BPA was consumed completely within 5 min and five chlorinated BPA congeners were observed, but no toxicity studies have been made.

Advanced oxidation processes (AOPs) combine ozone (O_3), ultraviolet (UV), hydrogen peroxide (H_2O_2) and/or catalyst to offer a powerful water treatment solutions for the reduction (removal) of residual organic compounds. Study showed that AOPs did not show a promising removal on perfluorinated compounds [Buxton et al.,1988]. High removal efficiency was observed on the destruction of estrogen hormones by using AOPs such as ozonation and photolysis reactions [Nakagawa et al., 2002, Liu et al., 2004]. However, the formations of by-products after these processes are unknown and may have estrogenic activities higher than their precursors [Andersen et al., 2003]. Ohko et al. (2001) investigated the photocatalytic degradation of BPA in water. They observed a fully mineralization of BPA and its intermediate products by UV irradiation after 20 h. Kaneco et al. (2004) also found that BPA could be completely mineralized in the TiO_2-catalyzed process under the UV-illumination of 11 h. Several studies examined O_3/H_2O_2 processes for the removal of 1, 4-dioxane in aqueous solutions [Adams et al., 1994, Bowman et al., 2001], the reported removal efficiencies on 1, 4-dioxane by using strong oxidation methods were approaching 100 %. These technologies all require a huge amount of capital cost on the instruments and facilities, and the formation of unknown by-products is very hard to avoid.

Biodegradation is another powerful tool for the removal of ECs. Takahashi et al. (2005) studied the removal of BPA in water medium by using Rumex crispus, and observed that BPA was completely removed after 15 days. Moreover, the use of plants such as Ipomoea Aquatica to remove BPA indicated a partial metabolization of BPA. Possibly, over 50% of the initial BPA content was polymerized or tightly bounded to the plant residues [Noureddin et al., 2004]. Chai et al. (2005) studied the removal of BPA by 26 fungi strains, and found 11 strains could biodegrade BPA at >50%. Because biodegradation of contaminated soil and water needs suitable conditions for the plants or strains to grow, these conditions are very hard to be met in the practical treatment of wastewater and contaminated soil and the time required is relative long. As a result, these technologies are very hard to be applied in large scale.

Adsorption technologies are also predominant treatment methods among water and wastewater treatment processes nowadays. Adsorption processes include physical adsorption [Li et al., 2008, Zhang et al., 2005] and ion-exchange process [Zhang et al., 2005]. Adsorption is largely used in uptaking organic contaminants from aqueous solutions. Typical solid media used are silica, alumina and activated carbon. Activated carbon is an adsorbent that has been extensively used for water purification since it has the ability to effectively remove various inorganic and organic substances and is also cost effective [Saha et al., 2010]. Fukuhara et al. (2006) investigated the removal of estrone and 17β-estradiol by using eight commercially activated carbons. The amount adsorbed for estrone and 17β-estradiol at equilibrium concentration was in the range of 25.6–73.5 mg/g and 21.3–67.6 mg/g, respectively.

However, after the carbon reaches its adsorption capacity, it is very hard to regenerate for reuse [Fukuhara et al., 2006]. And thus, the treatment of exhausted carbons generates more solid wastes and additional cost. Ion-exchange process therefore is considered to be a better approach for the remediation of pollutants due to the advantage of easy regeneration.

1.3 Ion-exchange technology

Ion-exchange is a reversible chemical reaction wherein ions from solution are exchanged for similarly charged ions attached to an immobile solid particle [Desilva et al., 1994]. These solid ion-exchangers are either naturally occurring inorganic zeolites or synthetically produced organic resins. More synthetic resins are generated nowadays because the characteristics of those resins can be designed for specific applications.

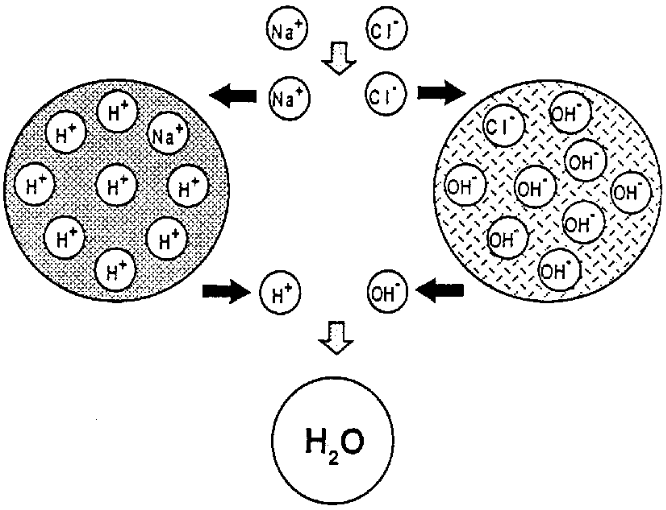

Figure 1.5 Schematic illustration of ion exchange process

Ion-exchange technology can be explained by Figure 1.5. When ions such as Na^+ and Cl^- come into contact with the ion-exchanger, they are exchanged with the similar charged ions (H^+ and OH^-) attached on the ion-exchanger, Na^+ and Cl^- ions are adsorbed onto the immobile solid phase while H+ and OH- are released into the solution and form H_2O.

Comparing ion-exchange technology with other water and wastewater treatment processes, ion-exchange technology has the advantage that it can treat a large volume.

[Gouthro et al., 1999, Desilva et al., 1994]. Ion-exchange technology has been applied to pharmaceutical purification, water softening processes, separation and purification in the food industry, catalyst and manufacture of ultra-pure water used in semiconductor processes, etc. [Bolto et al., 2002].

This technology is well established for the removal of heavy metal ions as well as organic contaminants. Studies were also reported using ion-exchange resins to remove nature organic matters (NOMs) in aqueous solution [Zhang et al., 2006, Bolto et al., 2002]. For example, ion-exchange technology is successfully applied to remove nickel ions. In order to separate nickel ion, cationic ion-exchange resins packed in the column was used, these resins can selectively exchange the nickel ion with hydrogen ion in wastewater. While the contaminated solution flows into the column, the resin separates nickel ion from the solution successfully [Levy et al., 1987]. After the resins reached their maximum adsorption capacity, the resin could be regenerated by acid in-situ [Plokhov et al., 2006]. The exhausted resin was easily regenerated using a concentrated solution of sodium chloride. Several research projects were developed on the denitrification of drinking water by anionic ion exchangers [Hongve et al., 1999]. Valderrama et al. (2007) studied the removal of polyaromatic hydrocarbons by using ion-exchange resins and activated carbon, they observed that the removal efficiency of polymeric ion exchange resins was lower than activated carbon, they indicated that the process is physical adsorption due to the large surface are of the adsorbents. Most of the organic compounds are neutral molecules in nature, so ion-exchange process is hardly observed.

There are indeed several factors that influence ion-exchange performance, such as solution pH [Lin et al., 2005], resin type and dosage [Bolto et al., 2002, Humbert et al., 2005], ionic strength [Hongve et al., 1999] and molecular weight of the adsorbates

[Fearing et al., 2004]. but the advantages seem to be obvious on the removal of pollutants:

- Generation of zero toxic substance, by-products free;
- High removal efficiency, normally more than 90%;
- Mature unit process in industry, easy application;
- Regeneration feature makes the technology financially preferable.

1.4 Emerging contaminants removal by ion-exchange technology

Limited research has been conducted on the application of ion-exchange technology in removal of emerging contaminants. Gu et al. (2003) studied on the perchlorate removal in wastewater by using ion-exchange resins, the removal efficiency was as high as 100%, and a novel regeneration technique for exhausted resins was developed and yielded 100% recovery. Bayburtskiy et al. (2007) studied the removal of surfactants by using different ion-exchange resins and found out that ion-exchange capacity depend strongly on the adsorbent nature. Neale et al. (2010) studied the usage of magnetic ion-exchange resins on the removal of estrone, it was observed at high pH (pH>10.4), 70 % of the estrone was removed by the resin while under the neutral condition, only 30 % was removed. Estrone has a pK_a of 10.4, which means estrone will ionize under pH of 10.4 and higher. The ion-exchange technology will be theoretically applicable for the removal of estrogen hormones with pK_a values. Saha et al. (2010) indicated that the hyper-cross-linked polymeric ion-exchange resins could be a good candidate to remove 17α-ethinylestradiol and 17β-estradiol, they also suggested that the adsorption mechanism could be a combination of ion-exchange and physical adsorption processes.

CHAPTER 2

PROJECT OBJECTIVES

The project objectives of this study include:

1. Batch investigation on the adsorption of four categories of ECs (estrogen hormones, perfluorinated compounds, bisphenol A and 1, 4-dioxane) onto various types of polymeric resins (MN100, MN200, A530E, A532E and C115).

(a) Determining the effect of different processing conditions for each category of contaminants including but not limited to: the initial concentration, resin dosage, contact time, pH and ionic strength;

(b) Application of different isotherm and kinetics models to the experimental data, and find out the relationship between the chemical structure and the adsorption behaviors;

(c) Proposing the possible mechanism for the adsorption.

2. Fixed-bed column study on the adsorption of mixture of hormones.

Investigate the breakthrough points on the adsorption of ECs mixture onto resins.

3. Making recommendations for future work.

CHAPTER 3

MATERIALS AND METHODS

3.1 Chemicals

The selected properties of the ECs used in this work are summarized in Table 3.1. All of them are purchased from Sigma-Aldrich Co.

3-o-methyl estrone was used as the internal standard for estrogen hormones analysis. Perfluorooctanoic acid-13C8 was used as the internal standard for PFCs analysis. Bisphenol-A-Ring-D8 and 1, 4-dioxane-D8 were used as the internal standards for BPA and 1, 4-dioxane analysis, respectively.

HPLC grade solvents such as methanol and toluene were obtained from Fisher Scientific. Millipore nitrocellulose filter papers (8 μm, 0.8 μm, and 0.45 μm) and amber glass bottles were also obtained from Fisher Scientific. Varian Bond Elute 3 mL/500 mg solid-phase extraction (SPE) cartridges were obtained from Varian Inc. WATERS oasis C18 HLB SPE columns were purchased from WATERS Cooperation, USA.

3.2 Ion-exchange resins and pretreatment

Five polymeric resins used in this study were provided by Purolite Inc, USA. MN100 and MN200 resins are macroporous special sorbents which are specially designed for the separation of hydrophobic organic species. MN100 resin is an anionic ion-exchange resin whereas MN200 resin is a non-functionalized polymer, both of them are hyper-cross-linked.

Table 3.1 Selected properties of emerging contaminants

Name	CAS number	Formula	Structure	Molecular Weight (g/mol)	Solubility (mg/L)	Log K_{ow}	pK_a
Estrogens							
17α-estradiol	57-91-0	$C_{18}H_{24}O_2$	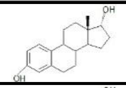	272.38	5.4–13.3[5]	4.01[5]	10.46 ± 0.03[3]
17β-estradiol	50-28-2	$C_{18}H_{24}O_2$	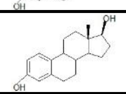	272.38	5.4–13.3[5]	4.01[5]	10.71[2]
17α-Dihydroequilin	651-55-8	$C_{18}H_{22}O_2$	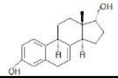	270.37	0.88[6]	4.34[6]	10.29 ± 0.02[3]
Equilin	474-86-2	$C_{18}H_{20}O_2$	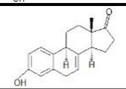	268.36	8.78[6]	4.22[6]	10.26 ± 0.04[3]
Estriol	50-27-1	$C_{18}H_{24}O_3$	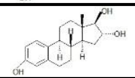	288.38	0.82[6]	2.77[6]	10.46[2]
Estrone	53-16-7	$C_{18}H_{22}O_2$	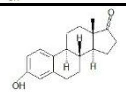	270.37	0.8–12.4[5]	3.13[5]	10.77[1]
17α-Ethinylestradiol	77538-56-8	$C_{20}H_{24}O_2$	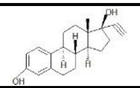	296.38	4.8–19.1[5]	3.67[5]	10.40 ± 0.01[3]
Gestodene	60282-87-3	$C_{21}H_{26}O_2$	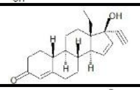	310.43	0.86[6]	4.43[6]	N/A
Medrogestone	977-79-7	$C_{23}H_{32}O_2$	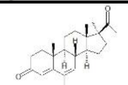	340.50	0.86[6]	5.03[6]	N/A
Norgestrel	6533-00-2	$C_{21}H_{28}O_2$	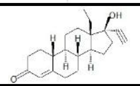	312.45	0.86[6]	4.27[6]	N/A
Progesterone	57-83-0	$C_{21}H_{30}O_2$	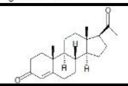	314.45	9.17[6]	4.18[6]	N/A

Trimegestone	74513-62-5	$C_{22}H_{30}O_3$	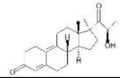	342.47	9.76[6]	4.25[6]	N/A
Perfluorinated compounds							
Perfluorotridecanoic acid	72629-94-8	$F_3C(CF_2)_{11}COOH$		664.11	N/A	N/A	<0[6]
Tricosafluorododecanoic acid	307-55-1	$F_3C(CF_2)_{10}COOH$		614.10	N/A	N/A	<0[6]
Perfluoroundecanoic acid	2058-94-8	$F_3C(CF_2)_9COOH$		564.09	N/A	N/A	<0[6]
Perfluorodecanoic acid	335-76-2	$F_3C(CF_2)_8COOH$	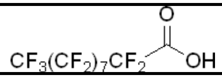	514.08	N/A	N/A	<0[6]
Perfluorooctanoic acid	335-67-1	$F_3C(CF_2)_6COOH$		414.07	N/A	N/A	<0[6]
Tridecafluorononanoic acid	27854-30-4	$F_3C\ (CF_2)_5(CH)_2$ COOH	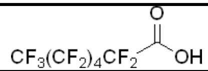	392.11	N/A	N/A	<0[6]
Perfluoroheptanoic acid	375-85-9	$F_3C(CF_2)_5COOH$	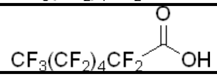	364.06	N/A	N/A	<0[6]
Undecafluorohexanoic acid	307-24-4	$F_3C(CF_2)_4COOH$	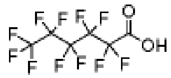	314.05	N/A	N/A	<0[6]
Heptadecafluorooctanesulfonic acid potassium salt	2795-39-3	$F_3C(CF_2)_7SO_3K$		538.22	N/A	N/A	<0[6]
Tridecafluorohexane-1-sulfonic acid potassium salt	3871-99-6	$F_3C(CF_2)_5SO_3K$	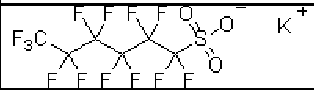	438.20	N/A	N/A	<0[6]
Bisphenol A	80-05-7	$C_{15}H_{16}O_2$	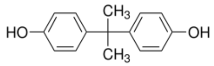	228.29	1.2[7]	3.2[7]	9.6[4]
1,4-dioxane	123-91-1	$C_4H_8O_2$	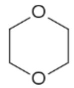	88.11	miscible	<0[6]	N/A

[1]Lewis et al., 1979

[2]Eger el al., 1972

[3]Hurwitz et al., 1977

[4]Zhang, et al., 2006

[5]Song, et al., 2009

[6]Data estimated by SPARC online

[7]Yoon, et al., 2003

Table 3.2 Physico-chemical properties of the polymeric resins

Resin	MN100	MN200	A530E	A532E	C115
Matrix	Polystyrene	Polystyrene	Polystyrene	Polystyrene	Porous polymethacrylic
Functional group	Tertiary Amine	None	Quaternary Ammonium	Bifunctional Quaternary amines	Carboxylic Acid
Physical form	Spherical beads	Spherical beads	Spherical beads	Spherical beads	Spherical beads
Total capacity(equiv./L)	0.1-0.3	n/a	0.6	0.75	3.5
Mean Diameter (μm)	535 ± 85	535 ± 85	725 ± 125	n/a	725 ± 125
Specific Gravity	1.09	1.04	1.4	n/a	1.1
Moisture Retention	57-61 %	57-61 %	50 - 57 %	36 - 45 %	46-53 %
Bet surface area (m^2/g)	857 ± 3 [1]	1116 ± 3 [1]	N/A	N/A	N/A
Point of zero charge	6.7 [1]	4.4 [1]	N/A	N/A	N/A

[1]Streat, M. and L. A. Sweetland (1997).

A532E and A530E resins are typical anionic resins with functional groups of tributyl amine (triethyl amine) and quaternary ammonium, respectively. C115 is a cationic ion-exchange resin with function group of carboxylic acid. The physical properties and specifications of resins used in this work are given in Table 3.2. Prior to use, the resins were washed with Milli-Q water to remove the adhering dirt and then dried at 333 K for 4 hours.

3.3 Experimental setup and methodology

3.3.1 Batch experiments

Batch experiments were conducted on a thermostatic mechanical shaker. 1 L (or 500 ml) amber bottles were used to hold model solutions. The batch experimental setup could be found in Appendix A.

Model solutions with each category of ECs were prepared by diluting the stock solution. Generally, after the preparation of the model solution, initial concentrations were tested immediately before the batch experiments. Various amounts of resins were released into the ambler bottles containing ECs model solutions. The samples were then moved to a thermostatic mechanical shaker with constant shaking (175 rpm) for a certain period of time.

The amount of ECs adsorbed by the ion-exchange resins was calculated by the following Equation 3.1:

$$q_e = \frac{C_0 - C_e}{M / V} \qquad \text{Equation 3.1}$$

Where q_e (μg/g) is the adsorption capacity of ion-exchange resins, C_0 and C_e (μg/L) are the initial and equilibrium concentrations in the model solution, respectively. V (L) is the volume of the model solution and M (g) is the mass of ion-exchange resins.

3.3.2 Fixed-bed Column experiments

Column used in this work were purchase from ACE Glass Inc., and is made of transparent glass with caps on both side. The diameter of the column is 1.1 cm. The pump was purchased from FMI metering Inc. Tubings, valves, pressure relief valves and check valves with stainless steel piping was purchased from Swagelok Inc. Ltd. The column experimental setup is shown in Appendix B. Model solutions of ECs with individual concentration of 100 μg/L were prepared in the carboys, and then pumped in the column continuously. Model solutions were replaced periodically and the changes of initial concentrations were noted. Samples were taken at the sample ports at different time until breakthrough was observed. Flow rate was checked randomly to ensure the constant experimental conditions.

3.4 Analytical methods

3.4.1 Analysis of estrogen hormones

The estrogen hormones samples were direct injected into UPLC/ESI/MS/MS for analysis unless the concentrations were below the detection limits of instrument (Appendix S for instrument detection limits data). Those samples with low concentrations were concentrated by using solid phase extraction before analysis on UPLC/ESI/MS/MS. Briefly, about 400 ml of water sample was passed through the Bond Elute C-18 SPE column at a flow rate of 5 ml/min. Before loading, the SPE cartridges were activated with 6 ml of methanol and then rinsed with 6 ml of Milli-Q water. After the sample was passed through the SPE column, the column was rinsed with Milli-Q water and then eluted with 6 ml of methanol. The methanol eluent was collected in a silanized test tube and fixed amount of the internal standard (3-o-methyl estrone) was added. Eluent was completely dried in a genevac centrifugal evaporator under the conditions of 317 K and 12 mbar. To the dried sample, 1.5 ml of methanol, 1.5 ml of water was added and vortexed. 2 ml of sample was then collected in a silanized LC vial and analyzed on UPLC/ESI/MS/MS.

3.4.2 Analysis of PFCs

The PFCs samples were direct injected into UPLC/ESI/MS/MS for analysis unless the concentrations were below the detection limits of instrument (Appendix S for instrument detection limits data). Those samples with low concentrations were concentrated by using solid phase extraction before analysis on UPLC/ESI/MS/MS. Briefly, 200 ml of water sample was passed through the WATERS Oasis C18 HLB SPE column at a flow rate of 5 ml/min. Before loading, the SPE cartridges were activated with 5 ml of methanol and then rinsed with 5 ml of Milli-Q water. After the sample was passed through the SPE column, the column was rinsed with 2 ml of Milli-Q water and then eluted with 6 ml of methanol. The methanol eluent was collected in a test tube and fixed amount of the internal standard (perfluorooctanoic acid-13C8) was added. Eluent was completely dried in a genevac centrifugal evaporator under the conditions of 318 K and 12 mbar. To the dried sample, 1.5 ml of methanol, 1.5 ml of water was added and vortexed. 2 ml of sample was then collected in a LC vial and analyzed on UPLC/ESI/MS/MS.

3.4.3 Analysis of BPA

BPA was analyzed on UPLC/ESI/MS/MS. Briefly, 10 ml of water sample was collected in an EPA vial, and fixed amount of the internal standard (bisphenol-A-Ring-D8) was spiked into the solution. After violate vortex, 2 ml of sample was then collected in a LC vial and analyzed on UPLC/ESI/MS/MS.

3.4.4. Analysis of 1-4-Dioxane

Liquid-liquid extraction was used to analyze 1, 4-dioxane. Briefly, 10 ml of water sample was placed in an EPA-vial and spiked with fixed amount of the internal standard (1, 4-dioxane-D8). 2 g of anhydrous sodium sulfate and 20 ml of methylene chloride were added and violate vortexed. After aqueous phase was discarded, 10 ml of water sample was added again to the organic phase. Mixture was vortexed and aqueous phase was again discarded. Small amount of sodium sulfate was added to remove the moisture content. Then the processed 1, 4-dioxane sample was analyzed on GC/MS/MS.

3.5. Analytical Instruments

3.5.1. Gas Chromatograph/Mass Spectrometry/Mass Spectrometry (GC/MS/MS) Analysis

Separation and detection of 1, 4-dioxane was performed by using a Waters Quattro micro GC™ of tandem quadrupole mass spectrometer. The gas chromatograph was coupled to a SPB^{TM}-624 capillary column (30mx0.25mmx1.4um film). The auto injections were made in splitless mode and 1 μL of injection volume was used. Helium was used as a carrier gas with flow rate of 1 ml/min. Injection temperature was 523 K and the head pressure was 60 kPa of Helium. The initial oven temperature was 308 K for 1 min and then ramped to 363 K at 7 K/min. Finally, the oven temperature was ramped to 473 K at 30 K/ min and held for 5 min. MS parameters: temperature of transfer line, 523 K; EI mode; electron energy, 70 eV; ion source temperature, 523 K.

3.5.2. Ultra Performance Liquid Chromatography/ Electro spray Ionization/ Mass Spectrometry/ Mass Spectrometry (UPLC/ESI/MS/MS) Analysis

Estrogen hormones, PFCs and BPA were analyized by using UPLC/ESI/MS/MS consisting of an UPLC (Waters Acquity UPLC™ system) coupled with a Waters Xevo™ mass spectrometer with a Z-Spray™ ESI source. The column used was Acquity UPLC®, BEH C18 column (1.7 µm particle size, 1.0×50mm, Waters, UK). LC was operated under the following conditions. A gradient mobile phase was used with methanol and water. Mobile phase flow rate was 0.6 ml/min. The injection volume of the sample was 10 µL. Gradient conditions were initiated with 30 % methanol and held for 30 seconds, followed by an increase to 100 % (5 min) and then held for 0.5 min. The proportion of water was then increased to 70 % and held for 0.5 min. The total run time for all samples was less than 6 min. The mass spectrometer was operated in the negative and positive electrospray ionization mode using multiple reaction monitoring (MRM) for different compounds. Nitrogen gas was used as both desolvation and nebulizer gas. Argon was used as collision gas.

3.6 Models

3.6.1. Isotherm models

Langmuir and Freundlich isotherm models were used for this study. The Langmuir isotherm model is based on the assumption that single adsorbate is retained on a homogeneous surface and forms only one molecular layer. The Langmuir isotherm model can be expressed in Equation 3.2:

$$q_e = \frac{q_0 b C_e}{1 + bC_e} \qquad \text{Equation 3.2}$$

Where q_e (μg/g) is the adsorption capacity at equilibrium, C_e (μg/L) is the equilibrium concentration, and q_0 (μg/g) and b (L/μg) are the Langmuir constants related to the maximum adsorption capacity and the adsorption energy, respectively. q_0 represents the maximum adsorption capacity of adsorbent with monolayer coverage of adsorbate. b represents the enthalpy of adsorption. Equation 3.2 is the non-linear form of the Langmuir isotherm equation. Change the Equation 3.2 into its linear form:

$$\frac{1}{q_e} = \frac{1}{bq_0}\frac{1}{C_e} + \frac{1}{q_0} \qquad \text{Equation 3.3}$$

From Equation 3.3, Langmuir parameters can be evaluated by plotting $1/q_e$ against $1/C_e$ and find the slope and the intercept by linear regression.

The Freundlich isotherm was also applied. This theoretical isotherm is proposed for the description of physical adsorption on heterogeneous surfaces in the submonolayer range. The Freundlich isotherm can be expressed in Equation 3.4:

$$q_e = K_f C_e^{\frac{1}{n}} \qquad \text{Equation 3.4}$$

Where K_f (μg/g)(L/g)$^{1/n}$ is the Freundlich constant and 'n' is the Freundlich exponent, Where C_e (μg/L) is the equilibrium concentration, q_e (μg/g) is the adsorption capacity at equilibrium. K_f and 'n' are constants incorporating all factors affecting the adsorption process such as temperature and intensity. Take logarithm on both sides and change Equation 3.4 into a linear expression:

$$\ln q_e = \ln K_f + \frac{1}{n} \ln C_e \qquad \text{Equation 3.5}$$

From Equation 3.5, Freundlich constants can be evaluated by plotting ln q_e against ln C_e and find the slope and the intercept by linear regression.

3.6.2. Kinetics models

Pseudo-first-order kinetics reaction equation can describe the solute adsorption rate [Shubha et al., 2001, Basagaoglu et al., 2002], which is one of the most important characteristics defining the efficiency of adsorption. The original pseudo-first-order equation is described in Equation 3.6:

$$\frac{dq}{dt} = (q - q_e) * k_1 \qquad \text{Equation 3.6}$$

Where q (μg/g) is the loading capacity and q_e (μg/g) is the maximum loading capacity. (q-qe) represents the driving force of an adsorbate adsorbed onto solid surface. Integrate the Equation 3.6, we have:

$$\int \frac{dq}{q - q_e} = k_1 \int dt \qquad \text{Equation 3.7}$$

$$\ln(q - q_e) \Big|_{q_0}^{q_t} = k_1 t \qquad \text{Equation 3.8}$$

Substitute the following boundary limits into Equation 3.8,

t=0 q=0 (clean adsorbents)

t=t q=q_t (loading at time t)

$t=\infty$ $\quad q=q_e$ (equilibrium concentration on adsorbents)

We have:

$$\ln\frac{q_t - q_e}{-q_e} = \ln(\frac{q_e - q_t}{q_e}) = k_1 t \qquad \text{Equation 3.9}$$

Change Equation 3.9 into the final following form showing in Equation 3.10 which is used predominantly during the adsorption studies [Shubha et al., 2001, Pan et al., 2010]:

$$\ln(q_e - q_t) = k_1 t + \ln q_e \qquad \text{Equation 3.10}$$

Where q_e and q_t (μg/g) are the amounts of ECs adsorbed onto resins at equilibrium and at time t, respectively. k_1 is the rate constant arising from the pseudo-first-order reaction model.

Pseudo-second-order was also applied to investigate the adsorption rate of emerging contaminants [Shubha et al., 2001, Basagaoglu et al., 2002]. The original equation for pseudo-second-order is shown in Equation 3.11:

$$\frac{dq}{dt} = (q - q_e)^2 k_2 \qquad \text{Equation 3.11}$$

Follow the same manner to derive the pseudo-first-order, we have:

$$\int \frac{dq}{(q - q_e)^2} = k_2 \int dt \qquad \text{Equation 3.12}$$

$$\frac{1}{q - q_e}\Big|_{q_0}^{q_t} = -k_2 t \qquad \text{Equation 3.13}$$

$$\frac{1}{q_t - q_e} + \frac{1}{q_e} = -k_2 t \qquad \text{Equation 3.14}$$

Change Equation 3.14 into the final following form showing in Equation 3.15:

$$\frac{1}{q_t} = \frac{1}{q_e} + \frac{1}{q_e^2 t k_2} \qquad \text{Equation 3.15}$$

Where q_e and q_t (μg/g) are the amounts of ECs adsorbed onto resins at equilibrium and at time t, respectively. k_2 is the rate constant obtained from the pseudo-second-order reaction model.

CHAPTER 4

RESULTS AND DISCUSSION

4.1. Removal of estrogen hormones

4.1.1. Screening test using 17β-estradiol

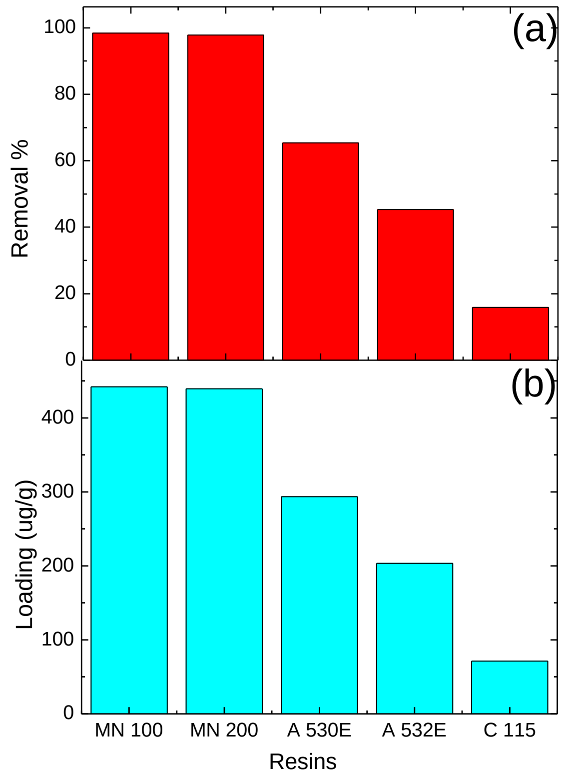

Figure 4.1 Screening test on the adsorption of 17β-estradiol onto various types of resins (initial concentration= 134.74 μg/L, pH= 7.0, contact time= 48 hours, sample volume= 1000 ml, temp= 295 K, resin dosage= 0.3 g/L)

Initially, experiments were conducted to test the efficiencies of various types of resins for the removal of 17β-estradiol. Results are given in Figure 4.1.

Figure 4.1(a) shows that the removal percentage of 17β-estradiol was 98 % for both MN100 and MN200 resins. The removal percentages (loadings) were 65 % (293 μg/g), 45 % (203 μg/g) and 16 % (71 μg/g) for A530E, A532E and C115 resins, respectively. Both MN100 and MN200 resins yielded higher removal efficiencies. MN100 resin has additional tertiary ammonium functional group (See Table 3.2) than

MN200 resin which might undergo ion-exchange reaction. However, under neutral pH, 17β-estradiol will not ionize due to its high pK_a value (10.32) (Table 3.1). Therefore, there is no ion-exchange type of reaction. So the adsorption capacities of MN100 and MN200 resins are similar, and the adsorption behavior might be due to physical adsorption. A530E and A532E resins are anionic resins and C115 resin is a cationic resin. This explains why the loading capacities of MN100 resin (442 μg/g) and MN200 resin (439 μg/g) were almost twice times higher than A530E resin (293 μg/g) and A532E resin (203 μg/g) as shown in Figure 4.1(b). Surface area of an adsorbent can be an important parameter influencing its capacity if physical adsorption is the case [Valderrama et al., 2007, Bolto et al., 2002, Humbert et al., 2005, Bayburtskiy et al., 2007]. Adsorbents with large surface area (800-1100 m^2/g, see Table 3.2) such as MN100 and MN200 resins can provide more active sites to interact with the 17β-estradiol molecules, and result in a higher adsorption capacity. MN100 and MN200 were selected to conduct further experiments on the removal of estrogen hormones mixture.

4.1.2. Effect of resin dosage and adsorption isotherm on the adsorption of estrogen hormones onto MN100 and MN200 resins

In wastewater treatment process, mixtures of substances, such as mixtures of pollutants, natural organic matters, and bacterial will be presented in water matrix [Staples et al., 1998]. In order to investigate the optimum amount of resin dosage on the removal of estrogen hormones mixture, various amounts of resins (range from 0.05 to 1.0 g/L) were spiked into 1 L of model solution containing 12 estrogen hormones mixture with constant mechanical shaking for 48 hours. Figure 4.2 shows the removal percentage of estrogen hormones as function of resin dosage. The removal percentage increased as the resin dosage increased, this is understandable because increasing resin amount can increase the effective surface area, and provide more active sites for the interaction with estrogen hormones. The result is in good agreement with earlier studies on the adsorption of heavy metal ions onto ion-exchange resins [Yoon et al., 2003, Kocaoba 2007, Yu et al., 2009] which also observed the increasing adsorption amount with increasing resin dosage.

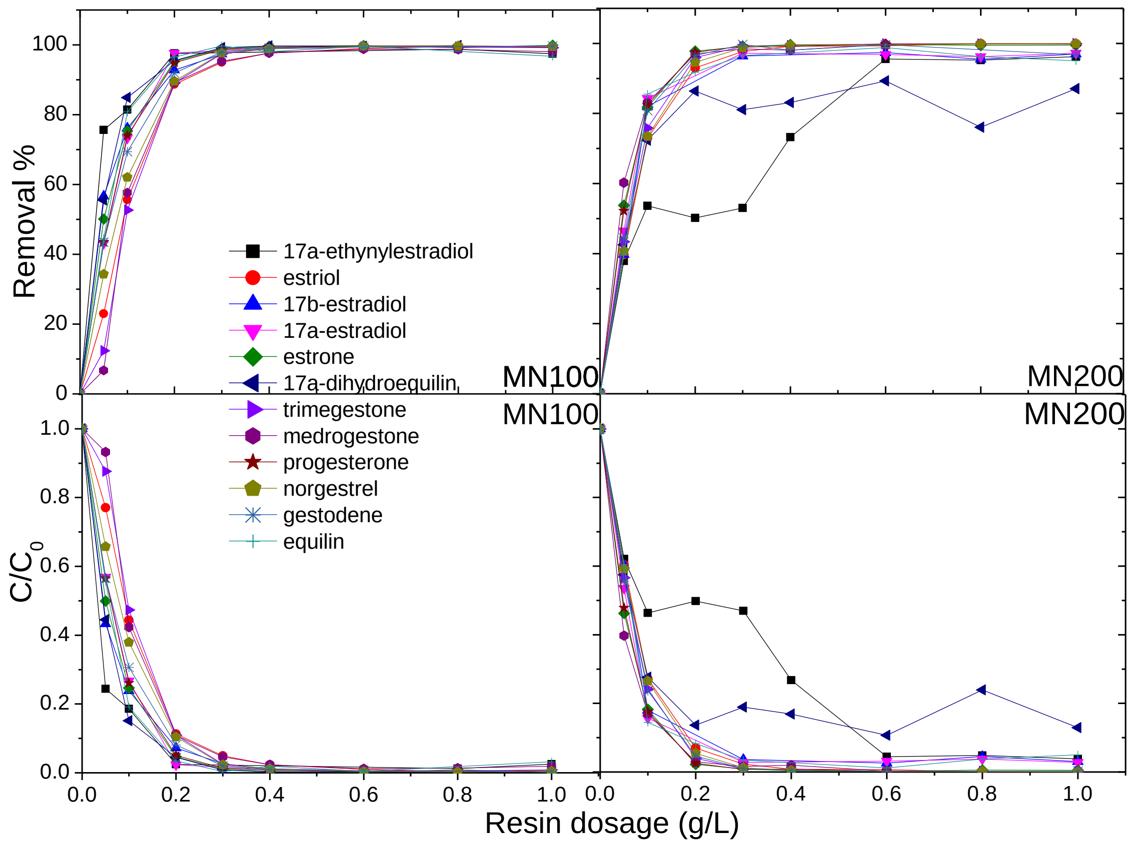

Figure 4.2 Effect of resin dosage on the adsorption of estrogen hormones mixture onto MN100 and MN200 resins (target initial concentration= 100 μg/L, pH= 7.0, contact time= 48 hours, sample volume= 1000 ml, temp= 295 K)

It may be noted from Figure 4.2 that at low resin dosage of 0.05 g/L, the adsorption efficiencies for 12 estrogen hormones onto MN100 resin are significant different. For example, 80 % 17α-ethinylestradiol was adsorbed onto MN100 resin while less than 5 % medrogestone was removed from the solution. Other 10 estrogens

(17α-estradiol, 17β-estradiol, 17α-dihydroequilin, estrone, estriol, equilin, gestodene, trimegestrone, norgestrel and progesterone) showed the removal percentage ranging from 22% to 56%. This result also indicate that at low resin dosage (0.05-0.2 g/L), MN100 resin tends to selectively remove estrogens due to the adsorption competition between estrogen molecules. The adsorption selectivity at low resin dosage was also noted for the adsorption of estrogens onto MN200 resin, but the trend was not as obvious as MN100 resin, as shown in Figure 4.2. Some estrogen hormones are favorable to be adsorbed onto the resin surface due to the higher hydrophobicity or the smaller molecular size than others. When the active sites in MN100 resin are less than MN200 resin (surface area of MN100 is less than MN200 resin as can be seen from Table 3.2), the molecules with favorable feathers will compete with other estrogen hormones to be adsorbed first onto the resin surface and thus, the adsorbents showed selectivity. Saha, et al. (2010) observed the adsorption of 17β-estradiol onto activated carbons was higher than 17α-ethinylestradiol because 17β-estradiol is more hydrophobic than 17α-ethinylestradiol, (solubility of 17α-ethinylestradiol is higher than 17β-estradiol as shown in Table 3.1). However, more additional experiments are needed to find out the main characteristics of the estrogens that affect the adsorption selectivity onto MN100 resin.

When the resin dosage of MN100 resin increased to 0.4 g/L and higher, all 12 estrogen hormones were 100 % adsorbed onto MN100 resin. As dosage of MN200 resin increased to 0.3 g/L, most of the estrogens were completely adsorbed onto the resin except for 17α-ethinylestradiol and 17α-dihydroequilin, as shown in Figure 4.2. This might be due to the structural properties of 17α-ethinylestradiol and 17α-dihydroequilin that lead to a special interaction with MN200 resin, or might just simply because of experimental error. The different behavior of these two estrogens needs additional investigation which will be addressed in our future research.

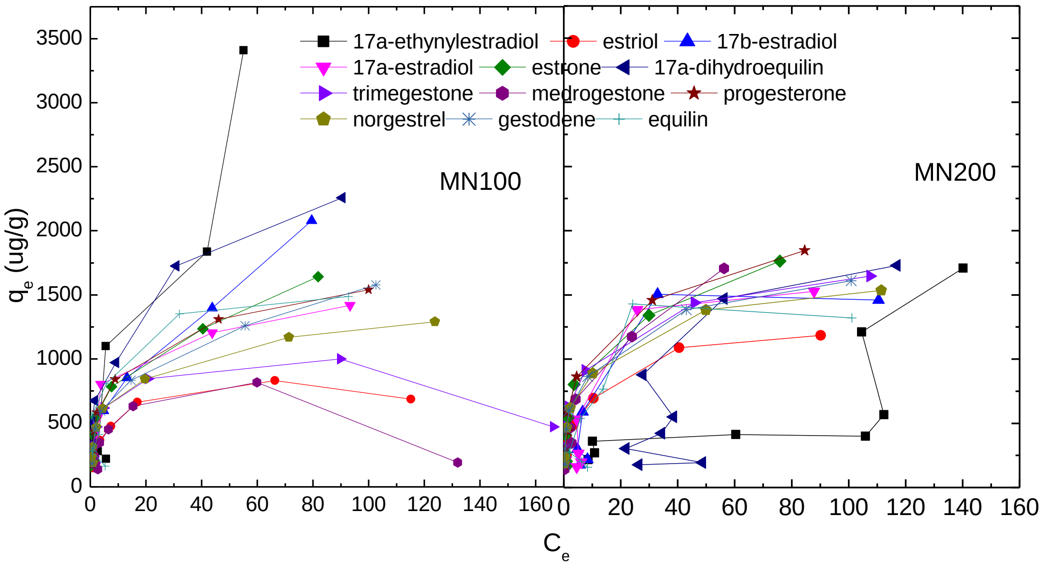

Figure 4.3 Isotherm plots on the adsorption of estrogen hormones onto MN100 and MN200 resins (target initial concentration= 100 μg/L, pH= 7.0, contact time= 48 hours, sample volume= 1000 ml, temp= 295 K)

Adsorption isotherms of 12 estrogens onto MN100 and MN200 resins are shown in Figure 4.3. It can be observed from the shapes of the isotherm plots that most of the estrogen hormones such as 17β-estradiol, 17α-estradiol and estrone are favorable to be adsorbed onto both MN100 and MN200 resins. In MN100 resin, medrogestone, estriol, trimegestone showed a significant lower adsorption affinity than the rest to the estrogen hormones. On the other hand, 17α-ethinylestradiol, 17α-dihydroequilin and 17β-estradiol did not reach their maximum capacities, as can be seen from Figure 4.3. The capacities of MN100 on the adsorption of most estrogens are distributed between 1000 μg/g to 1500 μg/g. In the case of MN200 resin, the adsorption capacities for most of the estrogen hormones were higher than 1500 μg/L and the maximum capacities were reached. The isotherm curves obtained for MN200 resin were not as disperse as for MN100 resin. In MN200 resin, 17α-ethinylestradiol and 17α-dihydroequilin showed an unexpected increasing trend as C_e increased, compared to the rest of the estrogens, this could be due to the experimental error as discussed earlier.

The Langmuir isotherm model is based on the assumption that a single adsorbate is retained on a homogeneous surface and forms only one molecular layer while the Freundlich isotherm, on the other hand, proposed for the description of a multilayer physical adsorption on heterogeneous surfaces. Both Langmuir and Freundlich models (Equation 3.3 and 3.5 in Chapter 3) are applied to fit the isotherm data.

As shown in Table 4.1, Freundlich isotherm model yielded reasonable correlation coefficient (R^2) values while Langmuir isotherm model failed to give a satisfactory fitting for most of the estrogen hormones. It was also noted that Freundlich model failed to give a satisfactory fitting on the adsorption of equilin and 17α-ethinylestradiol onto both resins, 17α-dihydroequilin onto MN200 resin and trimegestone onto MN100 resin (R^2 values for both resins were around 0.6 or less than 0.6, see Table 4.1). As can be seen from Figure 4.3, the adsorption behaviors of 17α-dihydroequilin and 17α-ethinylestradiol onto MN200 resin were unpredictable, and the adsorption of 17α-ethinylestradiol onto MN100 resin did not reach the maximum capacity, this might be a reason why the models failed to give a good fitting. In addition, during the adsorption of estrogens onto MN200 resin, the equilibrium concentrations of 17α-dihydroequilin at different dosage were not following the expected trend compared to the other estrogens, as shown in Figure 4.2. The reason why Freundlich model failed to give a satisfactory fitting for equilin might be due to the physical property of equilin. The solubility of equilin (Table 3.1) is 8.76 mg/L, which is relative higher than the rest of the estrogens. Higher solubility indicates a stronger water affinity, so equilin is harder to be adsorbed onto the resin surface than other estrogens. Additional experiments need to be conducted to confirm why isotherm models fail to give a reasonable fitting for the three estrogen hormones.

The adsorption capacities of estrogen hormones onto MN100 and MN200 resins were then compared with those of activated carbon, which has been used commonly for organic compound separation. The average adsorption capacity obtained for MN100 resin on the adsorption of 12 estrogen hormones was about 1250 μg/g, while for MN200 resin, it was about 1600 μg/g in this work. Saha et al. (2010) reported the maximum capacity was 428 μg/g for the adsorption of 17β-estradiol onto activated carbons which is lower than the capacity obtained in this work, possible reason might be that they used a very low initial concentration which was 4 μg/L compared to 100 μg/L in this work. The driving force at initial concentration of 100 μg/L is much stronger than at 4 μg/L, and thus yield higher adsorption amount. Kumar et al. (2009) studied the adsorption capacity of activated charcoal on the removal of estriol, the maximum capacity of activated charcoal on the adsorption of estriol was found even lower, which was 3.34μg/g. The lower adsorption capacity is not only due to the lower initial concentrations (5 μg/L), but also because of the surface area of activated charcoal (99.5 m^2/g) which is much lower than MN100 and MN200 resins (800-1100 m^2/g) in this work.

Table 4.1 Langmuir and Freundlich isotherm constants on the adsorption of estrogen hormones onto MN100 and MN200 resins

Estrogen Hormones	MN100						MN200					
	Langmuir constants			Freundlich constants			Langmuir constants			Freundlich constants		
	q_0(μg/g)	b(L/μg)	R^2	K_f(μg/g) (L/μg)$^{1/n}$	1/n	R^2	q_0(μg/g)	b(L/μg)	R^2	K_f(μg/g) (L/μg)$^{1/n}$	1/n	R^2
17α-Ethinylestradiol	2000	0.051	0.29	127.4	0.772	0.75	769	0.055	0.70	93.7	0.449	0.60
Estriol	556	0.643	0.74	214.8	0.309	0.88	556	4.500	0.81	323.1	0.3042	0.97
17β-Estradiol	1250	0.333	0.83	347.7	0.382	0.98	1667	0.032	0.53	95.8	0.6369	0.72
17α-Estradiol	1429	0.241	0.98	422.8	0.278	0.92	2500	0.022	0.54	90.3	0.6864	0.73
Estrone	667	1.667	0.61	349.1	0.348	0.86	714	1.000	0.37	336.0	0.4053	0.80
17α-Dihydroequilin	1429	0.636	0.85	463.4	0.364	0.94	1667	0.009	0.19	11.7	1.0283	0.40
Trimegestone	769	0.394	0.64	297.2	0.208	0.49	1000	1.250	0.87	416.4	0.3266	0.95
Medrogestone	400	0.490	0.29	151.8	0.454	0.79	769	1.182	0.87	308.3	0.4229	0.96
Progesterone	1111	0.391	0.72	308.2	0.382	0.89	909	1.833	0.93	425.1	0.3590	0.97
Norgestrel	833	0.600	0.73	295.0	0.349	0.87	909	1.375	0.90	386.9	0.3260	0.96
Gestodene	1429	0.241	0.98	295.9	0.376	0.94	1250	0.615	0.76	389.9	0.3358	0.90
Equilin	455	0.500	0.02	344.0	0.289	0.43	500	0.408	0.14	139.8	0.5223	0.54

4.1.3. Effect of contact time and adsorption kinetics on the adsorption of estrogen hormones onto MN100 and MN200 resins

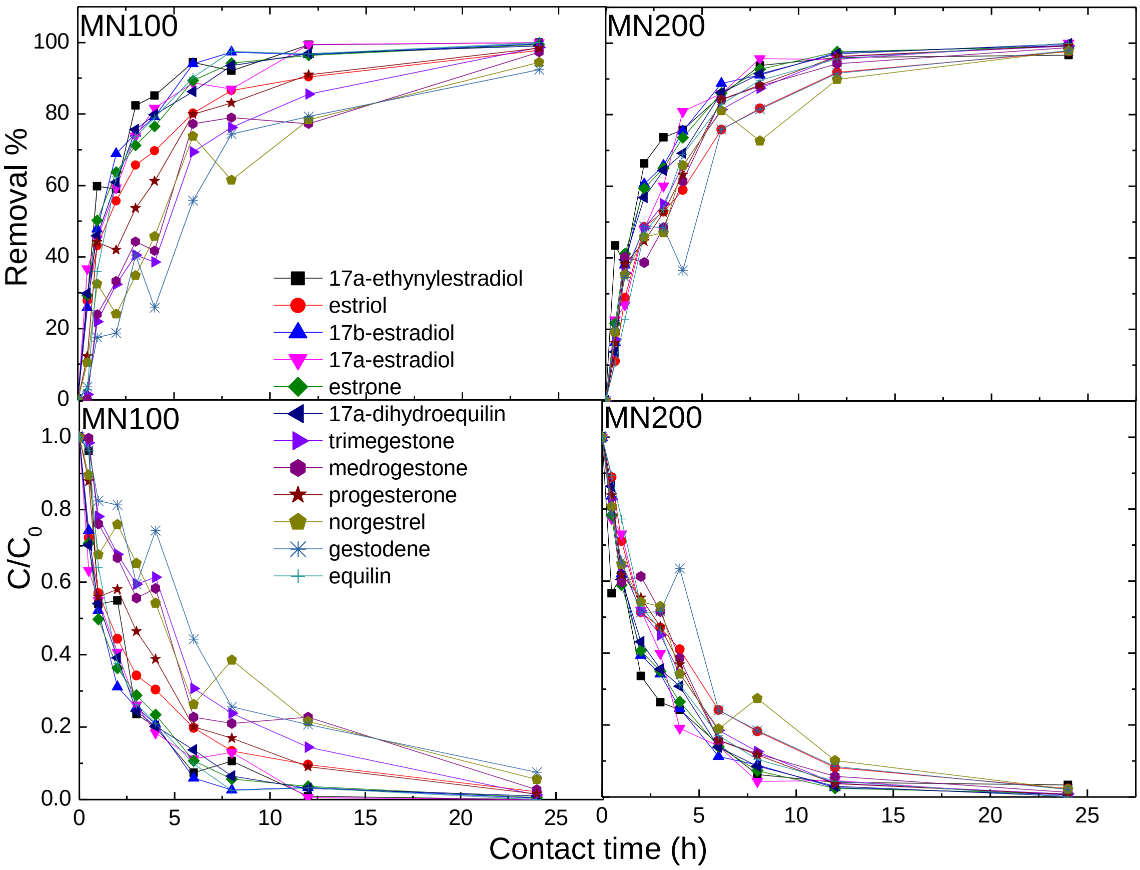

Figure 4.4 Effect of contact time and kinetics on the adsorption of estrogen hormones onto MN100 and MN200 resins (target initial concentration= 200 µg/L, resin dosage= 0.2 g/L, pH= 7.0, contact time= 48 hours, sample volume= 1000 ml, temp= 295 K)

The amount of time needed to reach the adsorption equilibrium is a critical parameter during the adsorption process. Figure 4.4 shows the removal efficiencies of both resins increased as a function of time until equilibrium was reached. MN200 resin reached the equilibrium faster than MN100 resin for all the estrogen hormones as seen in Figure 4.4. This result suggests that MN100 resin needed more time than MN200 resin to reach the equilibrium. MN200 resin with higher surface area can provide additional active sites for the interaction with estrogen molecules, and thus, shorten the time needed to reach the equilibrium. Since the adsorption of estrogen hormones onto the MN100 and MN200 resins is physical adsorption, the time needed for the resins to reach the equilibrium is not as quickly as uptaking metal ions using ion-exchange resin which normally reach the equilibrium with 4 hours [Pehlivan et al., 2006]

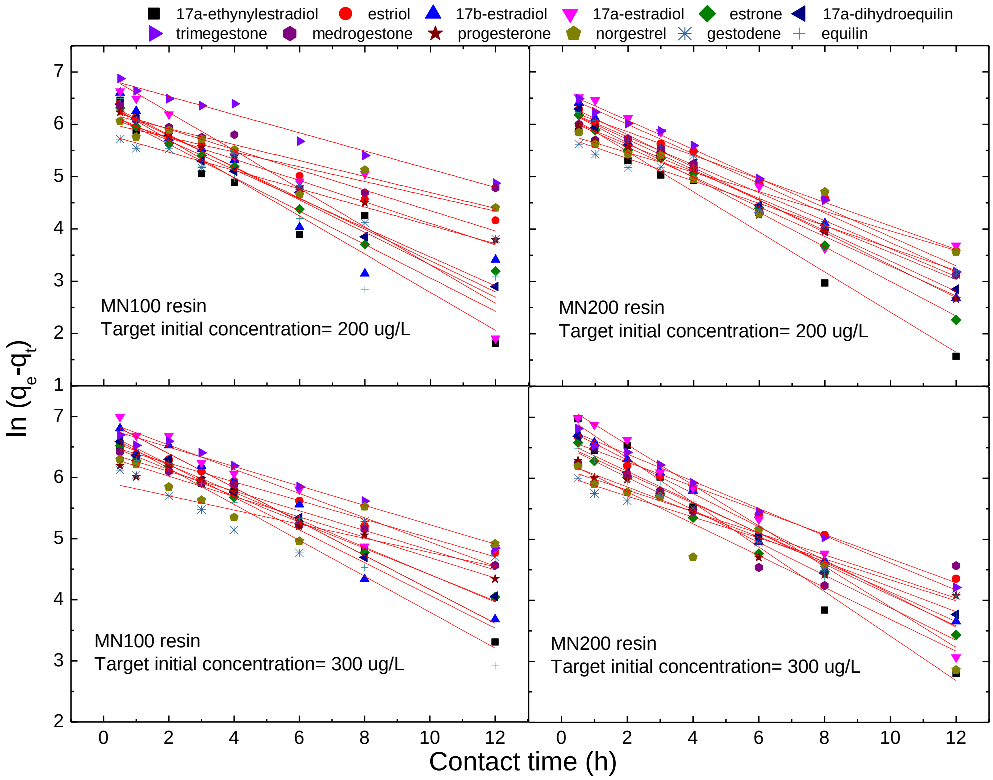

Figure 4.5 Linear plots of pseudo-first-order kinetics on the adsorption of estrogen hormones onto MN100 and MN200 resin with different target initial concentrations

Pseudo-first-order kinetic model (Equation 3.10 in Chapter 3) was used for the analysis of the adsorption process. q_e and k_1 are obtained by plotting $\ln(q_e - q_t)$ against t, and apply linear regression. Figure 4.5 shows pseudo-first-order plots on MN100 and MN200 resins with two target initial concentrations of estrogen hormones mixtures.

Table 4.2 Isotherm constants and correlation coefficients (R^2) on the adsorption of estrogen hormones onto MN100 and MN200 resins

Estrogen Hormones	MN100		MN200	
	200μg/L*	300μg/L*	200μg/L*	300μg/L*
	Pseudo-first-order rate constant k (h^{-1}) (R^2)			
17α-Ethinylestradiol	0.3641(0.9385)	0.2677(0.9800)	0.3825(0.9805)	0.3649(0.9826)
Estriol	0.1945(0.9681)	0.1531(0.9779)	0.2242(0.9920)	0.1977(0.9930)
17β-Estradiol	0.3105(0.8683)	0.2776(0.9604)	0.3105(0.9891)	0.2735(0.9907)
17α-Estradiol	0.3652(0.9024)	0.1984(0.9182)	0.2817(0.9055)	0.3326(0.9910)
Estrone	0.2775(0.9686)	0.2148(0.9953)	0.3297(0.9960)	0.2672(0.9887)
17α-Dihydroequilin	0.2987(0.9891)	0.2242(0.9903)	0.2898(0.9927)	0.2535(0.9791)
Trimegestone	0.1740(0.9719)	0.1586(0.9847)	0.2771(0.9925)	0.2229(0.9958)
Medrogestone	0.1525(0.8055)	0.1611(0.9715)	0.2576(0.9742)	0.1770(0.7750)
Progesterone	0.2047(0.9708)	0.1666(0.9625)	0.2835(0.9879)	0.2045(0.9432)
Norgestrel	0.1410(0.8456)	0.1101(0.6928)	0.1865(0.9126)	0.2612(0.9060)
Gestodene	0.1751(0.9367)	0.1156(0.7232)	0.2135(0.9420)	0.1716(0.9594)
Equilin	0.3194(0.8875)	0.2939(0.9669)	0.2662(0.9926)	0.2425(0.9834)

* Initial individual concentrations of estrogen hormones in solution

The rate constants and equilibrium adsorption capacities calculated from the pseudo-first-order equation as well as the correlation coefficients (R^2) are summarized in Table 4.2. As shown in Table 4.2, the R^2 was 0.6928 and 0.7750 for the adsorption of norgestrel (target initial concentration= 200 μg/L) onto MN100 resin and medrogestone onto MN200 (target initial concentration= 200 μg/L), respectively. Except for norgestrel and medrogetone, R^2 values of the model fitting for other estrogen hormones are higher than 0.8 which indicate a good linear fitting by using pseudo-first-order model. Other models such as pseudo-second-order model and intrapartical model were also applied. However, the results suggested that those models did not fit the experimental data reasonably. As a result, data was not presented in this work.

The adsorption rate constants obtained for lower initial concentration (target initial concentration= 200 μg/L) of estrogen hormones, were larger than that for higher initial concentration (target initial concentration= 300 μg/L) with few exceptions (medrogestone adsorbed onto MN100 and norgestrel adsorbed onto MN200) as shown in Table 4.2. This result suggests that at lower initial concentration, the estrogen hormones were adsorbed onto the resin surface faster. This could be explained by the large surface area (800-1100 m^2/g) of MN100 and MN200 resins [Streat and Sweetland, 1997] compare to the small amount of estrogen molecules. While at lower initial concentration, there may be unoccupied active sites in resins surrounded by less estrogen hormones molecules. Whenever the molecules come into physical contact with the active sites in the resin, they get adsorbed immediately. Saha et al. (2010) studied the adsorption rate of 17β-estradiol and 17α-ethinylestradiol onto activated carbon, they observed that the adsorption rate was independent of the initial concentration of 17β-estradiol and 17α-ethinylestradiol. The activated carbon used in their work has a surface area of 1679 m^2/g which is higher than the surface area of MN100 and MN200 resins. Large surface area of activated carbons provided more available active sites, so the adsorption rates were not affected too much as compared in this work.

As can be seen from Table 4.2, with same initial concentrations, MN200 resin had higher rate constants than MN100 resin for most estrogen hormones except for 17β-estradiol and equilin with both initial concentrations and 17α-estradiol and 17α-dihydroequilin with initial concentration of 200 μg/L. This means that MN200 resin could adsorb estrogen hormones faster than MN100 reins for most estrogens. The reason might be that MN200 resin is a non-functionalized resin, it tends to adsorb estrogen hormones indiscriminately due to the lack of specific interaction. In addition, the surface area of MN200 resin is larger than MN100 resin as can be seen from Table 3.2, there are more active sites available in MN200 resins, larger surface area increases the chances of estrogen molecules come into physical contact with the active sites in resins. This could be another reason that contributes to the faster removal of estrogen hormones by MN200 resin.

Another interesting observation from Figure 4.4 and Table 4.2 was that the adsorption rates for the five estrogens: trimegestone, progesterone, gestodene, medrogestone and norgestrel were relative slower than the rest of the estrogens regardless of the initial concentration and resin type. The five estrogens are relative bigger molecules as shown in Table 3.1. The molecular weights of these five compounds are higher than the rest of the estrogens, which could be a reason that makes their adsorption slower. Similar results reported by Yang and Xing (2010) indicated that a smaller molecule such as phenol is easier than bigger molecule such as proteins or natural organic matters to get adsorbed onto carbon nanotubes.

Hayduk-Laudie correlation equation is a useful relation to determine liquid diffusivity of an organic compound in water (Gustafson, K. E. and R. M. Dickhut, 1994). The Hayduk-Laudie correlation is given as Equation 16:

$$\mathbf{D_{aw}} = \frac{\mathbf{13.26 * 10^{-5}}}{\mathbf{(\mu)^{1.14} V_a^{0.589}}} \qquad \text{Equation 16}$$

Where μ (centipoise) is the viscosity of water (1.002 cp at 293 K), V_a (cm^3/mol) is the solute molar volume at normal boiling point estimated by Le Bas method, D_{AW} (cm^2/sec) is the diffusivity of solute in water (in dilute solution).

The diffusivities calculated from Equation 16 are shown in Table 4.3

Table 4.3 Diffusivity of estrogen hormones estimated by Hayduk-Laudie correlation equation

Estrogen hormones	Molar volume, V_a (cm^3/mol)	Diffusivity, D_{AW} (cm^2/sec)
17α-Ethinylestradiol	343.1	4.25E-06
Estriol	320.9	4.42E-06
17β-Estradiol	313.5	4.48E-06
17α-Estradiol	313.5	4.48E-06
Estrone	306.1	4.54E-06
17α-Dihydroequilin	306.1	4.54E-06
Trimegestone	402.3	3.87E-06
Medrogestone	417.1	3.79E-06
Progesterone	380.1	4.00E-06
Norgestrel	372.7	4.05E-06
Gestodene	365.3	4.09E-06
Equilin	298.7	4.61E-06

From Figure 4.3, we can see that the diffusivities of trimegestone, medrogestone, progesterone, norgestrel and gestodene are lower (ranging from 3.87-4.05 E-06 cm^2/sec) than the rest of the estrogens (ranging from 4.25-4.61 E-06 cm^2/sec). Diffusivity of a compound in water simply means the rate of a compound diffuse into the aqueous solution, the higher the diffusivity, the faster it diffuse into water. In our study, the estrogen hormones have to diffuse the water first before they get adsorbed onto the resin surface. So if the diffusivity is higher, for example, estrone (4.54E-06 cm^2/sec), the molecules diffuses into water will be faster than trimegestone (3.87 E-06 cm^2/sec). So estrone molecules will reach the resin surface and get adsorbed faster than trimegestone molecules. Diffusivity of the individual estrogen hormones and the associated pseudo-first-order rate constants are plotted in Figure 4.3:

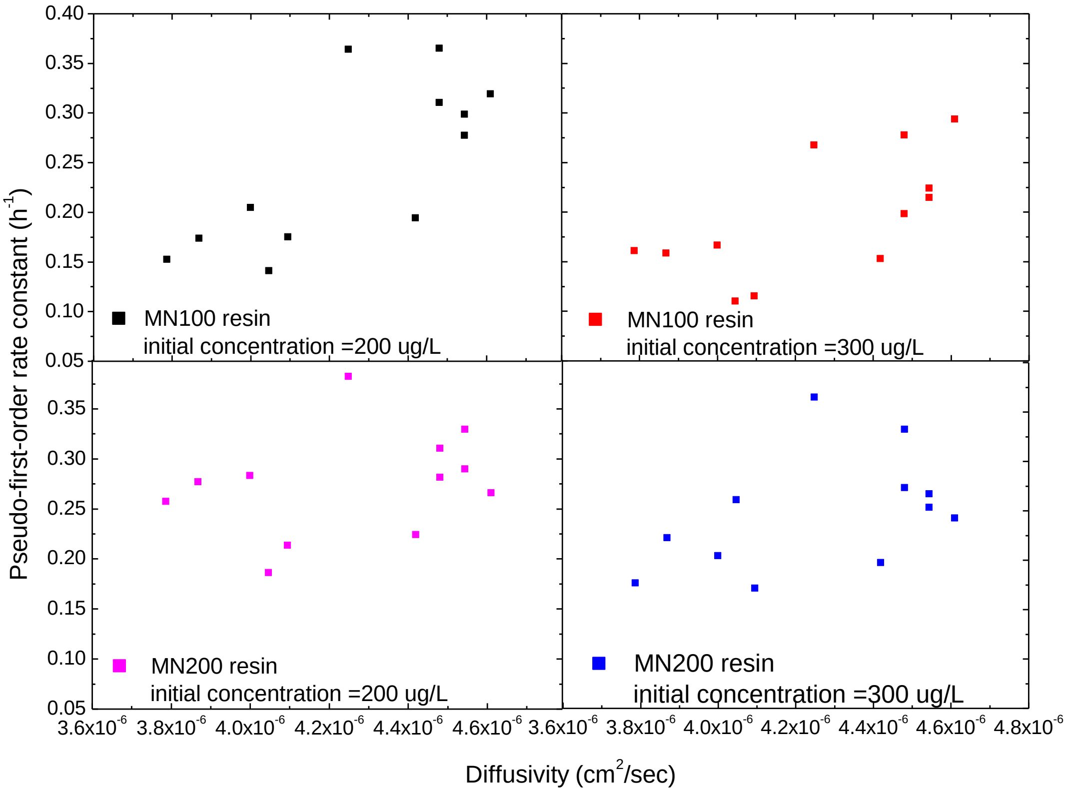

Figure 4.6 Relationship between pseudo-first-order rate constants and diffusivity of estrogen hormones

From Figure 4.6, we see a trend that as diffusivity of the estrogen hormones increased, the first-order-rate constants increased, which supported our previous assumption. But this trend was not strictly followed by every estrogen hormone. In addition, MN100 resins shows more definite trend than MN200 resin, as can be seen from Figure 4.6.

4.1.4. Effect of solution pH on the adsorption of estrogen hormones onto MN100 and MN200 resins

The solution pH can play an important role in the ion-exchange process [Kocaoba 2007, Lin and Juang 2005, Li et al., 2008]. In this set of experiments, solution pH was varied from 2 to 11. Estrogen hormones mixture was used to investigate the influence of solution pH on the adsorption process. Figure 4.7 shows the effect of solution pH on the adsorption of estrogen hormones mixture.

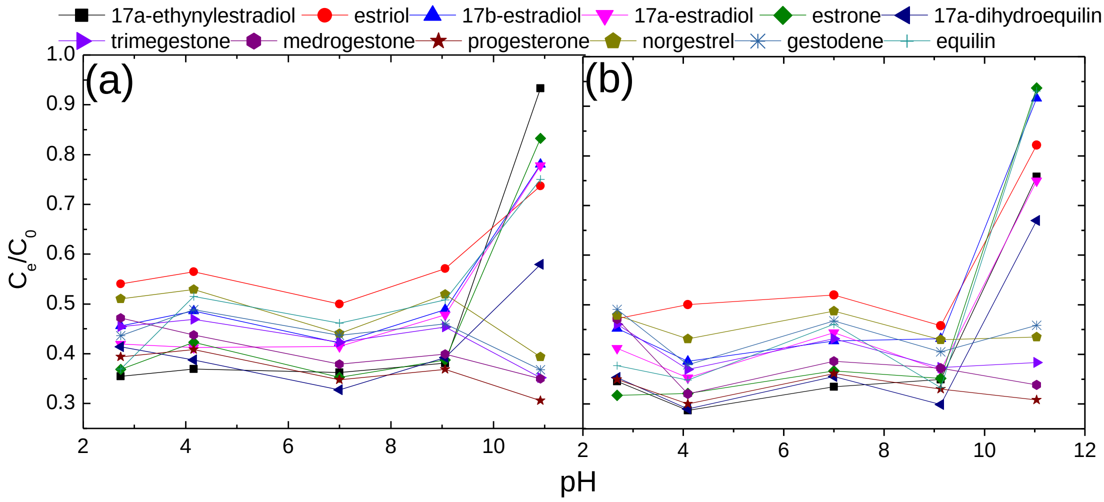

Figure 4.7 Effect of pH for the adsorption of estrogen hormones onto (a) MN100; (b) MN200 (target initial concentration= 100 µg/L, resin dosage= 0.2 g/L, contact time= 48 hours, sample volume= 1000 ml, temp= 295 K)

Figure 4.7 shows the ratio of the equilibrium concentration over the initial concentration as a function of solution pH. As pH increased from 2 to 9, no significant changes were observed on the adsorption efficiencies for all the estrogen hormones. However, when increasing pH from 9 to 11, the adsorption efficiencies of some estrogen hormones decreased. For example, while pH increased from 9 to 11, the amount of 17α-ethinylestradiol adsorbed onto MN100 resin decreased from 62 % to 7 %. Similar results were also noted in MN200 resin. Earlier reports showed that as solution pH increased to above 10, the adsorption capacities of 17β-estradiol and estrone onto solid adsorbents decreased [Li et al., 2008, Neale et al., 2010]. This is in good agreement with the results obtained in this work. However, for some of the estrogens such as norgestrel, gestodene, trimegestone, medrogestone and progesterone, no appreciable difference on adsorption efficiency was observed by increasing the pH from 2 to 11 for both MN100 and MN200 resins. The adsorption behaviors of MN100 and MN200 resins were similar due to their similar structures.

As can be seen from Figure 4.7, MN100 and MN200 resins clearly sort the estrogen hormones into two categories: (a) adsorption efficiencies remain the same as pH increases from 2 to 11 (trimegestone, progesterone, gestodene, medrogestone and norgestrel); (b) adsorption efficiencies remain the same when pH increases from 2 to 9 and decrease as pH increases from 9 to 11 (17α-ethinylestradiol, estriol, 17β-estradiol, 17α-estradiol, estrone, 17α-dihydroequilin and equilin). This difference might be explained by the physical properties of the estrogen hormones. Some of the estrogen hormones such as 17β-estradiol and equilin have lower pK_a values compare to other estrogens (See Table 3.1). When pH increases and approaches the pK_a values of the estrogen hormones, the molecules start to dissociate into charged species. The adsorption of the charged species onto the resin surface is not as efficient as neutral molecules due to the electrostatic interaction [Yang and Xing, 2010]. In addition, the reported point of zero charge for MN100 and MN200 resin are 6.7 and 4.4, respectively (Table 3.2), which means at higher pH of 10 and 11, the resin surface will be negatively charged and then repel the negatively charged estrogen hormone species, and thus decrease the adsorption efficiencies. On the other hand, estrogens such as trimegestone, progesterone, gestodene, medrogestone and norgestrel, they do not have pK_a values or have extremely high pK_a values as can be seen from Table 3.1 (trimegestone and progesterone do not have pK_a values due to the lack of dissociable functional groups), they remained neutral as pH increased to 9 and higher, so increasing pH did not affect the removal efficiencies of these estrogen hormones as much as those with relative lower pK_a values. The fact that low solution pH ($<pK_a$) is

favorable for the adsorption of 17β-estradiol and estrone onto the adsorbents is also noted elsewhere in the literature [Li et al., 2008].

4.1.5. Fixed-bed column study

Fixed-bed column experiment was conducted to verify the performance of the resins in practical use. The main column conditions are summarized in Table 4.4.

Table 4.4 Main column conditions on the adsorption of estrogen hormones

Resin	MN100
Target individual estrogen hormone concentration (μg/L)	100
Flow rate (ml/L)	32
Column diameter (cm)	1.1
Resin mass (g)	1.5
Bulk density (g/cm^3)	0.53
Bed depth (cm)	3
EBCT (min)	0.1
Run time (h)	52
Temperature (K)	295
pH	7.0

All the estrogen hormones were successfully adsorbed by MN100 resin within 10 hours (around 7000 bed volumes). The breakthrough points for all the estrogens were observed except for medrogestone. The effluent concentration of medrogestone was undetectable (below the instrument detection limits) throughout the column experiment and the average initial concentration was around 23.8 μg/L which is much lower than the desired initial concentration of 100 μg/L, as shown in Figure 4.8. The reason is unclear due to the lack of references on medrogestone. Possible reasons could be due to the adsorption onto the glassware or onto the Teflon tubings while pumping into the column.

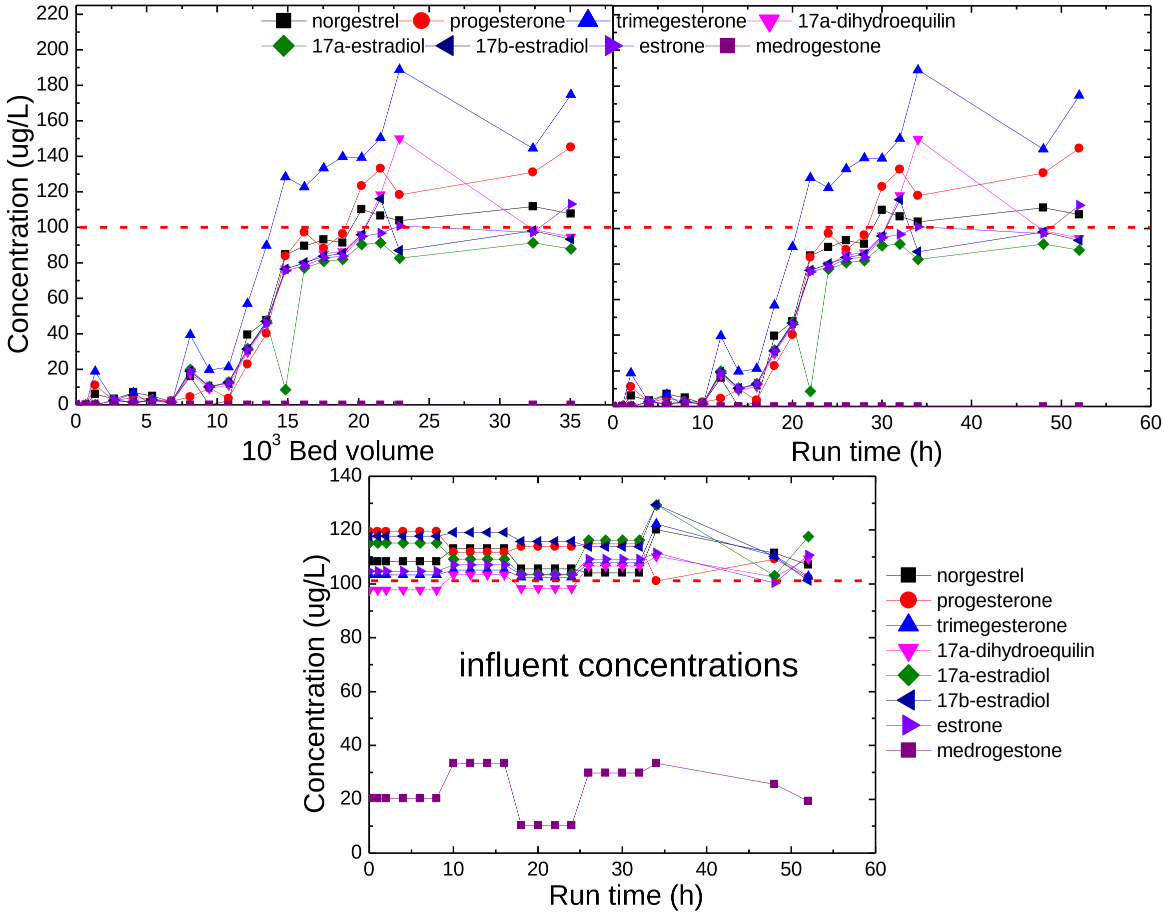

Figure 4.8 Fixed-bed column study with estrogen hormones mixture

Trimegestone was the first estrogen detected in the effluent, followed by progesterone, norgestrel, 17α-dihydroequilin, estrone, 17α-estrodial and 17β-estrodial. The elutions of 17α-estrodial and 17β-estrodial were simultaneous due to their similar structures. The results indicate that trimegestone is the most difficult estrogen to get adsorbed onto the resin, while 17α-estrodial and 17β-estrodial are strongly adsorbed onto the resin. Possible reason might be due to the size of the molecules. The molecular volume (MV) of trimegestone calculated by Le Bas method is 402.3 cm^3/mol which is the second highest among all 12 estrogen hormones used. The MV of 17α-estrodial and 17β-estrodial is 343.1 g/mol which is smaller than trimegestone

(Table 4.3). Similar results were also observed by Yang and Xing (2010), and indicated that a smaller molecule such as phonel is easier than bigger molecule such as protein or natural organic matters to get adsorbed onto the carbon nanotubes. These results suggest that the adsorption of estrogen hormones onto a fixed-bed column largely depends on the size of the individual molecules.

The result obtained from the column study was also associated well with the results observed from the batch investigations. As can be seen from Table 4.2, the first-order rate constants obtained for five estrogens (norgestrel, trimegestone, gestodene, progesterone and medrogestone) were smaller (ranging from 0.1410-0.2047 h^{-1}) than the rest of the estrogens (ranging from 0.1945-0.3652 h^{-1}) which means the adsorption of these five estrogen hormones onto the resins are slower than the rest of the other estrogens. These five estrogens are harder to get adsorbed, and thus, they are the first detected in the effluent of the column.

Another interesting result is that for some of the estrogens such as norgestrel, trimegestone and progesterone, their initial concentration in the influent was 100 μg/L, but the concentration detected in the effluent was higher than 100 μg/L after the breakthrough point. The model solution pumped into the column was changed periodically until the end of the column test and the concentration was analyzed each time after the replacement, but no appreciable difference was noted in the initial concentration as can be seen from Figure 4.8. This might suggest that when the resin reaches its adsorption capacity, it might release the adsorbed estrogens back into the water due to completion of adsorption. As discussed in the earlier, norgestrel, trimegestone and progesterone are harder to get adsorbed onto the resin due to their molecular size and weight. As a result, those estrogens are easier than other estrogens to desorb from the resin surface back into water.

Table 4.5 Comparison of maximum adsorption capacities from column study and the batch investigation

Estrogen hormones	Maximum loading from column study (μg/g)	Maximum loading calculated by Langmuir isotherm model (μg/g) [1]	Maximum loading observed from isotherm plots (μg/g) [2]
17β-Estradiol	3828.4	1250	>2500
17α-Estradiol	3894.0	1429	1500
Estrone	2973.8	667	1600
17α-Dihydroequilin	2632.7	1429	2250
Trimegestone	2181.7	769	750
Medrogestone	--	400	750
Progesterone	3042.8	1111	1250
Norgestrel	2786.6	833	1250

1 See Table 4.1 for Langmuir isotherm model prediction

2 See Figure 4.3 for isotherm plots

As can be seen from Table 4.5, the maximum loading capacities obtained from both Langmuir equation (Table 4.1) and isotherm plots (Figure 4.3) are lower than the data observed from column study. The maximum adsorption capacities estimated from isotherm plots are closer to column study data. This result might suggest that, in batch experiments, the resins did not reach the saturated status with the initial EC concentration of 100 μg/L. In addition, the adsorption capacities for trimegestone, medrogestone, progesterone and norgestrel estimated from both Langmuir isotherm equation and the isotherm plots of the five estrogens are lower than 17α-estradiol, 17β-estradiol, estrone and 17α-dihydroequilin, which indicate that trimegestone, medrogestone, progesterone and norgestrel are harder than 17α-estradiol, 17β-estradiol, estrone and 17α-dihydroequilin to get adsorbed onto the polymeric resins. This is in good agreement with the results obtained from column study as well as relationship between estrogen hormone diffusivity and their pseudo-first-order rate constants.

4.1.6. Estrogen hormones removal mechanism

The effects of resin dosage, contact time and solution pH as well as fixed-bed column study have been discussed already. We tried to depict the adsorption mechanism based on the experimental results.

Possible mechanisms used to describe the adsorption of estrogen hormones include: (1) physical adsorption (van der Waals forces, hydrophobic interaction); (2) hydrogen bonding; (3) electrostatic attraction or ion-exchange process; (4) coordination complexes or chemical adsorption. MN 200 resin is a polymeric resin without functionality, as a result, ion-exchange process is not possible. MN100 resin could undergo ion-exchange process due to the presence of tertiary ammonium functional group in the resin. However, most of the estrogen hormones used in this work could only be dissociated at pH over 10 (pK_a>10). The isotherm experiments conducted were under the neutral pH of 7, MN100 resin could not undergo ion-exchange process as well. So ion-exchange is not the mechanism for the adsorption of estrogen hormones under neutral pH.

Another possible adsorption mechanism is the formation of complexes or chemical bonding between adsorbent and adsorbate. Lei et al. (2008) studied the adsorption and oxidation of the target compounds by using Fe_2O_3 or Mn oxide, their results indicated that once the complexes is formed, it is very hard to reverse the process due to the formation of the strong chemical bonding. However, our regeneration tests for the resins (exhausted by the adsorption of estrogen hormones) showed that regeneration could be easily done by washing the exhausted resins with organic solvent such as methanol. This may be due to physical adsorption between resins and the estrogen molecules not the chemical bonding, so that we could regenerate the exhausted resins easily with methanol.

The point of zero charge of MN100 and MN200 resins are reported as 6.7 and 4.4, respectively [Street and Sweetland, 1997]. At neutral pH, both of the resins were negatively charged. But under pH of 7, all the estrogens are neutral molecules. Therefore, electrostatic attraction is not possible between them. So the possibility of the existence of electrostatic attraction is ruled out as well.

Hydrogen bonding could be formed only on MN100 resin because of the presence of tertiary ammonium functional group. It might form hydrogen bonding with estrogen hormones, as a result, yield better adsorption performance. However, by comparing the adsorption capacities between MN100 and MN200 resins, MN200 resin showed slightly better performance than MN100 resin based on the maximum adsorption capacities, as can be seen from the isotherm plots (Figure 4.3). So hydrogen bonding adsorption might exist but not the main mechanism contributes to the adsorption.

The above discussion suggests that the mechanism for the adsorption of estrogen hormones onto MN100 and MN200 resins might be physical adsorption, which may involve non-specific molecular interaction between the resins and the estrogens. Earlier reports indicated that the estrogen hormones could be adsorbed onto the particulates because of their hydrophobic nature [Lai et al., 2000]. K_{ow} is the distribution coefficient of a compound between organic and aqueous phase, and it could be used to predict adsorption on solids if the hydrophobic interaction is the case [Bertilsson and Bergh, 1999]. Most of the estrogen hormones used in this work has a log K_{ow} value ranging from 2.77 to 5.03 [Sedlak et al., 2000] (Also see Table 3.1 for the properties). The log K_{ow} values clearly indicate that estrogen hormones are a class of hydrophobic substances. The maximum adsorption capacities obtained from column test for estrone and 17β-estradiol onto MN100 resin were 2973.8 and 3828.4 μg/g, respectively (See Table 4.3). These numbers indicate that 17β-estradiol is more favorable to get adsorbed onto MN100 resin than estrone. The reported log K_{ow} values of 17β-estradiol and estrone were 4.01 and 3.13 [Sedlak et al., 2000], respectively. The results might indicate that the more hydrophobic (higher log K_{ow} value) the compound is, the higher tendency it will get adsorbed onto the resin and harder to detach. The first-order rate constants obtained from the kinetics study also indicated that estrogen hormones with higher hydrophobicity tend to yield higher adsorption rate, as can be seen from Table 4.2. To sum up, other interactions might also exist, but the main mechanism on the adsorption of estrogen hormones onto the MN100 and MN200 resins is highly possible due to the physical adsorption.

4.2. Removal of perfluorinated compounds

4.2.1. Screening test using perfluorooctanoic acid (PFOA)

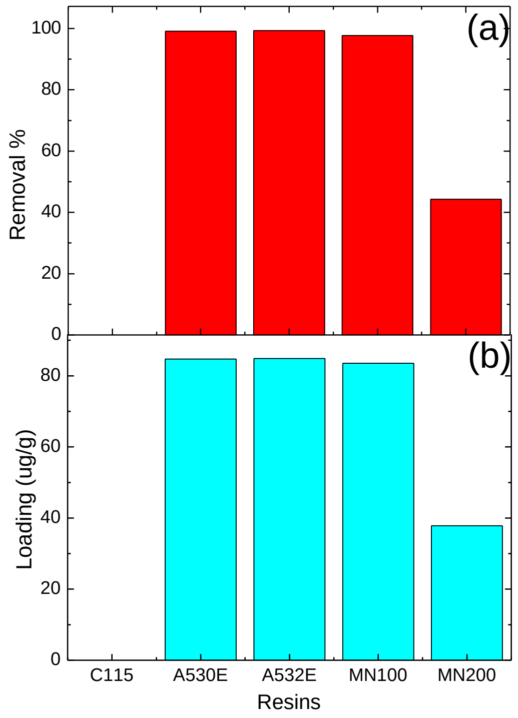

Figure 4.9 Screening test on the adsorption of perfluorooctanoic acid (PFOA) onto various types of resins: (a) removal efficiency; (b) loading capacity (initial concentration= 25.65 μg/L, pH= 7.0, contact time= 48 hours, sample volume= 1000 ml, temp= 295K)

In order to select proper resins for the adsorption of PFCs, five polymeric resins were subject to a screening test on the removal of perfluorooctanoic acid (PFOA). The screening test results are shown in Figure 4.9.

Except for C115 resin, all other resins tested showed removal of PFOA. The removal percentage (loading) of PFOA onto A530E, A532E, MN100 and MN200 resins were 99 % (84.7 μg/g), 99 % (84.8 μg/g), 98 % (83.5 μg/g) and 44 % (37.7 μg/g), respectively. C115 resin is a strong cationic resin, while A530E, A532E and MN100 resins are anionic resins. The better performance of anionic resins might suggest that the adsorption process is an anionic ion-exchange process. If this is the case, C115 could not remove any of the PFOA is understandable because C115 is a cationic resin, it will repel the negative charged species of PFOA due to electrostatic force. MN200 resin adsorbed a relative low amount of PFOA (44 %). The 44% removal may also be due to the physical adsorption caused by active sites on the resin surface as discussed in the previous chapter. A530E, A532E and MN100 resins were then selected for the further investigation.

4.2.2 Effect of resin dosage on the adsorption of perfluorooctanoic acid onto A530E, A532E and MN100 resins

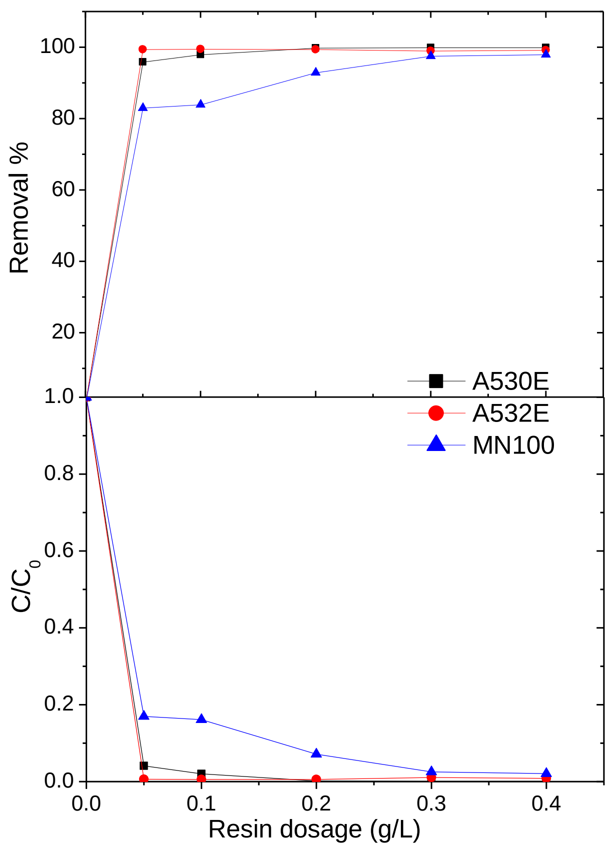

Figure 4.10 Effect of resin dosage on the adsorption of PFOA onto A530E, A532E and MN100 resins (initial concentration= 54.29 μg/L, pH= 7.0, contact time= 48 hours, sample volume= 1000 ml, temp= 295 K)

In order to investigate the optimum resin dosage needed to remove PFOA in aqueous solutions, experiments were conducted by adding various amounts of A532E, A530E and MN100 resins into PFOA model solution. The effects of resin dosage are shown in Figure 4.10.

As can be seen from Figure 4.10, the performance of resins A530E and A532E resin was similar. With the resin dosage of 0.05g/L, 99 % and 96 % of PFOA were adsorbed onto A532E and A530E resins, respectively. But with the same dosage, MN100 resin removed 83 % of PFOA. The adsorption capacity of MN100 resin is less than other two resins. This might be due to the relative low ion-exchange capacity of MN100 resin compared to A532E and A530E (total ion-exchange capacities of A532E, A530E and MN100 resins are 0.75, 0.6, 0.1-0.3 equiv./L, respectively). These results again indicated that the adsorption process is an ion-exchange process. When increasing the dosage to 0.3 g/L or higher, no appreciable differences were observed between the three resins since 100 % PFOA in the solution was adsorbed on to the resins.

4.2.3 Effect of contact time and adsorption kinetics on the adsorption of perfluorooctanoic acid onto A530E, A532E and MN100 resins

In order to investigate the rate for PFOA adsorbed onto the three selected resins, samples were taken and analyzed at different time interval. The results on the effect of contact time are shown in Figure 4.11. As can be observed from Figure 4.11, at the first 8 hours, the adsorption of PFOA onto all three resins was fast with the order of A532 resin>A530 resin>MN100 resin. About 80% of PFOA was removed by all three resins in 8 hours. After 8 hours, the adsorption rate decreased due to the low residue

PFOA concentration presented in aqueous solution. At lower target initial concentration (29.51 μg/L), A532E showed better performance than A530E and MN100 resins. While at higher target initial concentration (60.06 μg/L), the adsorption capacity of A532E was higher than A530E and MN100 resins, and the behaviors of A532E and A530E resins were similar after 12 hours. Both A532E and

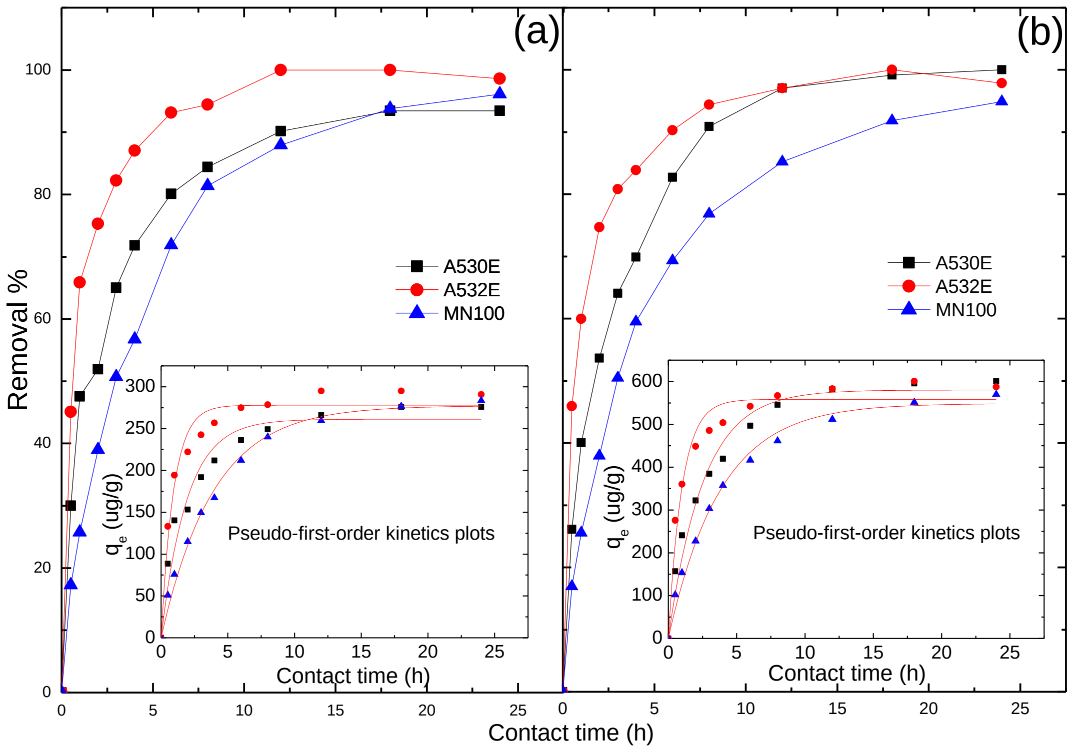

Figure 4.11 Effect of contact time and kinetics on the adsorption of PFOA onto A530E, A532E and MN100 resins (a) initial concentration= 29.51 μg/L; (b) initial concentration= 60.06 μg/L (pH= 7.0, contact time= 48 hours, sample volume= 1000 ml, temp=295K)

A530E resins yielded better adsorption performances than MN100 resin, as can be seen from Figure 4.11. For all three resins tested, 100 % of PFOA was removed from aqueous solution within 24 hours regardless of initial concentrations. A532E resin has bifunctional quaternary amines as its functional group, while A530E resins has single quaternary ammonium as its functional group. The bifunctional group increases the ion-exchange equivalent (See Table 3.2) and provides more ion-exchange sites to interact with negatively charged PFOA ions, therefore, yielded a faster adsorption rate than the other two resins.

Pseudo-first-order kinetics model was applied, as can be seen from Figure 4.11. This model can fit the experimental data well. The rate constants obtained from the model fitting are summarized into Table 4.6.

Table 4.6 Pseudo-first-order rate constants and correlation coefficients (R^2) on the adsorption of PFOA onto A532E, A530E and MN100 resins

Time (h)	Target concentration= 29.51 μg/L			Target concentration= 60.06 μg/L		
Resins	q_e (μg/g)	$k_1(h^{-1})$	R^2	q_e(μg/g)	$k_1(h^{-1})$	R^2
A532E	278	1.06	0.97	558.4	1.0	0.96
A530E	261	0.52	0.96	580.2	0.39	0.98
MN100	277	0.26	0.99	548.8	0.26	0.99

As can be seen from Table 4.6, R^2 values obtained in all cases are higher than 0.96, which indicate good fitting by using this model. At same initial concentration, the adsorption capacities calculated from the pseudo-first-order model for all three resins are similar. This is because the initial concentrations used for the kinetic study were very low (29.51 μg/L and 60.06 μg/L), 100 % PFOA was removed from solution after 24 hours, and the resins were not saturated or reached the maximum adsorption capacities. So the capacities calculated from the model do not represent the real maximum adsorption capacities of A532E, A530E and MN100 resins in the removal of PFOA.

4.2.4 Effect of initial concentration on the adsorption of PFOA onto A530E, A532E and MN100 resins

In order to investigate the effect of initial concentrations of PFOA, the starting concentrations were varied from 100-900 µg/L. After 48 hours of mechanical shaking, the residue concentrations were analyzed. The results are shown in Figure 4.12.

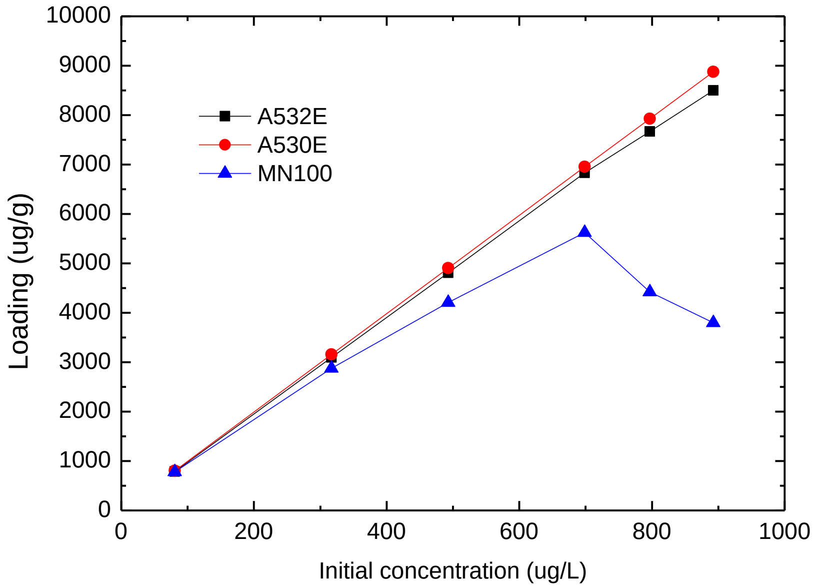

Figure 4.12 Effect of initial concentration on the adsorption of PFOA onto A530E, A532E and MN100 resins (resin dosage = 0.1 g/L, pH= 7.0, contact time= 48 hours, sample volume= 1000 ml, temp= 295 K)

As can be seen from Figure 4.12, as the initial concentration of PFOA increased from 100 µg/L to 900 µg/L, the resin loading capacities of A530E and A532E resins in the removal of PFOA increased linearly. At initial concentration of 900 µg/L, A532E and A530E resins showed loading capacities of $8.5*10^3$ and $8.8*10^3$ µg/g, respectively, and the maximum adsorption capacities for A532E and A530E were still not reached. In the case of MN100 resin, the loading capacity increased as initial concentration increased to around 700µg/L and started to decrease, as shown in

Figure 4.12. On the other hand, the loading capacity of MN100 resin was increasing when the initial concentration increased from 100 μg/L to 700 μg/L, then started to decrease. This might indicate that MN100 resin has reached its adsorption capacity. The maximum adsorption capacity of MN100 resin in the removal of PFOA is $5.6*10^3$. μg/g at initial concentration of 700 μg/L, as shown in Figure 4.12.

4.2.5 Effect of resin dosage and adsorption isotherm on the adsorption of perfluorinated compounds (PFCs) onto A530E, A532E and MN100 resins

In order to investigate the effect of resin dosage on the adsorption of 10 PFCs (perfluorotridecanoic acid, tricosafluorododecanoic acid, perfluoroundecanoic acid, perfluorodecanoic acid, heptadecafluorooctane sulfonic acid potassium salt, perfluorooctanoic acid, tridecafluorohexane sulfonic acid potassium salt, tridecafluorononanoic acid, perfluoroheptanoic acid and undecafluorohexanoic acid) onto A530E, A532E and MN100 resins, various amounts of resins (range from 0.025 to 0.2 g/L) were spiked into 1 L of model solution with 10 PFCs. The purpose of these experiments is also to find out the relationship between the adsorption behavior and the C-C chain length. The effect of resin dosage is shown in Figure 4.13. (During the experiments, tridecafluorohexane sulfonic acid potassium salt and tridecafluorononanoic acid showed negative removals and the initial concentrations were calculated to be less than 10μg/L, data can be found in Appendix L, but not participated in the following discussion).

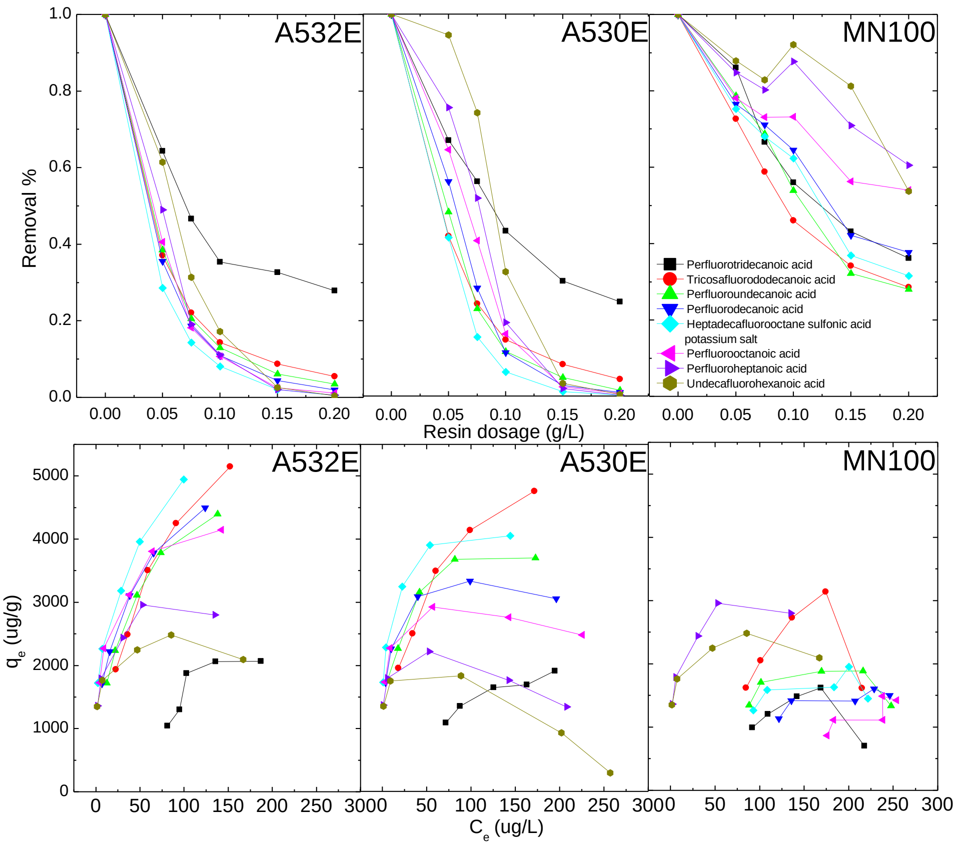

Figure 4.13 Effect of resin dosage and isotherm on the adsorption of PFCs onto (a) A530E; (b) A532E; (c) MN100 resins (target initial concentration= 300 μg/L, pH= 7.0, contact time= 48 hours, sample volume= 1000 ml, temp= 295 K)

As can be seen from Figure 4.13, most of the PFCs are favorable to get adsorbed onto A530E and A532E resins, but few of them are favorably adsorbed onto MN100 resin. For example, at resin dosage of 0.15 g/L, more than 90 % of PFCs were removed by the A530E and A532E resins except for perfluorotridecanoic acid. On the other hand, MN100 resin removed less than 70 % PFCs under the similar condition. These results again confirmed that the removal of PFCs is an ion-exchange process since A530E and A532E resins are anionic ion-exchange resins with higher ion-exchange equivalents and yield better adsorption capacities. Wang and Shih (2011) studied the adsorption of PFOA and PFOS onto alumina, and reported that the adsorption equilibrium was reached within 48 hours, and the adsorption behaviors of the PFCs was significantly affected by the solution pH and the ionic strength. In our work, we did not investigate the effect of the ionic strength, but we did see the adsorption efficiency of perfluorinated salt is higher than some of the perfluorinated acid, which was also observed by Wang and Shih (2011).

Isotherms for the adsorption of PFCs onto A532E, A530E and MN100 resins are also plotted in Figure 4.13. As can be seen in the case of A532E resin, only three PFCs reached the maximum adsorption capacities, they are perfluorotridecanoic acid, undecafluorohexanoic acid and perfluoroheptanoic acid. The maximum adsorption capacities for these three PFCs onto A532E were ranging from 2000-3000 μg/g. The adsorption capacities of A532E resin extended 4000 μg/g and still did not reach the maximum capacities for the rest of the PFCs (tricosafluorododecanoic acid, Perfluoroundecanoic acid, perfluorodecanoic acid, heptadecafluorooctane sulfonic acid potassium salt, perfluorooctanoic acid and tridecafluorononanoic acid). In the case of using A530E resin, all PFCs were reached the maximum adsorption capacities except for tricosafluorododecanoic acid which still remained unsaturated. The adsorption capacities for most PFCs adsorbed onto A530E were ranging from 1500-4000 μg/g (maximum capacity of A530E for the adsorption of tricosafluorododecanoic acid extended 4500μg/g). MN100 was the least efficient resin in the removal of PFCs, the maximum adsorption capacities with all the PFCs were below 3000 μg/g, as can be seen from Figure 4.13.

Freundlich and Langmuir models are applied to the isotherm data, the model constants and correlation coefficients (R^2) are summarized in Table 4.7. In the case of using A532E as the adsorbent, except for perfluorotridecanoic acid and undecafluorohexanoic acid, both isotherm models could provide good fittings for the rest of the PFCs, as can be seen from Table 4.7. It was observed from Figure 4.13, when the equilibrium concentration C_e increased, the loading capacities q_e for perfluorooctanoic acid, erfluoroheptanoic acid and undecafluorohexanoic acid decreased. That is why none of the models could yield reasonable fits for these three compounds.

Another interesting topic to the discussion is that the adsorption efficiency with the length of the PFCs molecules. At A532E resin dosage of 0.15 g/L, the removal percentages for perfluorotridecanoic acid and undecafluorohexanoic acid are 67 % and 97 %, respectively. Perfluorotridecanoic acid has the longest C-C chain among 10 PFCs used in this work, while undecafluorohexanoic acid has the shortest C-C chain (see Table 3.1 in Chapter 3). According to the experimental results, an assumption was proposed: longer C-C chain of PFCs yielded lower adsorption capacity. In order to verify this assumption, the number of C-C bonds in individual PFCs molecule is plotted against the Freundlich constants K_f (Table 4.7) from the adsorption of PFCs onto A532E and A530E resins. The relationship is shown in Figure 4.14.

Table 4.7 Langmuir and Freundlich isotherm constants on the adsorption of PFCs onto A532E and A530E resins

PFCs	A532E						A530E					
	Langmuir constants			Freundlich constants			Langmuir constants			Freundlich constants		
	q_0(μg/g)	b(L/μg)	R^2	K_f(μg/g) $(L/\mu g)^{1/n}$	1/n	R^2	q_0(μg/g)	b(L/μg)	R^2	K_f(μg/g) $(L/\mu g)^{1/n}$	1/n	R^2
Perfluorotridecanoic acid	4699.2	0.0048	0.5855	82.9	1.5880	0.5439	3016.3	0.0087	0.9419	147.2	2.0528	0.9217
Tricosafluorododecanoic acid	7403.4	0.0150	0.9968	449.3	2.0383	0.9787	5868.16	0.0243	0.9867	676.3	2.5941	0.9678
Perfluoroundecanoic acid	5246.9	0.0349	0.9886	720.6	2.2762	0.9763	3894.2	0.1130	0.9108	1310.6	4.6452	0.8863
Perfluorodecanoic acid	4881.6	0.0582	0.9410	911.8	2.9916	0.9952	3283.6	0.2796	0.9341	1661.9	7.3638	0.7373
Heptadecafluorooctane sulfonic acid potassium salt	4659.3	0.1502	0.7731	1283.4	3.4579	0.9864	3860.6	0.5458	0.8389	1864.8	5.9776	0.9469
Perfluorooctanoic acid	4143.8	0.1450	0.9269	1332.5	4.2276	0.9664	--	--	--	--	--	--
Perfluoroheptanoic acid	2837.2	0.4251	0.8716	1375.3	6.1500	0.8543	--	--	--	--	--	--
Undecafluorohexanoic acid	2258.6	1.0046	0.7577	1436.0	10.0100	0.6866	--	--	--	--	--	--

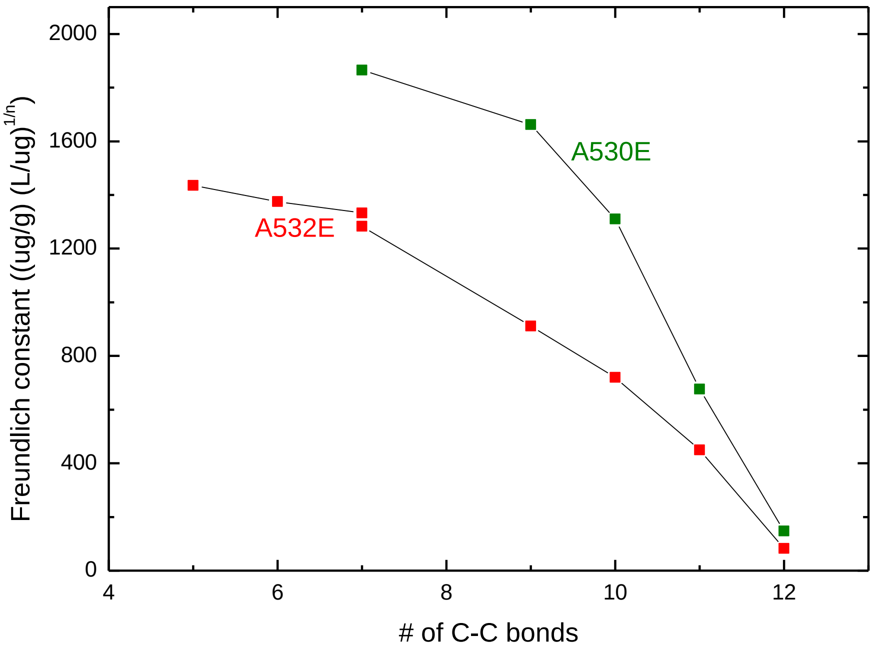

Figure 4.14 Relationship between PFCs molecular length and Freundlich isotherm constants

K_f calculated from Freundlich equation is an empirical constants reflecting the adsorption capacities and other adsorption factors while the number of C-C bonds in PFCs molecules simply indicate the length of the molecule. From Figure 4.14, an obvious relationship was found between the number of C-C bonds and Freundlich isotherm constants. As number of C-C bonds increases, the Freundlich isotherm constants decreases. Namely, as the length of the PFCs increases, the adsorption onto ion-exchange resins decreases. This might be due to the ion-exchange resins surface is favorable of exchanging shorter and smaller ions and form stable electron donor-acceptor complexes. Hansen et al. (2010) also observed the longer chain of PFCs yielded a lower adsorption capacity while using activated carbons as adsorbents. Similar trends can be found elsewhere in the literature [Yong, 2007]

4.2.6 PFCs removal mechanism

The nature of perfluorinated compounds (acids and salts) determines that they are easily dissociated into anionic ions [Carter et al., 2010]. As a result, ion-exchange process is proposed to be the main adsorption mechanism. Equation 17 showed the chemical process of the ion exchange process:

$$\mathbf{Resin \succ (CH_3)_3N^+Cl^- + CF_3(CF_2)_nCOOH = Resin \succ (CH_3)_3N^+CH_3(CF_2)_nCOO^- + HCl}$$

Equation 17

Where $\mathbf{Resin \succ (CH_3)_3N^+Cl^-}$ represents the resin structure with quaternary ammonium functional group ($\succ \mathbf{N^+Cl^-}$). $\mathbf{CF_3(CF_2)_nCOO^-}$ ions are exchanged with $\mathbf{Cl^-}$ ions and adsorbed in the resins.

The ion-exchange process can also be illustrated by using Figure 4.15. The status of dissociated PFCs and the anionic functional group on the resin surface is shown in Figure 4.15 (a). When PFCs ions come into physical contact with the resin surface as shown in Figure 4.15 (b), the negatively charged PFCs species ($\mathbf{CF_3(CF_2)_nCOO^-}$) undergo ion-exchange with $\mathbf{Cl^-}$ on the resin surface and get adsorbed. Meanwhile, $\mathbf{Cl^-}$ ions are released into the bulk solution. Wang and Shih (2011) also suggested the adsorption of PFOS onto alumina was due to the electrostatic interaction. They proposed that the sulfonate functional group in PFOS molecule interacts with the functional groups on the alumina which caused the high removal percentage. Senevirathna et al. (2010) studied the adsorption of PFCs onto granular activated carbon (GAC), ion-exchange polymers and non-ion-exchange polymers. They found out that at low concentrations of PFCs, the adsorption capacities were following the order of ion-exchange polymers>non-ion-exchange polymers>GAC.

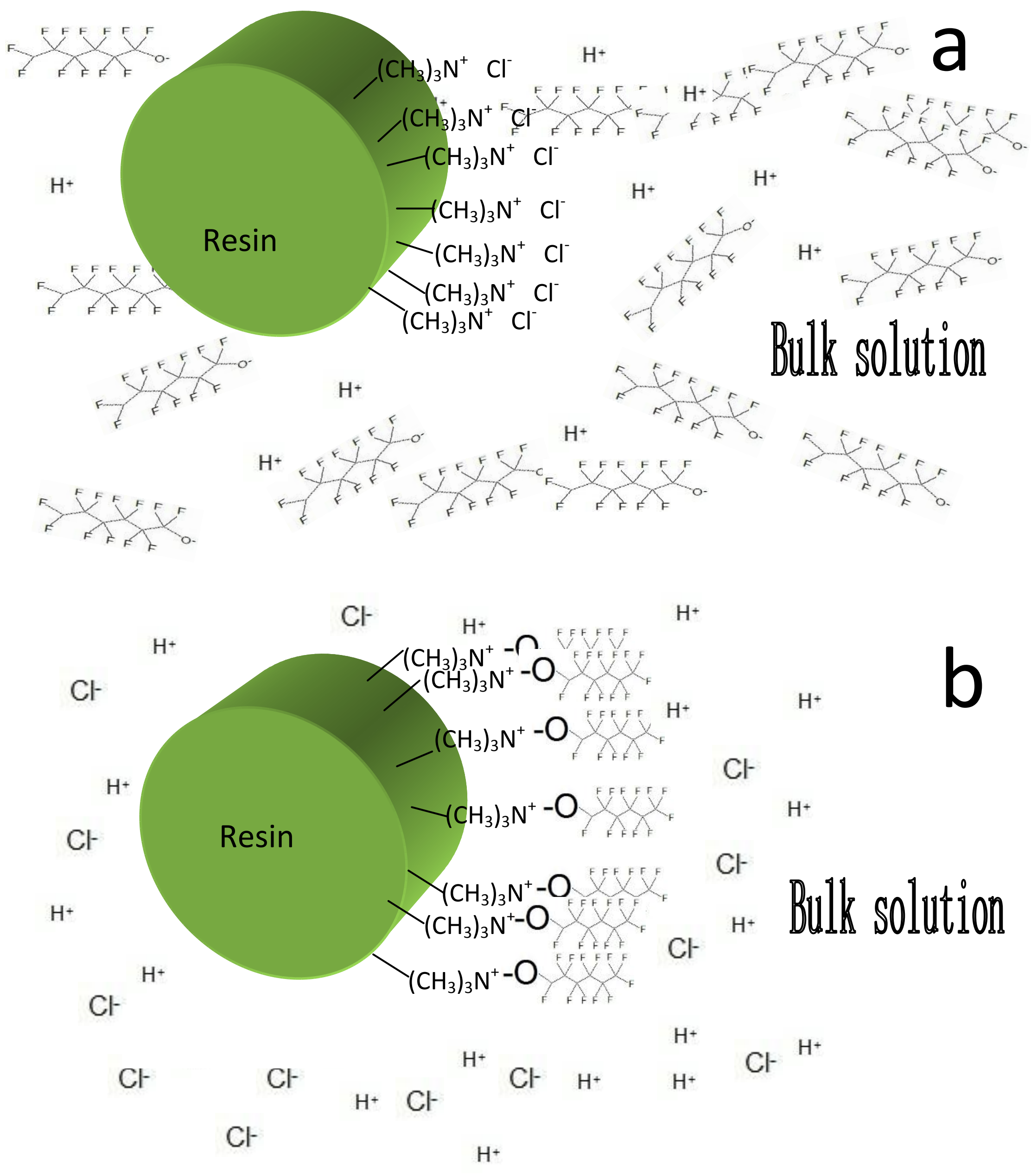

Figure 4.15 Schematic illustration of PFCs adsorbed on to the resin surface: (a) before adsorption; (b) after adsorption

4.3. Removal of Bisphenol A

4.3.1. Screening test on bisphenol A (BPA)

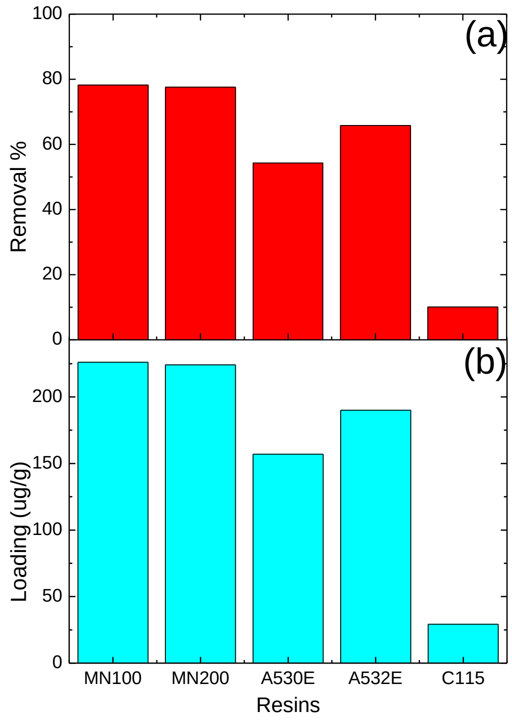

Figure 4.16 Screening test on the adsorption of BPA onto various types of resins (initial concentration= 86.67 μg/L, pH= 7.0, contact time= 48 hours, sample volume= 400 ml, temp= 295 K, resin dosage= 0.2 g/L)

Initially, experiments were conducted to test the removal efficiencies of bisphenol A (BPA) onto varies types of resins. The screening test results are shown in Figure 4.16.

The removal efficiencies (loadings) of BPA are 78 % (226 μg/g) and 77 % (224μg/g) onto MN100 and MN200 resins, respectively. About 54 % (156 μg/g), 66 % (189 μg/g) and 10 % (29 μg/g) of BPA was removed by A530E, A532E and C115 resins, respectively. The fact that MN100 and MN200 resins yielded better adsorption efficiencies is similar to the adsorption of estrogen hormones onto MN100 and MN200 resins, so the mechanism for the adsorption of BPA might also be due to physical adsorption. As discussed earlier, certain amount of BPA was also removed by A530E, A532E and C115 resin, the adsorption by these resins are also due to the physical adsorption of the resins. A530E, A532E and C115 are ion-exchange resins, while MN100 and MN200 are hyper-cross-linked polymers. Earlier reports indicated that the presence of functional groups decreased the surface area of the adsorbents [Saha et al., 2010, Streat and Sweetland, 1997]. Therefore, the adsorption efficiencies of BPA onto ion-exchange resins are not as high as compared to MN100 and MN200 resins. MN100 and MN200 resins were selected to conduct further experiments for the removal of BPA.

4.3.2 Effect of resin dosage and adsorption isotherm on the adsorption of BPA onto MN100 and MN200 resins.

In order to understand the effect of resin dosage on BPA removal efficiency, resin dosage was varied from 0.025 g/L to 0.15 g/L. Representative dosage-response data is shown in Figure 4.17. As displayed in Figure 4.17, both resins removed 80% of BPA at the dosage of 0.15 g/L. As resin dosage increased, the removal percentage increased, however, the amount of BPA adsorbed, per gram of resin, decreased. These results were expected because a certain amount of resin is enough for the adsorption of fixed amount of BPA, and thus, increasing the resin dosage decreases the overall capacity of the adsorbents. The result is also in good agreement with earlier studies using ion-exchange resins or adsorbents for the removal of heavy metal ions [Yoon et al., 2003, Kocaoba 2007, Yu et al., 2009].

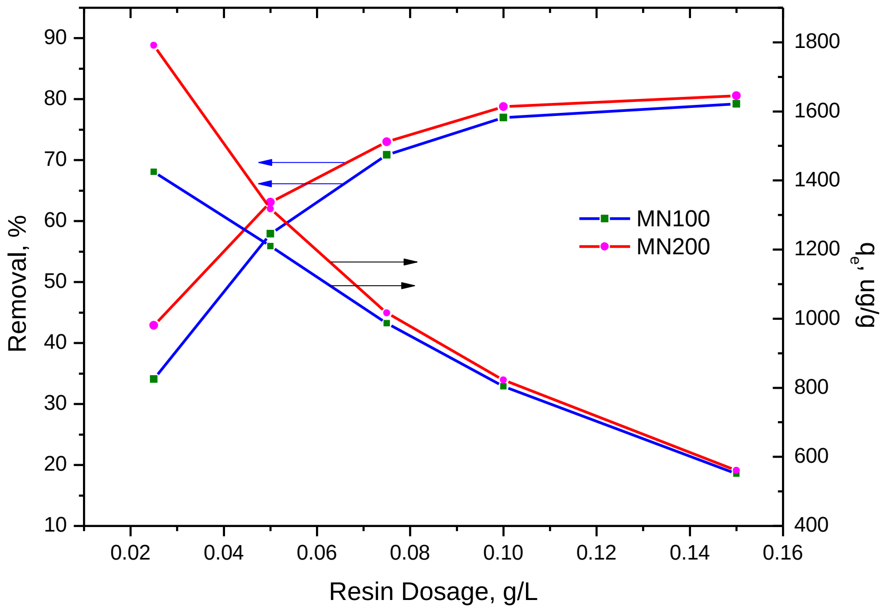

Figure 4.17 Effect of resin dosage on the adsorption of BPA onto MN100 and MN200 resins (initial concentration= 104.4 μg/L, pH= 7.0, contact time= 48 hours, sample volume= 400 ml, temp= 295 K)

By comparing the removal percentage of BPA under the same resin dosage, the adsorption efficiency of MN200 resin is slightly better than MN100 resin. For example, at resin dosage of 0.05 g/L, the adsorption capacity of MN100 and MN200 resins on the removal of BPA was 1424.65 μg/g and 1790.94 μg/g, respectively. This difference might be due to the presence of the tertiary amine functional groups in MN100 resin structure partially block the diffusion of BPA molecule into the internal surface of MN100 resin. Similar results were also observed by Saha et al. (2010), they observed the additional functional groups on the polymeric resins inhibited 17β-estradiol and 17α-ethinylestradiol molecules diffusing into the inner structure of the resins.

Non-linear regression of Langmuir and Freundlich isotherm models were used to fit the isotherm data for both resins. The results are shown in Figure 4.18.

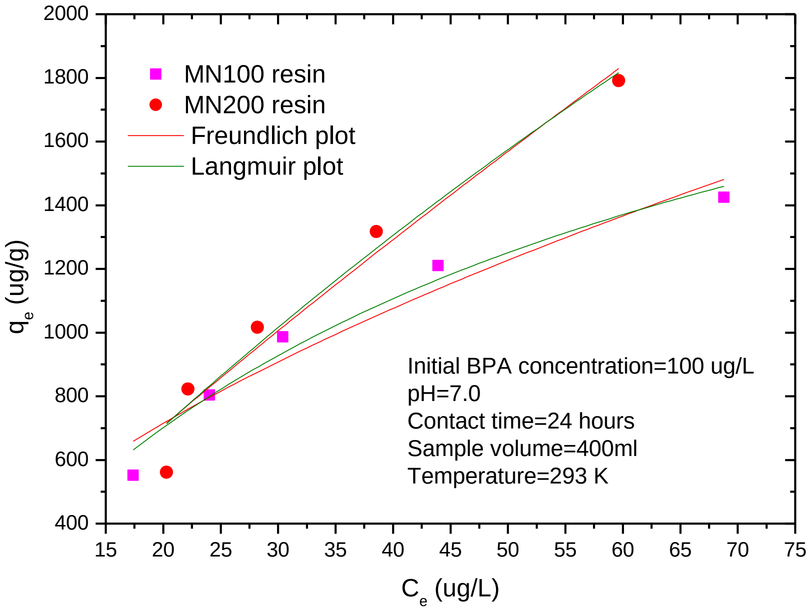

Figure 4.18 Langmuir and Freundlich isotherm plots on the adsorption of BPA onto MN100 and MN200 resins (initial concentration= 104.4 μg/L, pH= 7.0, contact time= 48 hours, sample volume= 400 ml, temp= 295 K)

As can be seen from Figure 4.18, the maximum adsorption capacity of MN200 resin is higher than MN100 resin. Both Langmuir isotherm model and Freundlich isotherm model fit the kinetics date well by comparing the R^2 values (>0.93). It can also be observed by the shapes of the Freundlich isotherm, that the adsorption of BPA onto MN200 resin is more favorable than on MN100 resin. Langmuir and Freundlich constants are present in Table 4.8. The Langmuir constant q_0 represents the maximum adsorption capacities of resins in the removal of BPA. q_0 observed for MN200 resin is 3.4 times higher than for MN100, which means the maximum adsorption capacity predicted for MN200 resin is 3.4 times higher than MN100 resin in the removal of BPA.

Table 4.8 Freundlich and Langmuir isotherm constants on the adsorption of BPA onto MN100 and MN200 resins

Resin	Freundlich $q_e = K_f C_e^{\frac{1}{n}}$			Langmuir $q_e = \frac{q_0 b C_e}{1 + bC_e}$		
	$K_f(\mu g/g)(L/\mu g)^{1/n}$	1/n	R^2	$q_0(\mu g/g)$	b(L/μg)	R^2
MN 100	52.02	1.15	0.95	2620.44	0.0183	0.97
MN 200	122.20	1.70	0.93	8945.43	0.0043	0.95

4.3.3 Effect of contact time and adsorption kinetics on the adsorption of BPA onto MN100 and MN200 resins

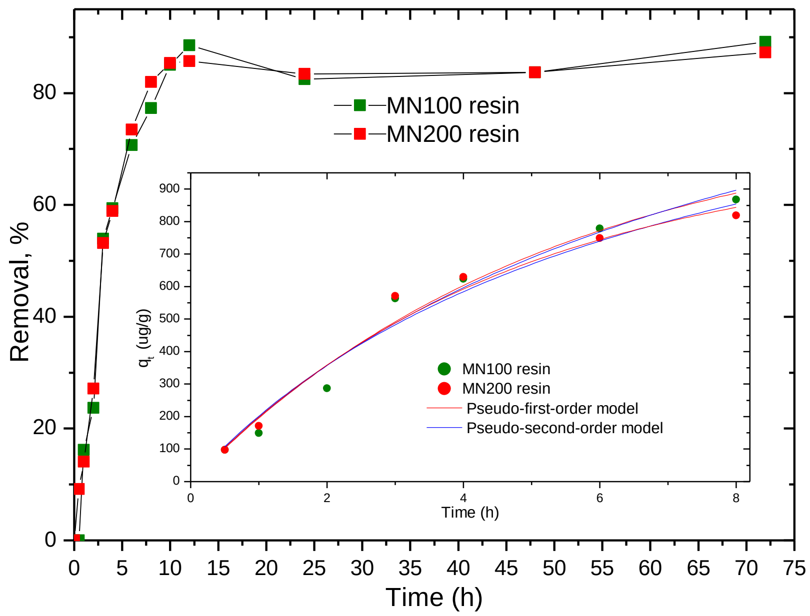

Figure 4.19 Effect of contact time and kinetics on the adsorption of BPA onto MN100 and MN200 resins and kinetics model fitting (initial concentration= 105.9 μg/L, pH= 7.0, contact time= 72 hours, sample volume= 1000 ml, temp= 295 K, resin dosage= 0.2 g/L)

The time needed to reach the adsorption equilibrium is also an important parameter to be investigated. Figure 4.19 shows the relationship between contact time and BPA removal efficiency. From Figure 4.19, it was observed that the adsorption equilibrium was reached in 12 hours for both resins. No significant differences were noted by comparing the removal efficiency of MN100 and MN200 resins.

Pseudo-first-order, pseudo-second-order were applied to the above data (Equation 3.10 and Equation 3.12 in Chapter 3). The equilibrium concentration, q_e, was calculated by taking the average concentration after 24 hours, 48 hours and 72 hours.

Table 4.9 Rate constants obtained from the kinetic models and the correlation coefficients

Resin	Experiment data		Pseudo-first-order $\ln(q_e - q_t) = k_1 t + \ln q_e$			Pseudo-second-order $\frac{1}{q_t} = \frac{1}{q_e} + \frac{1}{q_e^2 t k_2}$		
	C_0 (μg/g)	q_e(μg/g)	q_e (μg/g)	k_1(h^{-1})	R^2	q_e(μg/g)	k_2(g/μg h)	R^2
MN100	105.90	1008.54	1028.57	0.21	0.95	1587.94	9.16E^{-05}	0.94
MN200	105.90	1127.56	1142.24	0.19	0.97	1804.28	6.84E^{-05}	0.97

The non-linear pseudo-first-order and pseudo-second-order model fittings can also be seen from Figure 4.19. Rate constants obtained from different kinetic models are summarized in Table 4.9. The predicted adsorption capacities (q_e) by pseudo-first-order model and pseudo-second-order model are all higher than the experimental values, with the pseudo-second-order model having a value of 1.57 and 1.60 times higher than the experimental values for MN100 and MN200 resins, respectively. Both pseudo-first-order and pseudo-second-order yielded good fitting on both MN100 and MN200 resins (R^2 values higher than 0.94 in all cases).

4.3.4 Effect of solution pH on the adsorption of BPA onto MN100 and MN200 resins

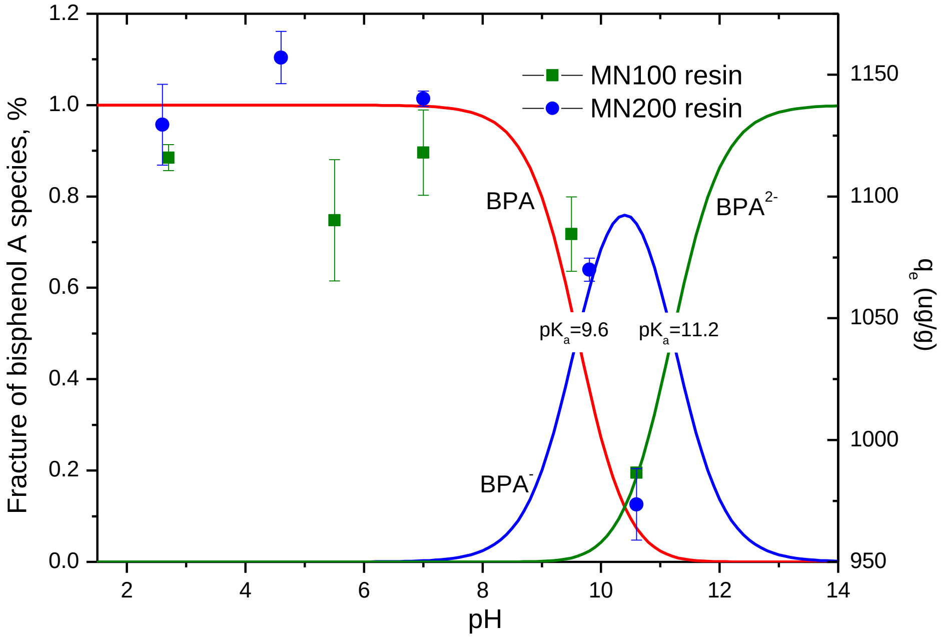

Figure 4.20 Effect of solution pH on the adsorption of BPA onto MN100 and MN200 resins (initial concentration= 128.17 μg/L, pH= 7.0, contact time= 24 hours, sample volume= 1000 ml, temp= 295 K, resin dosage= 0.2 g/L)

Solution pH can be an important parameter affecting the adsorption process. BPA is a compound with two phenyl groups in its structure. Numerous studies have shown that BPA has two pK_a values, pK_{a1}=9.6 and pK_{a2}=11.2 [Zhang et al., 2006, Tsai et al., 2006]. In order to investigate the effect of solution pH on the adsorption of BPA, the solution pH value was varied from 3 to 11. Figure 4.20 showed the adsorption capacity q_e against solution pH. A very clear trend can be seen from Figure 4.20. The amount of BPA adsorbed onto the resins decreases as the pH increases. At pH= 3, the adsorption capacity were noted as 1115.92 μg/g and 1129.44 μg/g for MN100 and MN200 resins, respectively. The adsorption capacities between MN100 and MN200 resins under low pH are similar due to the similar structure. No significant changes were observed by increasing the pH until the solution pH approached the pK_{a1} of BPA for both resins. At pH of 11, this is beyond the pK_{a1} value of BPA, the amount of BPA adsorbed onto the resins dropped to 987 μg/g and 974 μg/g. It was also observed that at pH of 9 and higher, the adsorption capacity of MN100 in removal of BPA became higher than MN200 resin, as can be seen from Figure 4.20. As discussed earlier, at high pH of 9 and higher, BPA molecules started to ionize, the charged species of BPA were undergoing ion-exchange process with the tertiary ammonium functional group in MN100 resin at high pH of 9 and higher which yield a relative higher adsorption capacity than MN200 resin. MN200 is a hyper-cross-linked resin without functional groups as mentioned in the previous section, so there is no ion-exchange reaction with MN200. The properties of MN100 and MN200 resins could be seen in Table 3.2. The pH values after the treatment were also measured, no significant differences were observed compared to the initial pH values.

4.3.5 Effect of ionic strength on the adsorption of BPA onto MN100 and MN200 resins

In order to investigate the effects of ionic strength, the adsorption kinetics of BPA onto MN100 resin was studied under different NaCl concentrations. The results are shown in Table 4.10. No significant differences on were observed after 25 mg/L of NaCl was added into the solution. The salting-out effect was not as obvious as reported by Liu et al. (2009) which lead to an enhancement of BPA adsorption onto MN100 resin. Adding salts caused a slight decrease in the pseudo-first-order rate constants. The decrease of k_1 relied on the fact that a small quantity of ionic strength could compete with BPA onto the active sites of MN100 resin and decrease the adsorption rate. This is in good agreement with the study by Liu et al. (2009) who also observed a decreasing of rate constant by adding salinity while conducting adsorption of bisphonel A onto activated carbon.

Table 4.10 Effect of ionic strength on the adsorption of BPA onto MN100 resin

Resin	NaCl (mg/L)	q_e (exp) (μg/g)	q_e (cal) (μg/g)	k_1 (h^{-1})	R^2
MN 100	0	1008.5	1028.6	0.21	0.95
	25	1036.8	1053.0	0.16	0.99
	100	1037.2	1043.8	0.15	0.99
	800	1051.4	1125.4	0.12	0.94

4.3.6 Regeneration experiments on BPA exhausted resins

One advantage of polymeric resins is their regeneration after usage. The exhausted resins can be recovered by regeneration solution such as salt solutions or organic solvents. Caetano et al. (2009) performed a regeneration test on MN200 resin by using 50:50 methanol: water (v/v) solution after the resin was exhausted by phenol, about 90±2% of the resins was recovered. In this work, different amounts of methanol were mixed with DI water to form a series of regeneration solutions, the results of regeneration tests for MN100 and MN200 resins exhausted by BPA are displayed in Figure 4.21. As can be seen from Figure 4.21, the recovery percentage of MN100 and MN200 resins by using pure methanol was 89% and 83%, respectively after 24 hours of mechanical shaking. The results showed that the highest recovery percentage was observed by using pure methanol which indicated that methanol is a very good regeneration agent for the exhausted resins.

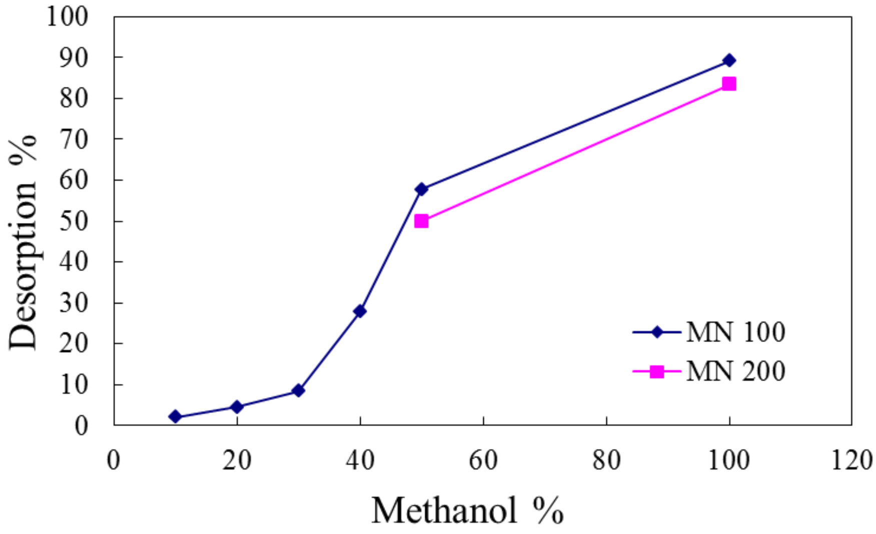

Figure 4.21 Regeneration tests on MN100 and MN200 resins by using gradient methanol-water solutions (contact time= 24 hours, regeneration solution volume= 100 ml, temperature= 295 K, resin dosage= 0.3 g/L)

4.3.7 BPA dsorption mechanis

The mechanism for the removal of bisphenol A is similar to that of estrogen hormones proposed earlier. Van der Waals force is one form of the physical adsorption force. This interaction is described as the sum of the attractive or repulsive forces between molecules or between parts of the same molecule, other than those due to covalent bonds or to the electrostatic interaction of ions. The hydrophobic properties of MN200 resin have been reported by Valderranma et al. (2007). This adsorption process is described as the attraction of BPA onto the hydrophobic solid. The evidence for the presence of such force is that the adsorption of BPA was significantly reduced when the pH approached to the pK_{a1} value of BPA [Zhang et al., 2006]. Van der Waals force is favorable for the adsorption of neutral molecules, and thus, when neutral BPA molecules start to ionize into charged species as pH increased to beyond its pK_a value, the adsorption capacity decreased.

4.4. 1, 4-Dioxane

4.4.1 Screening test on 1, 4-dioxane

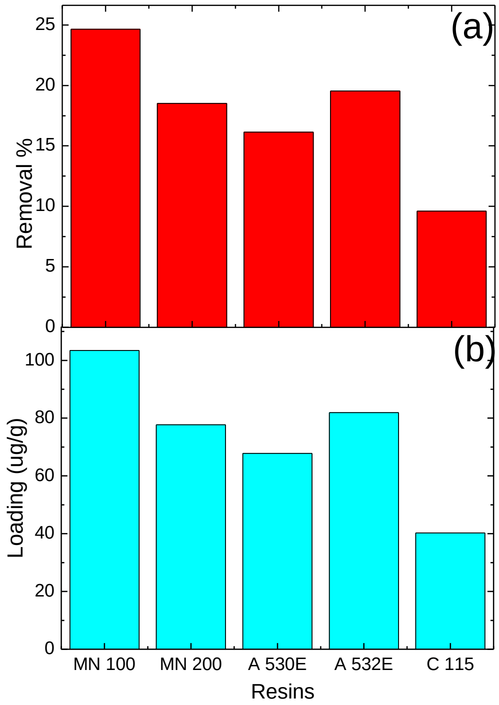

Figure 4.22 Screening test on the adsorption of 1, 4-dioxane onto various types of resins: (a) removal efficiency; (b) loading capacity (initial concentration= 125.87 μg/L, pH= 7.0, contact time= 48 hours, sample volume= 1000 ml, temp= 295 K, resin dosage= 0.3g/L)

Five resins were subject to a screening test by using 1,4-dioxane as adsorbate., Figure 4.22 shows the removal efficiency and loading capacity of the resins for of 1, 4-dioxane. All the resins were found to remove less than 30% of 1, 4-dioxane. The poor performance of resins is due to that the high water solubility of 1, 4-dioxane (miscible in water) which makes it very hard to adsorb from aqueous solutions [Zenker et al., 2003]. Physical adsorption approach seems to be inefficient to remove it. Another possible approach is to use ion-exchange adsorption, but because 1, 4-dioxane is extremely hard to ionize under normal conditions, and the functional groups in the resin structure will not interact with the neutral molecule which makes the ion-exchange approach impossible as well. So no further investigations were conducted on 1, 4-dioxane removal.

Chapter 5

CONCLUSIONS

In this work, five polymeric resins were used to remove emerging contaminants (ECs) of interests. The resins were found to be effective in removing estrogen hormones, PFCs and bisphenol A from aqueous solution. However, none of the resins could remove 1, 4-dioxane efficiently. It was observed that the adsorption behavior of the resins largely depends on different processing conditions such as the initial concentration, resin dosage, contact time, ionic strength and pH of the solution. The application of isotherm and kinetic models was also used and compared. The practical application of these resins in the removal of ECs was verified by using fixed bed column test.

For the removal of estrogen hormones, MN100 and MN200 resins were selected and a dosage of 0.3 g/L was needed to remove 95% of the estrogen hormones with the initial concentration of 100 μg/L. Freundlich isotherm model fits the experimental data well and yield relative high linear correlations (higher than 0.8) for all the estrogen hormones. Most of the resins could remove the estrogen hormones and reached the equilibrium within 24 hours. Pseudo-first-rate kinetic model could fit the experimental data well. Increasing pH to higher than 10 decreased the adsorption capacity for some of the estrogen hormones due to the relative low pK_a value of those hormones; for those estrogens with higher pK_a value, pH did not affect too much. Fixed-bed column test with MN100 resin could successfully retain estrogen hormones within 8 hours, trimegestone is the most difficult to adsorb while 17α-estradiol and 17β-estradiol were the easiest. Physical adsorption is the main mechanism for the removal of estrogen hormones.

In the case of removing PFCs by using A530E, A532E and MN100, a dosage of 0.05 g/L for both of A530E and A532E resins was needed to remove 100% of perfluorooctanoic acid (PFOA) with the initial concentration of 50 μg/L. All three resins could remove PFOA and reach the equilibrium within 20 hours with the initial concentration of 50 μg/L. Both of A530E and A532E resins did not reach the adsorption capacity by increasing the PFOA concentration from 100 μg/L to 1000 μg/L, meanwhile, MN100 resin reached the saturation status. The adsorption capacity for different PFCs was associated with the length of the molecules: the longer the chain is, the harder it will be adsorbed. Ion-exchange process is the main mechanism for the removal of PFCs by comparing the performance of A530E, A532E and MN100.

While using polymeric resins to remove bisphenol A, a dosage of 0.1 g/L for both of MN100 and MN200 resins was needed to remove 80% of bisphenol A with the initial concentration of 100 μg/L. Both non-linear Langmuir isotherm model and Freundlich model can fit the isotherm data well. Both resins could remove BPA and reach the equilibrium within 10 hours with the initial concentration of 100 μg/L. pseudo-first-order and pseudo-second-order kinetics models can fit the kinetics data well. Increasing pH decreased the adsorption capacity for both resins due to the disassociation of the BPA molecules at high pH of 11. Adding salt caused a slight decrease in the pseudo-first-order rate constants. The reason was that salinity could compete with BPA onto the active sites in resins and decreased the adsorption. 80% of the exhausted resin could be regenerated by using pure methanol. Physical adsorption mechanism was proposed to be the main mechanism on the adsorption of BPA onto polymeric resins.

The adsorption of 1, 4-dioxane onto polymeric resins was found inefficient. The poor performance of resins is due to the high water solubility of 1, 4-dioxane (miscible in water) which makes it very hard to extract from aqueous solutions and adsorbed onto the resin surface.

Chapter 6

PROPOSAL FOR THE FUTURE RESEARCH

Limited studies were found to conduct research on the adsorption of estrogens hormones, PFCs and BPA onto synthetic ion-exchange adsorbents, especially on the underlying adsorption mechanism of such ionizable organic compounds.

In these studies, we have examined the adsorption behaviors of estrogen hormones, PFCs and bisphenol A onto ion-exchange adsorbents. Future researches have been focused on the elucidation of adsorption mechanism, revealing the effects of molecule structure to the interaction between the organic compounds and adsorbents. The preliminary results have shown that some of the commercial available resins were successfully removing estrogens hormones, PFCs and phenol compound from aqueous solution. Based on the understanding of adsorption mechanism between them, a practical model may be hopefully proposed to reasonably predict adsorption behaviors of similar compounds onto ion-exchanger. The specific objectives of the future project will include:

1. Development of synthetic resins or adsorbents with certain functional groups, characterization and optimization of the resulted materials.
2. Examining and comparing the performance of synthetic resins with the available commercial resins and providing evaluations and suggestions, conducting regeneration tests.
3. Investigating the adsorption mechanism of estrogen hormones, PFCs, phenol compound onto both synthetic and commercial resins Using possible advanced statistical tools to assist the data analysis.

4. Proposing a mathematical model to predict adsorption behavior of similar-structure organic compounds onto investigated adsorbents and verifying its practicability and accuracy.

References

Abe, A. (1999). Distribution of 1,4-dioxane in relation to possible sources in the water environment. Science of the Total Environment 227(1): 41-47.)

Adams, C. D.,Scanlan, P. A.,Secrist, N. D., (1994). Oxidation and Biodegradability Enhancement of 1,4-Dioxane Using Hydrogen-Peroxide and Ozone. Environmental Science & Technology 28(11): 1812-1818.

Adams, C.,Wang, Y.,Loftin, K.,Meyer, M., (2002). Removal of antibiotics from surface and distilled water in conventional water treatment processes. Journal of Environmental Engineering-Asce 128(3): 253-260.

Andersen, H.,Siegrist, H.,Halling-Sorensen, B.,Ternes, T. A., (2003). Fate of estrogens in a municipal sewage treatment plant. Environmental Science & Technology 37(18): 4021-4026.

Auriol, M.,Filali-Meknassi, Y.,Tyagi, R. D.,Adams, C. D.,Surampalli, R. Y., (2006). Endocrine disrupting compounds removal from wastewater, a new challenge. Process Biochemistry 41(3): 525-539.

Auriol, M.,Filali-Meknassi, Y.,Tyagi, R. D.,Adams, C. D. (2007)., Laccase-catalyzed conversion of natural and synthetic hormones from a municipal wastewater. Water Research 41(15): 3281-3288.

Basagaoglu, H.,Ginn, T. R.,McCoy, B. J., (2002). Comment on "Model coupling intra-particle diffusion/sorption, nonlinear sorption, and biodegradation process" by H.K. Karapanagioti, C.M. Gossard, K.A. Strevett, R.L. Kolar, and D.A. Sabatini. J Contam Hydrol 57(3-4): 303-310; discussion 311-307.

Bayburtskiy, F. S.,Korenev, A. D.,Novozhilov, Y. A., (2007). Interaction of surfactants with ion polymeric sorbents. Oxidation Communications 30(2): 448-453.

Bertilsson, S. and S. Bergh (1999). Photochemical reactivity of XAD-4 and XAD-8 adsorbable dissolved organic compounds from humic waters. Chemosphere 39(13): 2289-2300.

Bolz, U.,Hagenmaier, H.,Korner, W., (2001). Phenolic xenoestrogens in surface water, sediments, and sewage sludge from Baden-Wurttemberg, south-west Germany. Environmental Pollution 115(2): 291-301.

Bolto, B.,Dixon, D.,Eldridge, R.,King, S.,Linge, K., (2002) Removal of natural organic matter by ion-exchange. Water Research 36(20): 5057-5065.

Bowman, R. H. (2001). Ozone-peroxide advanced oxidation water treatment system for treatment of chlorinated solvents and 1,4-dioxane. Abstracts of Papers of the American Chemical Society 221: U463-U463.

Buxton, G. V.,Greenstock, C. L.,Helman, W. P.,Ross, A. B., (1988). Critical-Review of Rate Constants for Reactions of Hydrated Electrons, Hydrogen-Atoms and Hydroxyl Radicals (.Oh/.O-) in Aqueous-Solution. Journal of Physical and Chemical Reference Data 17(2): 513-886.

Caetano, M.,Valderrama, C.,Farran, A.,Cortina, J. L., (2009). Phenol removal from aqueous solution by adsorption and ion-exchange mechanisms onto polymeric resins. J Colloid Interface Sci 338(2): 402-409.

Carter, K. E. and J. Farrell (2010). Removal of Perfluorooctane and Perfluorobutane Sulfonate from Water via Carbon Adsorption and Ion-exchange. Separation Science and Technology 45(6): 762-767.

Chang, H. S.,Choo, K. H.,Lee, B.,Choi, S. J., (2009). The methods of identification, analysis, and removal of endocrine disrupting compounds (EDCs) in water. Journal of Hazardous Materials 172(1): 1-12.

Chai, W.,Handa, Y.,Suzuki, M.,Saito, M.,Kato, N.,Horiuchi, C. A., (2005). Biodegradation of bisphenol A by fungi. Applied Biochemistry and Biotechnology 120(3): 175-182.

Chen, C.,Zhang, X. J.,Zhu, L. X.,Liu, J.,He, W. J.,Han, H. D., (2008). Disinfection by-products and their precursors in a water treatment plant in North China: Seasonal changes and fraction analysis. Science of the Total Environment 397(1-3): 140-147.

Desilva, F. (1994). The Ion-Exchange Deal. Chemical Engineering 101(7): 86-88.

FAO. (1999) Water quality management and control of water pollution. Proceedings of A Regional Workshop, Bangkok, Thailand, 26–30 October.

Fearing, D. A.,Banks, J.,Guyetand, S.,Eroles, C. M.,Jefferson, B.,Wilson, D., Hillis, P.,Campbell, A. T.,Parsons, S. A., (2004). Combination of ferric and MIEX (R) for the treatment of a humic rich water. Water Research 38(10): 2551-2558.

Fromme, H.,Kuchler, T.,Otto, T.,Pilz, K.,Muller, J.,Wenzel, A., (2002). Occurrence of phthalates and bisphenol A and F in the environment. Water Research 36(6): 1429-1438.

Fu, P. Q. and K. Kawamura (2010). Ubiquity of bisphenol A in the atmosphere. Environmental Pollution 158(10): 3138-3143.

Fukuhara, T.,Iwasaki, S.,Kawashima, M.,Shinohara, O.,Abe, I., (2006). Absorbability of estrone and 17beta-estradiol in water onto activated carbon. Water Research 40(2): 241-248.

Gabet-Giraud, V.,Miege, C.,Choubert, J. M.,Ruel, S. M.,Coquery, M., (2010). "Occurrence and removal of estrogens and beta blockers by various processes in wastewater treatment plants." Science of the Total Environment 408(19): 4257-4269.

Giesy, J. P. and K. Kannan (2001). Global distribution of perfluorooctane sulfonate in wildlife. Environmental Science & Technology 35(7): 1339-1342.

Gouthro, R. P. and L. Vaz (1999). Recovery and purification of nickel salts and chromic acid using Recoflo ion-exchange. Transactions of the Metal Finishers Association of India 8(4): 185-193.

Gu, B.,Dong, W.,Brown, G. M.,Cole, D. R., (2003). Complete degradation of perchlorate in ferric chloride and hydrochloric acid under controlled temperature and pressure. Environ Sci Technol 37(10): 2291-2295.

Gustafson, K. E. and R. M. Dickhut (1994). "Molecular Diffusivity of Polycyclic Aromatic Hydrocarbons in Aqueous Solution." Journal of Chemical & Engineering Data 39(2): 281-285.

Halling-Sorensen, B.,Nielsen, S. N.,Lanzky, P. F.,Ingerslev, F.,Lutzhoft, H. C. H.,Jorgensen, S. E., (1998). Occurrence, fate and effects of pharmaceutical substances in the environment - A review. Chemosphere 36(2): 357-394.

Hansen, M. C.,Borresen, M. H.,Schlabach, M.,Cornelissen, G., (2010). Sorption of perfluorinated compounds from contaminated water to activated carbon. Journal of Soils and Sediments 10(2): 179-185.

Hashimoto, T. and T. Murakami (2009). Removal and degradation characteristics of natural and synthetic estrogens by activated sludge in batch experiments. Water Research 43(3): 573-582.

He, P. J.,Phan, L.,Gu, G. W.,Hervouet, G., (2001). Reclaimed municipal wastewater - a potential water resource in China. Water Science and Technology 43(10): 51-58.

Humbert, H.,Gallard, H.,Suty, H.,Croue, J. P.,. (2005). Performance of selected anion-exchange resins for the treatment of a high DOC content surface water. Water Research 39(9): 1699-1708.

Hongve, D.,Baann, J.,Becher, G.,Beckmann, O. A., (1999). Experiences from operation and regeneration of an anionic exchanger for natural organic matter (NOM) removal. Water Science and Technology 40(9): 215-221.

Jin, Y.,Saito, N.,Harada, K. H.,Inoue, K.,Koizumi, A., (2007). Historical trends in human serum levels of perfluorooctanoate and perfluorooctane sulfonate in Shenyang, China. Tohoku J Exp Med 212(1): 63-70.

Kaneco, S.,Rahman, M. A.,Suzuki, T.,Katsumata, H.,Ohta, K., (2004). Optimization of solar photocatalytic degradation conditions of bisphenol A in water using titanium dioxide. Journal of Photochemistry and Photobiology a-Chemistry 163(3): 419-424.

Kim, S. D.,Cho, J.,Kim, I. S.,Vanderford, B. J.,Snyder, S. A., (2007). Occurrence and removal of pharmaceuticals and endocrine disruptors in South Korean surface, drinking, and waste waters. Water Research 41(5): 1013-1021.

Kocaoba, S. (2007). Comparison of Amberlite IR 120 and dolomite's performances for removal of heavy metals. J Hazard Mater 147(1-2): 488-496.

Kolpin, D. W.,Furlong, E. T.,Meyer, M. T.,Thurman, E. M.,Zaugg, S. D.,Barber, L. B.,Buxton, H. T., (2002). Pharmaceuticals, hormones, and other organic wastewater contaminants in US streams, 1999-2000: A national reconnaissance. Environmental Science & Technology 36(6): 1202-1211.

Kumar, A. K.,Mohan, S. V.,Sarma, P. N., (2009). "Sorptive removal of endocrine-disruptive compound (estriol, E3) from aqueous phase by batch and column studies: Kinetic and mechanistic evaluation." Journal of Hazardous Materials 164(2-3): 820-828.

Lai, K. M.,Johnson, K. L.,Scrimshaw, M. D.,Lester, J. N., (2000). Binding of waterborne steroid estrogens to solid phases in river and estuarine systems. Environmental Science & Technology 34(18): 3890-3894.

Lee, Y. and U. Von Gunten (2009). Transformation of 17-alpha-Ethinylestradiol during Water Chlorination: Effects of Bromide on Kinetics, Products, and Transformation Pathways. Environmental Science & Technology 43(2): 480-487.

Lei, C. H.,Bareno, J.,Wen, J. G.,Petrov, I.,Kang, S. H.,Abraham, D. P., (2008). "Local structure and composition studies of Li1.2Ni0.2Mn0.6O2 by analytical electron microscopy." Journal of Power Sources 178(1): 422-433.

Levy, F. and S. K. Doss (1987). Regeneration of Electroless Nickel Solution by Ion-Exchange. Plating and Surface Finishing 74(9): 80-81.

Li, F. S.,Yuasa, A.,Tanaka, H.,Katamine, Y., (2008). Adsorption and biotransformation of 17 beta-estradiol in biological activated carbon adsorbers. Adsorption-Journal of the International Adsorption Society 14(2-3): 389-398.

Lin, L. C. and R. S. Juang (2005). Ion-exchange equilibria of Cu(II) and Zn(II) from aqueous solutions with Chelex 100 and Amberlite IRC 748 resins. Chemical Engineering Journal 112(1-3): 211-218.

Liu, B. and X. L. Liu (2004). "Direct photolysis of estrogens in aqueous solutions." Science of the Total Environment 320 (2-3): 269-274.

Liu, G. F.,Ma, J.,Li, X. C.,Qin, Q. D. (2009). Adsorption of bisphenol A from aqueous solution onto activated carbons with different modification treatments. J Hazard Mater 164(2-3): 1275-1280.

Ma, R. W. and K. M. Shih (2010). Perfluorochemicals in wastewater treatment plants and sediments in Hong Kong. Environmental Pollution 158(5): 1354-1362.

Mclachlan, M. S.,Holmstrom, K. E.,Reth, M.,Berger, U., (2007). Riverine discharge of perfluorinated carboxylates from the European continent. Environmental Science & Technology 41(21): 7260-7265.

MSNBC, (2007): http://www.msnbc.msn.com/id/21494919/ns/us_news-environment/

Nakagawa, S.,Kenmochi, Y.,Tutumi, K.,Tanaka, T.,Hirasawa, I., (2002). A study on the degradation of endocrine disruptors and dioxins by ozonation and Advanced Oxidation Processes. Journal of Chemical Engineering of Japan 35(9): 840-847.

National Research Council (1999). *Hormonally Active Agents in the Environment.* National Academy Press, Washington, DC.

Neale, P. A.,Mastrup, M.,Borgmann, T.,Schafer, A. I., (2010). Sorption of micropollutant estrone to a water treatment ion-exchange resin. J Environ Monit 12(1): 311-317.

Noureddin, I. M.,Furumoto, T.,Ishida, Y.,Fukui, H., (2004). Absorption and metabolism of bisphenol A, a possible endocrine disruptor, in the aquatic edible plant, water convolvulus (Ipomoea aquatica). Biosci Biotechnol Biochem 68(6): 1398-1402.

Ohko, Y.,Ando, I.,Niwa, C.,Tatsuma, T.,Yamamura, T.,Nakashima, T.,Kubota, Y.,Fujishima, A., Degradation of bisphenol A in water by TiO_2 photocatalyst. Environmental Science & Technology 35(11): 2365-2368.

Pan, B. J.,Qiu, H.,Pan, B. C.,Nie, G. Z.,Xiao, L. L.,Lv, L.,Zhang, W. M.,Zhang, Q. X.,Zheng, S. R., (2010). "Highly efficient removal of heavy metals by polymer-supported nanosized hydrated Fe(III) oxides: Behavior and XPS study." Water Research 44(3): 815-824.

Pehlivan, E.,Altuna, T.,Cetin, S.,Bhanger, M. I. (2009). Lead sorption by waste biomass of hazelnut and almond shell. Journal of Hazardous Materials 167(1-3): 1203-1208.

Plokhov, E. S.,Mikhalenko, M. G.,Plokhov, S. V., (2006). Ion-exchange recovery of nickel(II) frown wash water formed in electroless plating in acid hypophosphite solutions. Russian Journal of Applied Chemistry 79(10): 1571-1575.

Routledge, E. J.,Sheahan, D.,Desbrow, C.,Brighty, G. C.,Waldock, M., Sumpter, J. P., (1998). Identification of estrogenic chemicals in STW effluents. 2. In vivo responses in trout and rouch. Environmental Toxicology and Chemistry 32(11): 1559-1565

Saha, B.,Karounou, E.,Streat, M., (2010). Removal of 17 beta-oestradiol and 17 alpha-ethinyl oestradiol from water by activated carbons and hypercrosslinked polymeric phases. Reactive & Functional Polymers 70(8): 531-544.

Sedlak, D. L.,Gray, J. L.,Pinkston, K. E., (2000). Contaminants in recycled water." Environmental Science & Technology 34(23): 509a-515a

Senevirathna S.T.M.L.D., Tanaka S., Fujii S., Kunacheva C., Harada H., Shivakoti B.R., Okamoto R. (2010), A comparative study of adsorption of perfluorooctane sulfonate (PFOS) onto granular activated carbon, ion-exchange polymers and non-ion-exchange polymers. Chemosphere 80 647–651

Shubha, K. P.,Raji, C.,Anirudhan, T. S., (2001). Immobilization of heavy metals from aqueous solutions using polyacrylamide grafted hydrous tin (IV) oxide gel having carboxylate functional groups. Water Res 35(1): 300-310.

Sinclair, E. and K. Kannan (2006). Mass loading and fate of perfluoroalkyl surfactants in wastewater treatment plants. Environmental Science & Technology 40(5): 1408-1414.

Staples, C. A.,Dorn, P. B.,Klecka, G. M.,O'Block, S. T.,Harris, L. R., (1998). A review of the environmental fate, effects, and exposures of bisphenol A. Chemosphere 36(10): 2149-2173.

Streat, M. and L. A. Sweetland (1997). Physical and adsorptive properties of Hypersol-Macronet (TM) polymers. Reactive & Functional Polymers 35(1-2): 99-109.

Sundstrom, D. W.,Klei, H. E.,Tsui, T.,Nayar, S., (1979). Response of Biological Reactors to the Addition of Powdered Activated Carbon. Water Research 13(12): 1225-1231.

Takahashi, S.,Chi, X. J.,Yamaguchi, Y.,Suzuki, H.,Sugaya, S.,Kita, K., Hiroshima, K.,Yamamori, H.,Ichinose, M.,Suzuki, N., (2001). Mutagenicity of bisphenol A and its suppression by interferon-alpha in human RSa cells. Mutation Research-Genetic Toxicology and Environmental Mutagenesis 490(2): 199-207.

Takahashi, S. Tsukamoto, A. Kawaguchi, A. Sakamoto, H. Morikawa (2005). Phytoremediators from abandoned rice field, Plant Biotechnol. 22 167–170.

Tsai, W. T.,Hsu, H. C.,Su, T. Y.,Lin, K. Y.,Lin, C. M., (2006). Adsorption characteristics of bisphenol-A in aqueous solutions onto hydrophobic zeolite. Journal of Colloid and Interface Science 299(2): 513-519.

US Food and Drug Administration. (2008) Draft assessment of bisphenol A for use in food contact applications.

Valderrama, C.,Cortina, J. L.,Farran, A.,Gamisans, X.,Lao, C. (2007). Kinetics of sorption of polyaromatic hydrocarbons onto granular activated carbon and Macronet hyper-cross-linked polymers (MN200). Journal of Colloid and Interface Science 310(1): 35-46.

Vandenberg, L. N.,Hauser, R.,Marcus, M.,Olea, N.,Welshons, W. V., (2007). Human exposure to bisphenol A (BPA). Reproductive Toxicology 24(2): 139-177.

Wang F. and Shih K. (2011), Adsorptionof perfluorooctanesulfonate (PFOS) and perfluorooctanoate (PFOA) on alumina: Influence of solution pH and cations. Water Res 45(9): 2925-2930

Yamamoto, T. and A. Yasuhara (2002). Chlorination of bisphenol A in aqueous media: formation of chlorinated bisphenol A congeners and degradation to chlorinated phenolic compounds. Chemosphere 46(8): 1215-1223.

Yang, K. and B. S. Xing (2010). "Adsorption of Organic Compounds by Carbon Nanomaterials in Aqueous Phase: Polanyi Theory and Its Application." Chemical Reviews 110(10): 5989-6008.

Yong, Q. (2007). "Study on treatment technologies for perfluorochemicals in wastewater," Kyoto University.

Yoon, Y.,Westerhoff, P.,Snyder, S. A.,Esparza, M., (2003). , HPLC-fluorescence detection and adsorption of bisphenol A, 17beta-estradiol, and 17alpha-ethynyl estradiol on powdered activated carbon. Water Res 37(14): 3530-3537.

Yoon, Y.,Ryu, J.,Oh, J.,Choi, B. G.,Snyder, S. A., (2010). Effect of gamma irradiation on Burkholderia thailandensis (Burkholderia pseudomallei surrogate) survival under combinations of pH and NaCl. Radiation Physics and Chemistry 79(4): 545-548.

Yu, Z. H.,Qi, T.,Qu, J. K.,Wang, L. N.,Chu, J. L.,. Removal of Ca(II) and Mg(II) from potassium chromate solution on Amberlite IRC 748 synthetic resin by ion-exchange. J Hazard Mater 167(1-3): 406-412.

Zenker, M. J.,Borden, R. C.,Barlaz, M. A., (2003). Occurrence and treatment of 1,4-dioxane in aqueous environments. Environmental Engineering Science 20(5): 423-432.

Zhang, Y. P. and J. L. Zhou (2005). Removal of estrone and 17 beta-estradiol from water by adsorption. Water Research 39(16): 3991-4003.

Zhang, Y.,Causserand, C.,Aimar, P.,Cravedi, J. P. (2006). Removal of bisphenol A by a nanofiltration membrane in view of drinking water production. Water Research 40(20): 3793-3799.

Zhang, R.,Vigneswaran, S.,Ngo, H. H.,Nguyen, H. (2006). Magnetic ion-exchange (MIEX (R)) resin as a pre-treatment to a submerged membrane system in the treatment of biologically treated wastewater. Desalination 192(1-3): 296-302.

Zhao, Z.,Knowlton, K. F.,Love, N. G.,Ogejo, J. A., (2010). "Estrogen Removal from Dairy Manure by Pilot-Scale Treatment Reactors." Transactions of the Asabe 53(4): 1295-1301.

Appendices

Appendix A

Experimental setup for batch investigation

Appendix B

Experimental setup for column studies

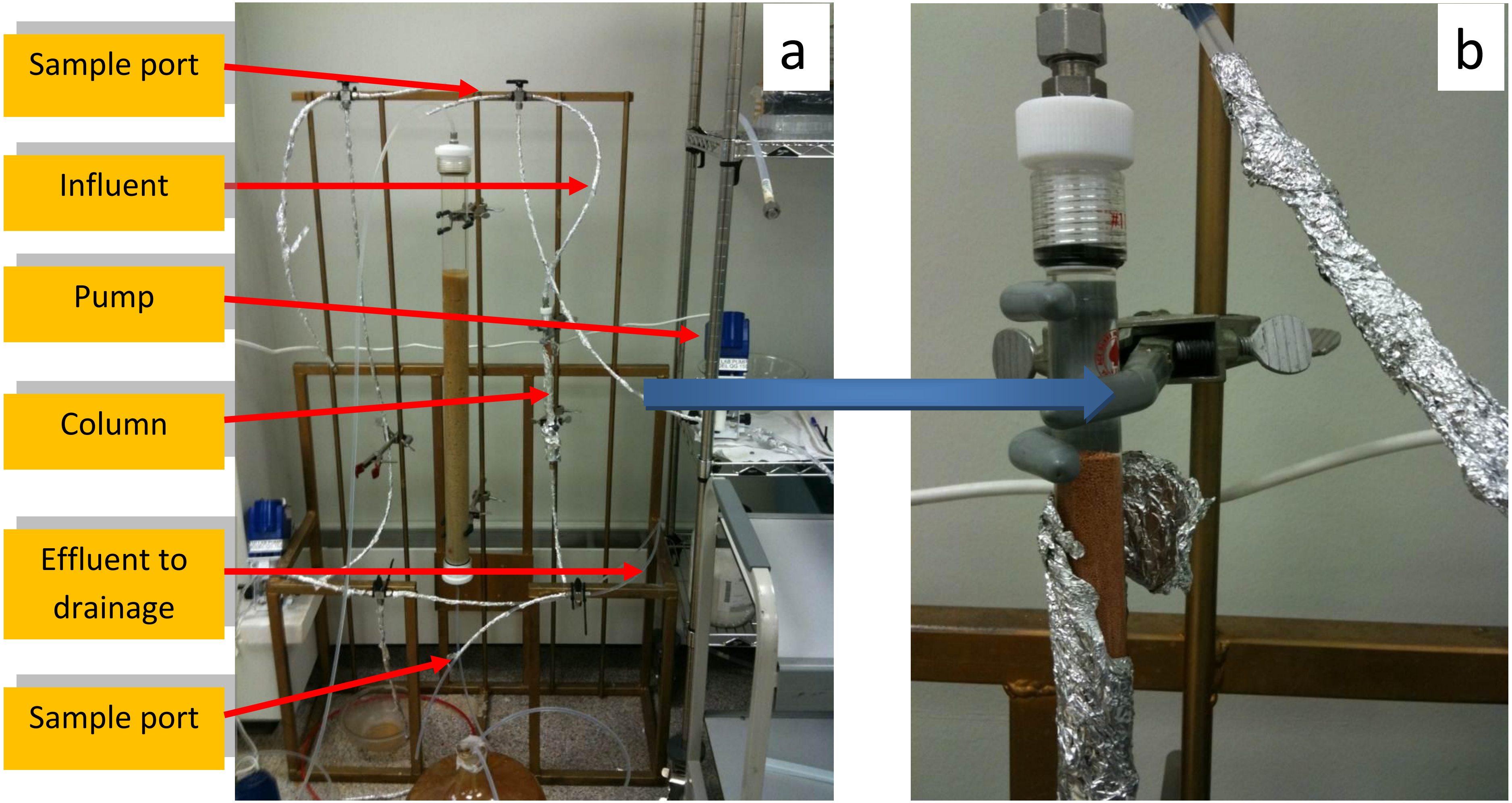

Appendix C Experimental details for Figure 4.1

Screening test for the adsorption of 17β-estradiol onto various types of resins

Conditions: (initial concentration= 134.74 μg/L, pH= 7.0, contact time= 48 hours, sample volume= 1000 ml, temp= 295 K, resin dosage= 0.3 g/L)

Resins	Peak Area	Concentration （μg/L)	Removal %	Loading (μg/g)
*initial	12030	134.74	--	--
MN 100	8468	2.12	98.43	442.08
MN 200	9157	2.90	97.85	439.48
A 530E	9423	46.70	65.34	293.46
A 532E	9044	73.74	45.27	203.32
C 115	10160	113.36	15.87	71.28

*Initial represents the actual initial concentrations of the model solution

Appendix D (a)

Experimental details for Figure 4.2 Effect of resin dosage on the adsorption of estrogen hormones mixture onto MN100 resins

Conditions: (target initial concentration= 100 μg/L, pH= 7.0, contact time= 48 hours, sample volume= 1000 ml, temp= 295 K)

Numbers showed in the following table are concentrations with unit of μg/L

Dosage (g/L)	17α-Ethinylestradiol	Estriol	17β-Estradiol	17α-Estradiol	Estrone	17α-Dihydroequilin	Trimegestone	Medrogestone	Progesterone	Norgestrel	Gestodene	Equilin
*Initial	230.10	156.71	190.76	175.26	174.91	200.22	196.94	172.80	185.20	182.59	190.49	182.13
0.05	55.09	115.12	79.53	93.31	81.88	90.42	166.34	132.02	99.93	123.75	102.56	92.80
0.1	41.96	66.30	43.77	43.80	40.46	30.79	89.81	59.90	46.08	71.34	55.60	31.99
0.2	5.60	16.90	13.24	3.86	7.61	9.21	20.75	15.35	8.96	19.65	14.68	5.81
0.3	BDL	7.41	2.60	2.65	1.81	1.62	4.81	6.58	2.44	4.45	3.71	0.58
0.4	BDL	3.49	BDL	1.68	0.62	0.55	2.19	3.34	1.34	2.17	1.64	3.22
0.6	BDL	1.47	BDL	BDL	0.26	0.80	1.19	1.69	0.62	0.78	1.02	0.67
0.8	2.78	0.56	BDL	BDL	1.37	0.34	1.11	1.95	0.61	0.52	BDL	BDL
1	5.70	1.01	BDL	BDL	0.21	BDL	1.59	2.70	0.91	0.95	0.65	5.38

*Initial represents the actual initial concentrations of the model solution

BDL=below detection limits

Appendix D (b)

Experimental details for Figure 4.2 Effect of resin dosage on the adsorption of estrogen hormones mixture onto MN200 resins

Conditions: (target initial concentration= 100 μg/L, pH= 7.0, contact time= 48 hours, sample volume= 1000 ml, temp= 295 K)

Numbers showed in the following table are concentrations with unit of μg/L

Dosage (g/L)	17α-Ethinylestradiol	Estriol	17β-Estradiol	17α-Estradiol	Estrone	17α-Dihydroequilin	Trimegestone	Medrogestone	Progesterone	Norgestrel	Gestodene	Equilin
*Initial	230.10	156.71	190.76	175.26	174.91	200.22	196.94	172.80	185.20	182.59	190.49	182.13
0.05	140.18	90.17	110.52	87.84	75.85	116.88	107.47	56.26	84.60	111.42	100.85	101.10
0.1	104.53	40.50	32.97	25.75	29.89	56.16	45.89	23.96	31.04	49.90	42.99	24.16
0.2	112.34	10.45	BDL	BDL	3.63	27.72	7.59	4.23	4.50	10.19	8.39	13.80
0.3	105.92	3.40	6.65	4.57	1.47	38.49	1.65	2.24	1.30	2.30	1.77	5.80
0.4	60.39	1.22	BDL	BDL	0.66	34.27	1.17	2.76	1.55	0.98	0.84	BDL
0.6	10.11	1.01	4.80	5.16	0.38	21.73	0.24	0.38	0.31	BDL	0.36	1.97
0.8	10.81	0.10	8.31	6.16	0.95	48.62	0.35	0.21	0.16	0.38	BDL	6.33
1	8.60	0.10	5.60	4.54	0.82	26.31	0.19	0.25	0.15	0.16	0.43	8.32

*Initial represents the actual initial concentrations of the model solution

BDL=below detection limits

Appendix E (a)

Experimental details for Figure 4.4 Effect of contact time on the adsorption of estrogen hormones onto MN100 resins

Conditions: (target initial concentration= 200 μg/L, pH= 7.0, contact time= 48 hours, sample volume= 1000 ml, temp= 295 K)

Numbers showed in the following table are concentrations with unit of μg/L

Time (h)	17α-Ethinylestradiol	Estriol	17β-Estradiol	17α-Estradiol	Estrone	17α-Dihydroequilin	Trimegestone	Medrogestone	Progesterone	Norgestrel	Gestodene	Equilin
*initial	266.68	255.67	299.75	361.10	236.11	256.66	297.73	179.00	176.09	119.49	102.40	204.42
0.5	191.50	184.73	222.56	228.38	167.07	180.15	258.52	151.28	154.58	109.13	89.39	198.31
1	107.36	145.60	156.60	198.60	117.46	138.75	174.25	98.06	98.48	75.45	59.95	130.93
2	158.33	164.32	134.95	212.53	123.92	145.29	395.37	240.88	147.99	215.56	138.65	111.19
3	67.40	125.77	109.53	135.28	97.61	90.01	283.95	168.28	117.40	179.94	123.18	77.04
4	59.21	115.60	92.96	98.90	82.38	77.27	272.28	155.38	101.69	169.46	113.25	64.19
6	22.04	75.81	26.77	60.96	37.88	52.84	136.85	61.08	53.05	60.20	41.75	30.02
8	30.77	50.05	11.65	68.57	19.65	24.22	103.11	54.80	43.36	85.89	62.16	12.38
12	2.70	36.17	14.76	2.97	12.60	11.65	63.06	59.51	23.39	48.35	31.06	7.60
24	BDL	8.37	1.56	BDL	1.96	3.85	6.02	7.43	4.13	13.03	11.81	10.88

BDL=below detection limits

Appendix E (b)

Experimental details for Figure 4.4 Effect of contact time on the adsorption of estrogen hormones onto MN200 resins

Conditions: (target initial concentration= 200 μg/L, pH= 7.0, contact time= 48 hours, sample volume= 1000 ml, temp= 295 K)

Numbers showed in the following table are concentrations with unit of μg/L

Time (h)	17α-Ethynylestradiol	Estriol	17β-Estradiol	17α-Estradiol	Estrone	17α-Dihydroequilin	Trimegestone	Medrogestone	Progesterone	Norgestrel	Gestodene	Equilin
*initial	199.13	185.70	220.14	261.61	185.93	187.84	240.77	152.29	142.78	97.79	80.76	169.13
0.5	112.68	165.05	184.02	202.22	145.68	162.11	199.45	122.83	119.69	86.17	66.45	151.19
1	122.54	132.08	136.42	191.21	109.54	113.68	154.61	91.01	88.18	66.63	52.87	130.63
2	41.61	95.42	86.67	135.85	75.55	81.02	124.54	93.39	79.04	109.02	88.95	89.70
3	74.59	87.47	75.24	104.49	64.99	66.72	108.26	78.52	67.52	98.66	78.55	78.46
4	54.66	76.17	54.12	49.94	49.13	57.79	82.56	58.73	52.55	83.34	68.51	52.74
6	29.08	44.91	24.76	36.97	25.98	26.01	44.67	24.12	22.51	24.96	19.60	28.82
8	12.47	33.83	19.63	11.33	13.53	16.12	30.38	18.28	16.69	36.14	26.45	17.62
12	8.07	15.12	5.73	11.97	4.49	5.57	9.21	8.75	5.30	13.38	9.10	7.46
24	6.63	4.35	1.33	BDL	1.59	0.39	1.98	1.93	1.00	2.84	2.26	BDL

BDL=below detection limits

Appendix F (a)

Experimental details for Figure 4.6 Effect of pH for the adsorption of estrogen hormones onto MN100 resin

Conditions: (target initial concentration= 100 μg/L, resin dosage= 0.2 g/L, contact time= 48 hours, sample volume= 1000 ml, temp= 295 K)

Numbers showing in the below table is concentrations with unit of μg/L.

pH	17α-Ethinylestradiol	Estriol	17β-Estradiol	17α-Estradiol	Estrone	17α-Dihydroequilin	Trimegestone	Medrogestone	Progesterone	Norgestrel	Gestodene	Equilin
*Initial	123.82	112.84	146.88	102.94	105.86	118.43	126.83	115.81	109.12	111.52	134.22	113.42
2.73	43.91	60.94	66.98	43.19	39.01	49.01	57.63	54.67	42.94	56.87	58.52	41.88
4.16	45.69	63.68	71.31	42.44	44.78	45.85	59.50	50.66	44.55	59.03	65.55	58.43
7	44.85	56.40	61.88	42.67	37.35	38.77	53.65	43.90	37.91	49.16	58.66	52.32
9.06	47.23	64.41	71.76	49.19	41.00	46.44	57.52	46.23	40.22	57.92	61.71	57.60
10.92	115.52	83.18	114.62	80.07	88.14	68.58	44.66	40.49	33.40	43.90	49.35	85.07

Appendix F (b)

Experimental details for Figure 4.6 Effect of pH for the adsorption of estrogen hormones onto MN200 resin

Conditions: (target initial concentration= 100 µg/L, resin dosage= 0.2 g/L, contact time= 48 hours, sample volume= 1000 ml, temp= 295 K)

Numbers showing in the below table is concentrations with unit of µg/L.

pH	17α-Ethinylestradiol	Estriol	17β-Estradiol	17α-Estradiol	Estrone	17α-Dihydroequilin	Trimegestone	Medrogestone	Progesterone	Norgestrel	Gestodene	Equilin
*Initial	123.82	112.84	146.88	102.94	105.86	118.43	126.83	115.81	109.12	111.52	134.22	113.42
2.73	42.81	53.27	66.41	42.46	33.62	41.82	58.41	54.57	38.15	53.34	65.84	42.80
4.16	35.56	56.47	56.69	36.31	34.02	34.37	46.87	37.08	32.77	48.10	50.87	39.47
7	41.42	58.63	62.70	45.69	38.84	42.10	54.73	44.73	39.44	54.35	62.71	52.26
9.06	43.28	51.67	63.39	37.88	37.23	35.39	47.39	43.10	36.03	47.89	54.38	37.77
10.92	93.87	92.71	134.56	77.16	99.15	79.33	48.63	39.20	33.62	48.52	61.54	105.55

Appendix G

Experimental details for Figure 4.7 Fixed-bed column study with estrogen hormones mixture

Conditions:

(Resin used: MN100, target concentration=100 µg/L, flow rate= 32 ml/min, column diameter= 1.1 cm, resin mass= 1.5 g, bed depth= 3 cm, EBCT= 0.1 min, running time= 52 hours, temperature= 295 K)

Numbers showing in the below table is concentrations with unit of µg/L at different time interval. Numbers in the bucket represents the initial concentrations.

Time (h)	Norgestrel	Progesterone	Trimegestrone	17α-dihydroequilin	17α-Estradiol	17β-Estradiol	Estrone	Medrogestone
0	BDL (108.3)	BDL(119.5)	BDL(103.4)	BDL(97.9)	BDL(115.2)	BDL(117.8)	BDL(104.8)	BDL(20.4)
1	BDL(108.3)	BDL(119.5)	BDL(103.4)	BDL(97.9)	BDL(115.2)	BDL(117.8)	BDL(104.8)	BDL(20.4)
2	6.09(108.3)	11.13(119.5)	18.76(103.4)	0.33(97.9)	0.23(115.2)	0.16(117.8)	BDL (104.8)	BDL(20.4)
4	3.50(108.3)	2.44(119.5)	2.17(103.4)	2.40(97.9)	2.81(115.2)	2.78(117.8)	2.86(104.8)	BDL(20.4)
6	7.02(108.3)	4.43(119.5)	6.75(103.4)	1.46(97.9)	1.58(115.2)	1.48(117.8)	1.58(104.8)	BDL(20.4)
8	4.93(108.3)	3.19(119.5)	BDL (103.4)	2.35(97.9)	3.04(115.2)	2.82(117.8)	2.76(104.8)	BDL(20.4)
10	1.80(113.2)	2.38(111.8)	BDL(105.2)	1.11(103.6)	1.58(109.3)	1.53(119.2)	1.61(107.2)	BDL(33.5)
12	16.17(113.2)	4.62(111.8)	39.65(105.2)	17.82(103.6)	19.89(109.3)	19.19(119.2)	18.82(107.2)	BDL(33.5)
14	0.00(113.2)	9.65(111.8)	19.76(105.2)	9.32(103.6)	10.50(109.3)	10.11(119.2)	10.24(107.2)	BDL(33.5)
16	2.52(113.2)	3.61(111.8)	21.31(105.2)	11.44(103.6)	12.94(109.3)	12.49(119.2)	12.61(107.2)	BDL(33.5)
18	39.59(105.7)	22.93(113.9)	56.97(102.5)	29.93(98.5)	31.81(103.7)	31.27(115.9)	31.10(103.5)	BDL(10.3)
20	47.79(105.7)	40.28(113.9)	89.67(102.5)	45.75(98.5)	47.35(103.7)	46.99(115.9)	46.14(103.5)	BDL(10.3)
22	84.70(105.7)	83.81(113.9)	128.40(102.5)	76.75(98.5)	8.68(103.7)	76.57(115.9)	75.64(103.5)	BDL(10.3)
24	89.48(105.7)	97.20(113.9)	122.71(102.5)	79.85(98.5)	77.17(103.7)	80.15(115.9)	78.37(103.5)	BDL(10.3)

26	93.29(104.2)	88.23(115.0)	133.47(107.9)	85.20(106.7)	80.84(116.3)	83.79(113.9)	83.05(109.3)	BDL(29.9)
28	91.41(104.2)	96.29(115.0)	139.67(107.9)	86.61(106.7)	81.95(116.3)	85.37(113.9)	83.77(109.3)	BDL(29.9)
30	110.24(104.2)	123.44(115.0)	139.42(107.9)	96.16(106.7)	90.51(116.3)	95.90(113.9)	94.93(109.3)	BDL(29.9)
32	106.69(104.2)	133.23(115.0)	150.43(107.9)	118.70(106.7)	91.33(116.3)	116.13(113.9)	96.80(109.3)	BDL(29.9)
34	103.78(120.2)	118.46(101.2)	188.86(122.3)	150.25(110.3)	82.74(129.3)	87.12(129.5)	100.99(111.5)	BDL(33.5)
48	111.75(111.5)	131.18(109.3)	144.47(110.4)	98.85(102.7)	91.36(103.2)	98.08(110.3)	97.30(100.4.)	BDL(25.7)
52	107.77(107.1)	145.12(102.4)	174.73(102.8)	94.82(109.6)	87.85(117.6)	93.39(101.3)	113.18(110.8)	BDL(19.4)
Average initial Concentration	108.695	114.515	105.775	101.78	112.045	117.13	106.035	23.82

BDL=below detection limits

Appendix H

Experimental details for Figure 4.8 Screening test on the adsorption of perfluorooctanoic acid (PFOA) onto various types of resins

Conditions: (initial concentration= 25.65 µg/L, pH=7.0, contact time= 48 hours, sample volume= 1000 ml, temp= 295 K, resin dosage=0.3g/L)

Resins	Peak Area of PFOA	Concentration (µg/L)	Removal%	Loading (µg/g)
*Initial	58406	25.65	--	--
C115	59330	26.06	-	-
A530E	526	0.23	99.10	84.73
A532E	426	0.19	99.27	84.88
MN100	1339	0.59	97.71	83.54
MN200	32559	14.30	44.25	37.83

*Initial represents the actual initial concentrations of the model solution

Appendix I

Experimental details for Figure 4.9 Effect of resin dosage on the adsorption of PFOA onto A530E, A532E and MN100 resins

Conditions: (initial concentration= 54.29 μg/L, pH= 7.0, contact time= 48 hours, sample volume= 1000 ml, temp= 295 K)

Numbers showed in the following table are concentrations with unit of μg/L

Resin dosage (g/L)	MN100	A530E	A532E
*Initial	54.29	54.29	54.29
0.05	9. 1	2.23	0.34
0.1	8.75	1.09	0 30
0.2	3.86	0.09	0.31
0.3	1.37	0.05	0.58
0.4	1.12	0.07	0.46

*Initial represents the actual initial concentrations of the model solution

Appendix J

Experimental details for Figure 4.10 Effect of contact time on the adsorption of PFOA onto A530E, A532E and MN100 reins

Conditions: (pH= 7.0, contact time= 52 hours, sample volume= 1000 ml, temperature= 295 K, resin dosage= 0.1 g/L)

Numbers showed in the following table are concentrations with unit of μg/L

Time (h)	Target concentration= 25 μg/L			Target concentration= 50 μg/L		
Resins	A530E	A532E	MM100	A530E	A532E	MM100
*Initial	29.51	29.51	29.51	60.06	60.06	60.06
0.5	20.65	16.20	24.42	44.37	32.47	49.88
1	15.48	10.08	21.92	35.99	24.05	44.71
2	14.19	7.30	18.01	27.85	15.18	37.28
3	10.33	5.25	14.56	21.59	11.51	29.74
4	8.32	3.82	12.77	18.09	9.67	24.32
6	5.88	2.02	8.30	10.36	5.83	18.40
8	4.60	1.65	5.50	5.47	3.36	13.91
12	2.91	BDL	3.56	1.77	1.76	8.87
18	1.93	BDL	1.83	0.50	BDL	4.88
24	0.89	0.42	1.15	BDL	1.29	3.05
52	BDL	BDL	BDL	BDL	BDL	1.15

*Initial represents the actual initial concentrations of the model solution

BDL=below detection limits

Appendix K

Experimental details for Figure 4.11 Effect of initial concentration on the adsorption of PFOA onto A530E, A532E and MN100 resins

Conditions: (resin dosage = 0.1 g/L, pH= 7.0, contact time= 48 hours, sample volume= 1000 ml, temp= 295 K)

Numbers showed in the following table are concentrations with unit of µg/L

Initial concentration (µg/L)	A530E	A532E	MN100
100	0.77	1.80	3.22
300	1.38	9.80	27.99
400	1.87	7.54	58.28
600	2.41	11.88	116.64
800	4.17	15.48	356.32
1000	5.60	30.37	574.3

Appendix L

Experimental details for Figure 4.12 Effect of resin dosage and isotherm on the adsorption of PFCs onto (a) A530E; (b) A532E; (c) MN100 resins

Conditions: (target concentration= 300 μg/L pH= 7.0, contact time= 48 hours, sample volume= 1000 ml, temperature= 295 K)

Numbers showed in the following table are concentrations with unit of μg/L

A532E	1	2	3	4	5	6	7	8	9	10
*Initial	194.37	171.58	172.55	195.97	144.19	225.55	222.98	146.46	207.69	257.05
0.05	194.37	171.58	172.55	195.97	144.19	225.55	222.98	146.46	207.69	257.05
0.08	163.00	98.82	81.77	98.83	53.62	142.47	107.92	97.85	142.54	168.82
0.10	125.44	60.24	41.69	39.72	22.10	56.80	35.11	47.19	52.92	74.05
0.15	87.33	34.17	17.46	9.86	4.02	8.48	3.90	7.74	5.51	7.64
0.20	71.65	18.12	5.50	3.59	0.95	2.67	0.44	4.81	0.62	1.04
A530E										
*Initial	194.37	171.58	172.55	195.97	144.19	225.55	222.98	146.46	207.69	257.05
0.05	186.77	152.00	137.86	123.94	99.28	142.08	129.54	16.75	134.71	167.03
0.08	135.43	90.62	73.52	65.19	49.68	63.87	50.16	54.18	52.58	85.38
0.10	102.62	58.72	46.53	38.02	28.30	37.61	27.72	19.95	30.45	46.79
0.15	94.77	35.84	21.89	15.39	7.27	8.83	5.55	0.00	5.65	7.15
0.20	80.84	22.43	12.47	6.82	2.03	4.09	1.44	1.35	1.67	1.28
MN100										
*Initial	252.88	295.59	314.33	321.28	293.92	325.09	6.61	149.87	259.61	298.77
0.05	217.75	214.86	247.36	246.11	221.39	253.92	5.26	240.77	220.17	262.47
0.08	168.52	173.93	216.20	228.62	199.95	237.78	4.87	188.09	208.35	247.72
0.10	141.67	136.16	169.40	207.18	183.19	238.09	4.92	6.06	227.64	275.20
0.15	109.07	101.15	101.19	135.63	108.48	182.87	3.61	3.59	184.21	242.69
0.20	91.63	84.60	88.10	121.38	92.95	175.51	3.38	20.79	157.22	160.65

1 Perfluorotridecanoic acid 2 Tricosafluorododecanoic acid 3 Perfluoroundecanoic acid
4 Perfluorodecanoic acid 5 Heptadecafluorooctane sulfonic acid potassium salt
6 Perfluorooctanoic acid 7 Tridecafluorohexane-1-sulfonic acid potassium salt
8 Tridecafluorononanoic acid 9 Perfluoroheptanoic acid 10 Undecafluorohexanoic acid

*Initial represents the actual initial concentrations of the model solution

Appendix M

Experimental details for Figure 4.14 Screening test on the adsorption of BPA onto various types of resins

Conditions: (initial concentration= 86.67 μg/L, pH= 7.0, contact time= 48 hours, sample volume= 400 ml, temp= 295 K, resin dosage= 0.2 g/L)

Numbers showed in the following table are concentrations with unit of μg/L

Resins	Peak Area of BPA	Peak Area of BPA-D	Normalized Peak Area	Concentration (μg/L)	Removal (%)	Loading (μg/g)
*Initial	22390	12741	1.76	86.67	--	--
MN100	4550	11905	0.38	18.85	78.25	226.07
MN200	4591	11648	0.39	19.44	77.57	224.10
A530E	9821	12240	0.80	39.57	54.34	156.99
A532E	8045	13371	0.60	29.68	65.76	189.98
C115	19641	12431	1.58	77.93	10.09	29.14

*Initial represents the actual initial concentrations of the model solution

Appendix N

Experimental details for Figure 4.15 Effect of resin dosage on the adsorption of BPA onto MN100 and MN200 resins

Conditions: (initial concentration= 104.4 μg/L, pH= 7.0, contact time= 48 hours, sample volume= 400 ml, temp= 295 K)

MN 100	Peak Area of BPA	Peak Area of BPA-D	Normalized Peak Area	Concentration (μg/L)
*Initial 1	20063	8937	2.24	110.29
*Initial 2	19101	9521	2.01	98.56
0.025	16124	11512	1.40	68.81
0.05	10130	11329	0.89	43.93
0.075	6667	10769	0.62	30.42
0.1	5409	11055	0.49	24.04
0.15	5020	11360	0.44	21.71
MN 200				
*Initial 1	20063	8937	2.24	110.29
*Initial 2	19101	9521	2.01	98.56
0.025	13438	11067	1.21	59.66
0.05	9385	11958	0.78	38.56
0.075	5745	10004	0.57	28.21
0.1	4474	9919	0.45	22.16
0.15	4549	11009	0.41	20.30

*Initial 1 and initial 2 represent duplicate analysis of initial concentration, the average was taken for the analysis purpose

Appendix O

Experimental details for Figure 4.16 Effect of contact time on the adsorption of BPA onto MN100 and MN200 resins and kinetics model fitting

Conditions: (initial concentration= 105.9 µg/L, pH= 7.0, contact time= 72 hours, sample volume= 1000 ml, temp= 295 K, resin dosage= 0.2 g/L)

MN100	Peak Area of BPA	Peak Area of BPA-D	Normalized Peak Area	Concentration (µg/L)
*Initial 1	20219	9644	2.10	103.00
*Initial 2	20130	9090	2.21	108.80
0.5	17758	8202	2.17	106.37
1	15375	8513	1.81	88.73
2	13956	8486	1.64	80.80
3	13484	13581	0.99	48.78
4	11229	12835	0.87	42.98
6	6964	11034	0.63	31.01
8	6447	13175	0.49	24.04
10	4204	13024	0.32	15.86
12	2944	11946	0.25	12.11
24	3877	10264	0.38	18.56
48	3763	10722	0.35	17.24
72	2685	11503	0.23	11.47
MN200				
0.5	18302	9350	1.96	96.17
1	16581	8952	1.85	91.00
2	13611	8667	1.57	77.16
3	9411	9323	1.01	49.59
4	7365	8311	0.89	43.54
6	4885	8552	0.57	28.06
8	3706	9540	0.39	19.09
10	2608	8261	0.32	15.51
12	2294	7445	0.31	15.14
24	4145	11613	0.36	17.54
48	3763	10722	0.35	17.24
72	3064	11172	0.27	13.47

*Initial 1 and initial 2 represent duplicate analysis of initial concentration, the average was taken for the analysis purpose

Appendix P

Experimental details for Figure 4.17 Effect of solution pH on the adsorption of BPA onto MN100 and MN200 resins

Conditions: (initial concentration= 128.17 µg/L, pH= 7.0, contact time= 24 hours, sample volume= 1000 ml, temp= 295 K, resin dosage= 0.2 g/L)

MN 100	Peak Area of BPA	Peak Area of BPA-D	Normalized Peak Area	Concentration (µg/L)	pH after the treatment
*Initial 1	46545	16452	2.83	139.00	7.2
*Initial 2	38759	16230	2.39	117.33	7.2
2.7	5436	15613	0.35	17.11	2.8
5.5	6927	15740	0.44	21.62	5.9
7	4491	15107	0.30	14.61	6.7
9.5	7413	17152	0.43	21.23	9.4
10.6	14309	23989	0.60	29.31	10.7
MN 200					
2.6	4306	15600	0.28	13.56	2.6
4.6	4363	15834	0.28	13.54	4.3
7	4625	15709	0.29	14.46	5.7
9.8	7860	18655	0.42	20.70	9.9
10.6	14382	21902	0.66	32.26	10.8

*Initial 1 and initial 2 represent duplicate analysis of initial concentrations, the average was taken for the calculation

Appendix Q

Experimental details for Figure 4.19 Regeneration test on MN100 and MN200 resins by using gradient methanol-water solutions

Conditions: (contact time= 24 hours, regeneration solution volume= 100 ml, temperature= 295 K, resin dosage= 0.3 g/L)

MN100	Peak Area of BPA	Peak Area of BPA-D	Normalized Peak Area	Conc. After desorption	Mass after desorption (μg)	Mass adsorbed (μg)	Desorption %
*10% Me	843	4946	0.17	8.37	0.84	41.47	2.02
20% Me	2024	5418	0.37	18.35	1.84	41.48	4.42
30% Me	4212	5930	0.71	34.90	3.49	42.01	8.31
40% Me	14477	6142	2.36	115.80	11.58	41.68	27.79
50% Me	30858	6274	4.92	241.64	24.16	41.84	57.75
100% Me	36369	4819	7.55	370.78	37.08	41.56	89.21
MN200							
50% Me	34373	7604	4.52	222.09	22.21	44.42	50.00
100% Me	40905	5307	7.71	378.68	37.87	45.42	83.37

*10% Me represent that the regeneration solution is consist of 10% methanol (volume: volume)

Appendix R

Experimental details for Figure 4.20 Screening test for the adsorption of 1, 4-dioxane onto various types of resins

Conditions: (initial concentration= 125.87 μg/L, pH= 7.0, contact time= 48 hours, sample volume= 1000 ml, temp= 295 K, resin dosage= 0.3 g/L)

Resins	Peak Area of 1, 4-dioxane	Concentration (μg/L)	Removal %	Loading (μg/g)
*Initial	12030	125.87	--	--
MN 100	8468	94.84	24.65	103.43
MN 200	9157	102.56	18.52	77.71
A 530E	9423	105.54	16.15	67.77
A 532E	9044	101.29	19.53	81.92
C 112	10160	113.79	9.60	40.26

*Initial represents the actual initial concentrations of the model solution

Appendix S

Instrument detection limits (IDL) for estrogen hormones, 1, 4-dioxane and PFOA unit (ng/L) (Solid Phase Extraction followed by UPLC/MS/MS)

Compounds	IDL
17a-ethinyl estradiol	7.68
Estriol	26.33
17b-estradiol	0.98
17a-estradiol	2.99
Estrone	35.35
17a-dihydroequilin	15.10
Trimegesterone	0.16
Medrogesterone	0.04
Progesterone	0.01
Norgestrel	0.03
Gestodene	0.02
Equilin	7.73
PFOA*	250
BPA*	1000

* Instrument detection limits by direct injection